

Mescape. A probabilistic mesoscopic model for fire evacuation in large gatherings

Lorenzo Contini

**Fire Safety Engineering
Lund University
Sweden**

Report 5669, Lund 2022

Master Thesis in Fire Safety Engineering

Mescape. A probabilistic mesoscopic model for fire evacuation in large gatherings
Lorenzo Contini

Report 5669
ISRN: LUTVDG/TVBB—5669--SE

Number of pages: 80
Illustrations: 58

Keywords: human behaviour, crowd evacuation, mesoscopic modelling, hydraulic model, large gatherings, fire safety, performance-based design, quantitative risk assessment, consequence analysis, uncertainty analysis, probabilistic modelling.

Abstract: This study presents a mesoscopic model that predicts pedestrian evacuation in large gatherings with probabilistic methods. The model is based on a coarse network representation of buildings, where occupants are treated at a different scale according to their location. A microscopic approach is used to represent people in the initial enclosure: here individual characteristics and behaviours are attributed to each occupant through random sampling from user-defined probabilistic parameter distributions, and individual timelines are used to determine the initial flow of evacuees. A macroscopic representation is implemented in the following parts of egress routes, where occupants are treated as a homogeneous crowd with uniform characteristics. The SFPE hydraulic model is used to predict movement until a place of safety. Two automatic iterative processes are implemented within the evacuation model to address variability and uncertainty. In the first step, behavioural uncertainty is investigated by running the same evacuation scenario multiple times until results meet user-defined converge criteria based on inferential statistics. In the second step, input parameters/distributions are modified automatically to predict evacuation in different scenarios for quantitative risk assessment. Multiple tests show good agreement between the results of the mesoscopic model and a microscopic model employed for benchmarking (Pathfinder used in SFPE mode). For horizontal egress routes, the proposed tool provides detailed and accurate outputs (evacuation curves, flow rates, queue size, etc.) with short computational time. For vertical egress routes, mesoscopic predictions capture well the qualitative evolution of the egress process, but quantitative results are underestimated and necessitate additional investigation. Lastly, a quantitative risk assessment is performed for a case study, in which the proposed model is used for the calculation of the evacuation curve in several scenarios. The efficiency of modelling and calculation processes highlights that the proposed model represents a valuable contribution for the probabilistic analysis of fire evacuation in large gatherings.

© Copyright: Fire Safety Engineering, Lund University. Lund 2022.

Fire Safety Engineering
Lund University
P.O. Box 118
SE-221 00 Lund
Sweden

<http://www.brand.lth.se>

Telephone: +46 46 222 73 60



HOST UNIVERSITY: Lund University

FACULTY: Faculty of Engineering, LTH

DEPARTMENT:

Department of Building and Environmental Technology,
Division of Fire Safety Engineering

Academic Year 2021-2022

Mescape. A probabilistic mesoscopic model for fire evacuation in large gatherings

Lorenzo Contini

Supervisor: Prof. Enrico Ronchi

Master thesis submitted in the Erasmus+ Study Programme

International Master of Science in Fire Safety Engineering

DISCLAIMER

This thesis is submitted in partial fulfilment of the requirements for the degree of *The International Master of Science in Fire Safety Engineering (IMFSE)*. This thesis has never been submitted for any degree or examination to any other University/programme. The author(s) declare(s) that this thesis is original work except where stated. This declaration constitutes an assertion that full and accurate references and citations have been included for all material, directly included and indirectly contributing to the thesis. The author(s) gives (give) permission to make this master thesis available for consultation and to copy parts of this master thesis for personal use. In the case of any other use, the limitations of the copyright have to be respected, in particular with regard to the obligation to state expressly the source when quoting results from this master thesis. The thesis supervisor must be informed when data or results are used.

Read and approved,



Lorenzo Contini

May 11th, 2022

Abstract (EN)

This study presents a mesoscopic model that predicts pedestrian evacuation in large gatherings with probabilistic methods. The model is based on a coarse network representation of buildings, where occupants are treated at a different scale according to their location.

A microscopic approach is used to represent people in the initial enclosure: here individual characteristics and behaviours are attributed to each occupant through random sampling from user-defined probabilistic parameter distributions, and individual timelines are used to determine the initial flow of evacuees. A macroscopic representation is implemented in the following parts of egress routes, where occupants are treated as a homogeneous crowd with uniform characteristics. The SFPE hydraulic model is used to predict movement until a place of safety.

Two automatic iterative processes are implemented within the evacuation model to address variability and uncertainty. In the first step, behavioural uncertainty is investigated by running the same evacuation scenario multiple times until results meet user-defined converge criteria based on inferential statistics. In the second step, input parameters/distributions are modified automatically to predict evacuation in different scenarios for quantitative risk assessment.

Multiple tests show good agreement between the results of the proposed mesoscopic model and a microscopic model employed for benchmarking (Pathfinder used in SFPE mode). For horizontal egress routes, the proposed tool provides detailed and accurate outputs (evacuation curves, flow rates, queue size, etc.) with short computational time. For vertical egress routes, mesoscopic predictions capture well the qualitative evolution of the egress process, but quantitative results are underestimated and necessitate additional investigation.

Lastly, a quantitative risk assessment is performed for a case study, in which the proposed model is used for the calculation of the evacuation curve in several scenarios. The efficiency of modelling and calculation processes highlights that the proposed model represents a valuable contribution for the probabilistic analysis of fire evacuation in large gatherings.

Keywords: human behaviour, crowd evacuation, mesoscopic modelling, hydraulic model, large gatherings, fire safety, performance-based design, quantitative risk assessment, consequence analysis, uncertainty analysis, probabilistic modelling.

Abstract (IT)

In questa tesi viene presentato un modello mesoscopico utile a predire l'evacuazione di edifici affollati con approccio probabilistico. Il modello si basa su una schematizzazione degli edifici a rete grossolana, in cui gli occupanti sono rappresentati con un diverso livello di dettaglio a seconda della loro posizione.

L'approccio microscopico è utilizzato per rappresentare le persone nell'ambito iniziale: qui a ciascun occupante vengono attribuite caratteristiche e comportamenti individuali attraverso un campionamento casuale da distribuzioni probabilistiche di parametri definite dall'utente; delle linee temporali individuali vengono utilizzate per determinare il flusso iniziale di occupanti. Nelle parti successive delle vie d'esodo è implementata una rappresentazione macroscopica, dove gli occupanti sono trattati come una folla omogenea di persone con caratteristiche uniformi. Il modello idraulico SFPE viene utilizzato per prevedere il movimento fino a un luogo sicuro.

Due processi iterativi automatici sono implementati all'interno del modello di evacuazione per trattare la variabilità e le incertezze sui dati di input. Nella prima fase, l'incertezza comportamentale viene esaminata ripetendo il calcolo dello stesso scenario di evacuazione più volte fino a quando i risultati soddisfano i criteri di convergenza definiti dall'utente basati sulla statistica inferenziale. Nella seconda fase, i parametri/distribuzioni di input vengono modificati automaticamente per simulare l'evacuazione in diversi scenari ai fini di una valutazione quantitativa del rischio.

Diversi test mostrano una buona corrispondenza tra i risultati del modello mesoscopico e un modello microscopico impiegato per l'analisi comparativa (Pathfinder utilizzato in modalità SFPE). Per le vie d'esodo orizzontali, lo strumento proposto fornisce risultati dettagliati e accurati (curve di evacuazione, flussi, dimensioni della coda, ecc.) in un breve tempo di calcolo. Per le vie di uscita verticali, le previsioni mesoscopiche colgono bene l'evoluzione qualitativa del processo d'esodo, ma i risultati quantitativi sono sottostimati e richiedono ulteriori indagini.

Infine, viene eseguita una valutazione quantitativa del rischio applicata a un caso di studio, in cui il modello proposto è utilizzato per il calcolo della curva di evacuazione in diversi scenari. L'efficacia dei processi di modellazione e calcolo evidenzia che il modello proposto rappresenta un valido contributo per l'analisi probabilistica dell'evacuazione da incendi in edifici affollati.

Parole chiave: comportamento umano, evacuazione della folla, modellazione mesoscopica, modello idraulico, edifici affollati, sicurezza antincendio, valutazione del rischio, analisi delle conseguenze, analisi dell'incertezza, approccio probabilistico.

Table of contents

Abstract (EN)	I
Abstract (IT)	II
Table of contents	III
List of symbols	V
List of acronyms	VII
List of figures	VIII
List of tables	XI
1 Introduction	1
1.1 Background.....	1
1.2 Aim and objectives	3
1.3 Methods	3
1.4 Limitations.....	4
2 Risk-informed fire safety engineering	5
2.1 Approaches to fire risk management	5
2.2 Advantages of probabilistic evacuation modelling.....	7
2.3 General probabilistic framework	9
3 Mesoscopic evacuation modelling of large gatherings	11
3.1 Advantages of mesoscopic evacuation modelling.....	11
3.2 Review of existing mesoscopic models	12
3.3 Proposed mesoscopic model.....	13
3.4 Application field	19
4 Conceptual and mathematical description of the proposed model	20
4.1 Model setup and deterministic run	22
4.2 Iterative runs for convergence	38
4.3 Iterative runs for the analysis of multiple scenarios	43
4.4 Consequence analysis	44
5 Application of the proposed model and discussion of the results	45
5.1 Test scenarios.....	45
5.2 Case study	60
5.3 Performance of the proposed model	71
6 Conclusion and outlook	74
Acknowledgements	76

References 77
Appendices 82
 Appendix A: Inferential statistics..... 82
 Appendix B: User manual 86
 Appendix C: Test scenarios – Setup of the evacuation models 89
 Appendix D: Case study – Modelling assumptions and inputs..... 95
 Appendix E: Case study – Fire modelling 100
 Appendix F: Case study – Setup of the evacuation models 102
 Appendix G: Case study – Quantitative risk assessment 110

List of symbols

a	[-]	Constant for SFPE hydraulic model (0.266 for metric units)
A	[m ²]	Floor area of a zone
ASET	[s]	Available safe egress time
BL	[m]	Boundary layer clearance
c	[-]	Consequences of a design scenario
CL	[%]	Confidence level
D	[pers/m ²]	Occupants' density
F	[year ⁻¹]	Frequency of N or more persons exposed to untenable conditions
F _c	[pers/s]	Component flow
F _{c,max}	[pers/s]	Maximum component flow or component capacity
F _{pres}	[pers/s]	Presentation flow
F _s	[pers/s]	Specific flow
F _{s,max}	[pers/s]	Maximum specific flow
HRR	[kW]	Heat release rate
i (subscript)	[-]	Individual number of design scenarios
j (subscript)	[-]	Individual number of occupants
k (subscript)	[-]	Individual number of nodes
k	[-]	Egress component constant
L	[m]	Distance
L _{trav}	[m]	Travel distance
n (subscript)	[-]	Individual number of simulation runs
N	[pers]	Number of persons exposed to untenable conditions
p	[-]	Likelihood of a design scenario
p _{pres}	[-]	Number of persons presenting at the exit of a zone
P ₀	[pers]	Initial number of occupants
P _{evacuated}	[pers]	Cumulative number of occupants that have evacuated a zone/node
P _{remaining} or P	[pers]	Cumulative number of occupants that are still within a zone/node
Q	[pers]	Number of persons in a queue
RSET	[s]	Required safe egress time
s	[-]	Design scenario
S	[m/s]	Adjusted walking speed (according to occupants' density)

S_{\max}	[m/s]	Unimpeded walking speed
S_x	[varies]	Sample standard deviation for variable x
t	[s]	Time
t_a	[s]	Activation time of fire suppression systems
t_d	[s]	Detection time
t_{d+n}	[s]	Sum of detection time and notification time
t_e	[s]	Evacuation time
t_{first}	[s]	Time when the first occupant flows through a component
t_{flow}	[s]	Flow time
t_{last}	[s]	Time when the last occupant flows through a component
t_n	[s]	Notification time
t_{pre}	[s]	Pre-evacuation time
t_{pres}	[s]	Presentation time
$t_{q,\text{off}}$	[s]	Time when a queue dissolves at a component
$t_{q,\text{on}}$	[s]	Time when a queue forms at a component
t_{trav}	[s]	Travel time
t_w	[s]	Waiting time
W	[m]	Measured component width
W_e	[m]	Effective component width
x	[m]	Occupant distance from the door in x direction
X	[m]	Dimension of a zone in x direction (side with door)
\bar{X} (bar)	[varies]	Sample mean for variable x
y	[m]	Occupant distance from the door in y direction
Y	[m]	Dimension of a zone in y direction
y_s	[kg/kg]	Soot yield
z	[-]	Z score (inferential statistics)
ZET	[s]	Zone evacuation time
α	[-]	Alpha value (inferential statistics)
α_g	[kW/s ²]	Fire growth rate
Δ	[s]	Standard error
Δ_d	[s]	Design standard error
ΔH_c	[MJ/kg]	Heat of combustion
Δt	[s]	Time step duration

Δt_{flow}	[s]	Flow duration
Δt_{queue}	[s]	Queue duration
μ	[varies]	Population mean for variable x
σ	[varies]	Population standard deviation for variable x
ν	[-]	Degrees of freedom (inferential statistics)
χ^2	[-]	Chi-squared value (inferential statistics)
χ_r	[-]	Radiative fraction

List of acronyms

ALARP	As low as reasonably practicable
CA	Cellular automata
CFAST	Consolidated model of Fire and Smoke Transport
CFD	Computational fluid dynamics
CR	Convergence run
DR	Deterministic run
FDS	Fire Dynamics Simulator
FRA	Fire risk assessment
FSE	Fire safety engineering
HBiF	Human behaviour in fire
NIST	National Institute of Standards and Technology
PBD	Performance-based design
PS	Path shape
QRA	Quantitative risk assessment
VBA	Visual Basic application

List of figures

Figure 1 – Approaches to fire risk management	6
Figure 2 – Example of uncertainty analysis of a QRA from (Frantzich, 1998).....	10
Figure 3 – Conceptual representation of the proposed mesoscopic approach	14
Figure 4 – Workflow for the analysis of a single risk scenario.....	21
Figure 5 – Examples of networks with a single flow	23
Figure 6 – Example of network with multiple flows	23
Figure 7 – Example of networks for stairs	23
Figure 8 – Example of a zone with its population and travel distances with/without obstacles	24
Figure 9 – Example of a zone converted into virtual nodes.....	24
Figure 10 – Adjustment of walking speed as a function of density	25
Figure 11 – Representation of individual presentation time $t_{pres,j}$ in an enclosure with automatic fire detection and notification systems	27
Figure 12 – Example of presentation flow $F_{pres}(t)$ at the door location (a) and evacuation curve $P(t)$ from a zone (b) in free flow conditions	27
Figure 13 – Example of component flow $F_{c,k}(t)$ (a) and evacuation curve $P_k(t)$ (b) at a node k in free flow conditions ($F_{c,k-1}(t) \leq F_{c,k,max}$).....	28
Figure 14 – Network representation of a node where $F_{c,k-1}(t) > F_{c,k,max}$ before queue (a), during queue formation (b) and during queue reduction (c)	29
Figure 15 – Example of outflow $F_{c,k}(t)$ (a) and evacuation curve $P_k(t)$ (b) at a node k when a queue forms ($F_{c,k-1}(t) > F_{c,k,max}$) which dissolves before the end of the flow ($t_{k,q,off} < t_{k,last}$)	30
Figure 16 – Example of outflow $F_{c,k}(t)$ (a) and evacuation curve $P_k(t)$ (b) at a node k when a queue forms ($F_{c,k-1}(t) > F_{c,k,max}$) which dissolves at the end of the flow ($t_{k,q,off}$ $= t_{k,last}$).....	30
Figure 17 – Examples of queue curve $Q_k(t)$ at a node k which dissolves before the end of the flow ($t_{k,q,off} < t_{k,last}$) (a) or at the end of the flow ($t_{k,q,off} = t_{k,last}$) (b)	31
Figure 18 – Combined representation of SFPE fundamental diagrams of $F_s(D)$ and $S(D)$ for horizontal movement. The dotted lines represent the graphical derivation of S from F_s	32
Figure 19 – Example of corridor without doors (a) and evacuation curve through it (b).	33
Figure 20 – Example of corridor with doors	33
Figure 21 – Example of transition from a door to a corridor (node 1 \rightarrow node 2) and from a corridor to a door (node 2 \rightarrow node 3) where the maximum capacity of the latter is reached	35

Figure 22 – Example of evacuation curve at different locations along a corridor with two doors, where the exit is narrower than the entrance.	35
Figure 23 – Example of a zone followed by a transit.....	36
Figure 24 – Example of a stair with two doors (a) and evacuation curve through it (b) where the exit is narrower than the entrance.	37
Figure 25 – Example of a sample of ZETs obtained from 500 repeated runs of the evacuation model for a single scenario.....	40
Figure 26 – Example the evolution of the sample mean <i>ZET</i> (continuous line) and of the 95% confidence interval (dotted lines) calculated after every model run.	40
Figure 27 – Example the evolution of the standard error Δ which decreases as the number of simulations n increases.....	41
Figure 28 – Example of a sample of evacuation curves obtained from 50 repeated runs of the evacuation model for a single scenario (continuous thin lines), mean evacuation curve (continuous thick line), and the design evacuation curve for the 99 th percentile (dashed line).....	42
Figure 29 – Example of a group of evacuation curves obtained for the same node of a network from 10 different evacuation scenarios with variable initial occupant density.....	43
Figure 30 – Example of evacuation curve at different locations along an egress path in case of zero consequences (a) and undesired consequences (b).....	44
Figure 31 – Scenario T1 – Spatial distribution of occupants within the zone ($D = 0.5$ pers/m ²).....	49
Figure 32 – Scenario T1 – Uniform distribution of individual walking speed S_j [m/s].....	49
Figure 33 – Scenario T1 – Log-normal distribution of individual pre-evacuation time $t_{pre,j}$ [s].....	49
Figure 34 – Scenario T1 – Pathfinder geometry (a) and mesoscopic network (b).....	50
Figure 35 – Scenario T1 – Evacuation curves obtained with the proposed mesoscopic model and Pathfinder, for six combinations of occupant density D [pers/m ²] and door width W [m]	50
Figure 36 – Scenario T2 – Pathfinder geometry (a) and mesoscopic network (b).....	52
Figure 37 – Scenario T2 – Evacuation curves obtained with the proposed mesoscopic model and Pathfinder, for four combinations of door and corridor width.	52
Figure 38 – Scenario T2 – Results from 10 randomly-chosen Pathfinder simulations representing the flow rate of occupants through the first door.....	53
Figure 39 – Scenario T2 – Results from 10 randomly-chosen Pathfinder simulations representing the flow rate of occupants through the second door	53
Figure 40 – Scenario T2 – Results from 10 randomly-chosen Pathfinder simulations representing the occupant density in the corridor.....	54

Figure 41 – Scenario T2 – Results from 10 randomly-chosen Pathfinder simulations representing the average walking speed in the corridor	54
Figure 42 – Scenario T3 – Pathfinder geometry (a) and mesoscopic network (b).....	55
Figure 43 – Scenario T3 – Evacuation curve obtained with the proposed mesoscopic model and Pathfinder, for a transit	55
Figure 44 – Scenario T4 – Pathfinder geometry (a) and mesoscopic network (b).....	56
Figure 45 – Scenario T4 – Evacuation curves obtained with the proposed mesoscopic model and Pathfinder, for a stair with 19.1 cm (7.5 in) risers and 25.4 cm (10 in) treads	57
Figure 46 – Scenario T4 – Evacuation curves obtained with the proposed mesoscopic model and Pathfinder, for a stair with 16.5 cm (6.5 in) risers and 33 cm (13 in) treads.....	57
Figure 47 – Scenario T5 – Pathfinder geometry (a) and mesoscopic network (b).....	59
Figure 48 – Scenario T5 – Evacuation curve obtained with the proposed mesoscopic model and Pathfinder, for two groups of occupants merging for simultaneous and phased evacuation.....	59
Figure 49 – Case study – Floor plans and cross section of the food court.....	61
Figure 50 – Case study – Event tree.....	63
Figure 51 – Case study, Network 1 – Evacuation curve obtained with the proposed mesoscopic model and Pathfinder. The curve represents the sum of the occupants of zones 1, 2 and 3	65
Figure 52 – Case study, Network 2 – Evacuation curve obtained with the proposed mesoscopic model and Pathfinder	65
Figure 53 – Case study, Network 3 – Evacuation curve obtained with the proposed mesoscopic model and Pathfinder	66
Figure 54 – Case study, Network 4 – Evacuation curve obtained with the proposed mesoscopic model and Pathfinder	66
Figure 55 – Case study, Network 5 – Evacuation curve obtained with the proposed mesoscopic model and Pathfinder	67
Figure 56 – Case study, Network 6 – Evacuation curve obtained with the proposed mesoscopic model and Pathfinder	67
Figure 57 – Case study, Network 1 – Evacuation curve obtained with the proposed mesoscopic model and Pathfinder. The curve represents the occupants of zone 1	68
Figure 58 – Case study, Network 1 – Evacuation curve obtained with the proposed mesoscopic model and Pathfinder. The curve represents the occupants of zone 2	68
Figure 59 – Case study, Network 1 – Evacuation curves obtained with the proposed mesoscopic model for 10 evacuation scenarios presented in Table 9.	70

Figure 60 – Case study, Network 1 – FN curve for the occupants of the 2 nd floor.....	70
Figure 61 – Representation of a confidence interval centered at X with a confidence level of approximately 95%. Figure from (Devore, 2012).....	83
Figure 62 – Representation of one hundred confidence intervals with confidence level of approximately 95%. Asterisks identify intervals that do not include the population mean μ . Figure from (Devore, 2012).....	84
Figure 63 – Case study – Customer visits to similar facilities located in the analysed train station. Figure from www.google.com	96
Figure 64 – Case study – Heat release rate curves	97
Figure 65 – Case study – Timeline of the evacuation process in case of success of the automatic detection and notification system	99
Figure 66 – Case study – Timeline of the evacuation process in case of failure of the automatic detection and notification system	99
Figure 67 – Case study – 3D view of CFAST.....	100
Figure 68 – Case study – Smoke layer temperature obtained with CFAST	101
Figure 69 – Case study – Smoke layer height obtained with CFAST.....	101
Figure 70 – Case study – 3D views of Pathfinder model.....	103
Figure 71 – Case study – 2D views of Pathfinder model.....	104
Figure 72 – Case study – Simplification of the building geometry into zones and nodes	105

List of tables

Table 1 – Maximum specific flow $F_{s,max}$, unimpeded walking speed S_{max} and constant k for different types of egress components from (Gwynne & Rosenbaum, 2016)	37
Table 2 – Values of z for commonly used percentiles	42
Table 3 – Input point values for test scenarios.....	47
Table 4 – Input distributions for test scenarios	47
Table 5 – Boundary layer clearance from (Gwynne & Rosenbaum, 2016).....	47
Table 6 – Values of α and $z_{\alpha/2}$ for commonly used confidence levels.....	83
Table 7 – Case study – Design occupant loads and associated probability	96
Table 8 – Case study – Design fire scenarios.....	97
Table 9 – Case study – Design evacuation scenarios.....	98
Table 10 – Case study – ASETs obtained with CFAST	100
Table 11 – Case study, Network 1 – Consequences of risk scenarios	110
Table 12 – Case study, Network 1 – Likelihood of risk scenarios.....	111
Table 13 – Case study, Network 1 – Consequences and frequency of risk scenarios	112

1 Introduction

1.1 Background

Fire safety engineering has made great advancements over the last few decades, and performance-based design (PBD) has become a key methodology to assess and implement fire safety into the built environment. Calculation models are an essential tool that allows designers to predict fire development, smoke spread, occupant evacuation, structural response, and the interaction between these processes.

Meanwhile, fundamental advancements in computing capability have paved the way for the development of sophisticated computerised tools, such as fire models based on computational fluid dynamics (CFD), evacuation models based on a microscopic representation of occupants, or structural models based on finite element modelling (FEM). Since they rely on first principles, advanced models are widely applicable and provide deeper insight into physical phenomena than simpler empirical correlations. Therefore, in the fire engineering community we are witnessing a move towards refined computerised tools (Baker et al., 2022; Lovreglio, Ronchi & Kinsey, 2020), which may be often preferred not only for the design of exceptional buildings but also for ordinary applications.

Since high model sophistication leads to high computational cost, often a limited number of design scenarios can be investigated with advanced simulators in order to cope with project constraints. Consequently, performance-based designs are often assessed with deterministic approaches. However, research has demonstrated that deterministic evaluation methods of complex phenomena such as fire and human behaviour involve large uncertainties, and a priori modelling can lead to remarkable errors in the prediction of the physical quantities of interest (Rein et al., 2009). This can be due to a number of reasons, including: a limited understanding of physical phenomena and their underlying science, which is reflected in model formulation and simplifying assumptions (model uncertainty); difficulty in collecting data from experimental tests and in extrapolating laboratory results to real world conditions (measurement uncertainty); the scarcity of data bases from real accidents and the stochastic nature of many design parameters (input uncertainty). When it comes to egress, behavioural uncertainty adds to the list, making evacuation modelling one of the most challenging tasks in a performance-based design (Averill, 2011; Ronchi, Reneke & Peacock, 2014). In fact, even if accurate engineering models and data sets are available, a deterministic approach is still unable to cope with the variability associated with combustion phenomena or populations of persons. For example, it would always be impossible to predict the first item ignited, its location, the exact number of occupants in a room at a given time, a person's walking speed or how quickly he/she will react to fire cues, etc. These are random variables in the real world.

An alternative approach is to work in a probabilistic environment. With quantitative risk analysis (QRA) complex systems are investigated systematically taking into account the probabilities of different scenarios and the uncertainties that characterise stochastic variables. For this purpose, many advanced evacuation models allow to consider variability in the form of input parameter distributions from which the model draws random values at every run. Nevertheless, the output of a single simulation is deterministic: it only represents one possible outcome among the infinite combinations of stochastic variables. Behavioural uncertainty has to be addressed by running

multiple times the same scenario, but when working with advanced simulation models the set setup, calculation and postprocessing of hundreds of simulations may represent labour-intensive and time-consuming tasks. The challenge is how to handle uncertainties in a practical manner.

In cases where empirical models are applicable, simpler simulation tools can be used in combination with probabilistic methods to cover uncertainties and get a better representation of the safety level. The downside of this technique is that analytical/empirical modelling provides coarser results than sophisticated simulators, and this might prevent engineers to capture all the physical phenomena that contribute to the real scenario outcome.

A number of probabilistic methodologies have been developed in previous research, such as in (Chen & Mao, 2018; Kong et al., 2014; Van Weyenberge et al., 2016). However, in some studies the evacuation process is represented in a simplistic way where the only output of the model is the required safe egress time (RSET). In other cases, the analysis requires the use of deterministic advanced models supported by analytical and numerical models, which demand to users a high level of competency and engineering time. To the knowledge of the author, research has not yet been conducted to develop a simple probabilistic tool which is able to predict the whole evacuation curve (number of occupants remaining within an enclosure as a function of time).

In the light of these considerations, fire safety engineers often face the conundrum of choosing between advanced computer models used in a deterministic manner, which provide refined but uncertain results, or simpler empirical models that produce coarser outputs with quantifiable uncertainty. The purpose of this study is to address this problem, applied to evacuation modelling, from a third perspective. The aim is to develop a tool for the analysis of egress which is simple enough to be easily implemented in a probabilistic environment, allowing users to account for probability and uncertainty, but sufficiently refined to capture all the significant quantities that characterise the evacuation process in large gatherings.

The methodology that is proposed to satisfy this need is mesoscopic modelling, which is a technique that incorporates the feature of both the macroscopic and microscopic tools that are commonly used by engineers to analyse the evacuation process from building fires. Macroscopic models treat occupants as a homogeneous and continuous flow moving along a sequence of egress components as a fluid in a hydraulic network. Since only average quantities are used (e.g., density, flow, speed, etc.), engineering calculations represent an efficient design tool, but involve many simplifications that may lead to coarse results. The second category of models treats building occupants at microscopic level. People are represented as autonomous agents that can move independently throughout the geometry, considering individual characteristics of the population. Thus, the results of microscopic computer models are characterised by a greater level of detail at the cost of greater simulation time and amount of output data (Hurley et al., 2016; O'Connor et al., 2019).

A number of mesoscopic models have been developed to predict pedestrian evacuation (Dressler et al., 2010; Hanisch et al., 2003; Shi, Lee & Ma, 2018; Teknomo & Gerilla, 2008; Tolujew & Alcalá, 2004; Xiong, Tang & Zhao, 2013; Zambrano et al., 2020). However, in most cases the two approaches are layered and run in parallel in order to predict the optimal evacuation strategy which is not necessarily the aim of probabilistic performance-based design. In other cases, the microscopic component is based on a grid-representation of the geometry, which comes with several limitations in terms of density predictions. The idea behind this study is to develop a mesoscopic model based on a network representation of buildings, where the microscopic and

macroscopic calculations are executed in different regions. This technique will provide accurate predictions of the initial outflow and the formation of queues in the parts of the building characterised by the largest number of occupants and the presence of hazardous conditions. In the following parts of the building, where no direct threat to life is foreseen, a coarser level of detail will reduce computational time and allow integration in the probabilistic environment.

1.2 Aim and objectives

The aim of this study is to develop a probabilistic evacuation model for quantitative fire risk assessment. The tool will be designed to perform probabilistic analyses in order to address the problem of variability and uncertainty about initial conditions and human behaviour.

Therefore, the model proposed in this study is developed to meet the following objectives:

- Allow modellers to input distributions of stochastic/uncertain variables (section 3.3).
- Produce outputs that are not limited to RSET, but also include information about densities, flowrates, queuing times, and all the crucial variables necessary to correctly predict the evacuation process in large gatherings (section 4.1).
- Automatically perform an ideal number of repeated simulations using random sampling techniques until model predictions converge, and produce and plot design output data to be used for consequence analysis (section 4.2).
- Automatically reiterate the calculation for a range of evacuation scenarios for quantitative risk assessments and uncertainty analyses (section 4.3).

Reliability, ease of use and computing speed will be essential for a tool that aims to facilitate the use of probabilistic methodologies for practical engineering problems. Hence, these characteristics will be tested and illustrated through the application of the proposed model to a case study (chapter 5).

1.3 Methods

In order to meet the objectives defined in the previous section, this study is conducted according to four main stages.

The first step consists in the definition of the probabilistic framework in which the proposed evacuation model is intended to be used. Therefore, chapter 2 provides an overview of the approaches to risk and uncertainty that are commonly used in fire safety engineering practice and highlights the context in which the evacuation model is developed. This clarifies how it should work and which outputs are required for future integration with other sub-models of the probabilistic framework.

Next, the mesoscopic approach to evacuation modelling is investigated. A literature review is carried out in chapter 3 to analyse existing mesoscopic models. This is then used as a basis to formulate the conceptual description of the proposed method, as well as to identify its key components and its ideal application field.

Furthermore, the workflow and the mathematical description of the proposed mesoscopic evacuation model are established, as presented in chapter 4. Consequently, the model is implemented using Visual Basic for Application in Microsoft Excel.

Finally, a benchmarking study is carried out to assess how the model performs and compares to microscopic approaches. Pathfinder (Thunderhead Engineering, 2021) is used for this purpose. Both models are applied to five basic scenarios and to a complex facility. In the second case, the whole QRA process is also performed with the mesoscopic tool. The results and their discussion are presented in chapter 5.

1.4 Limitations

The evacuation model that will be developed with this study is meant to be used as a sub-model in a probabilistic framework, where other sub-models (not within the scope of this work) are used to predict the fire dynamics and the risk to the life of occupants. Since probabilistic fire modelling is typically performed with analytical/zone models, which are applicable to ordinary fire compartments, the evacuation model is intended to be used in the same context. This means that it is initially developed to simulate the evacuation from enclosures of limited size and regular shape and layout, where the formation of a smoke layer is possible, hence falling within the application field of empirical fire models.

Fire development and occupants' evacuation are coupled phenomena in a real fire emergency. For example, the smoke spread has an influence on evacuees' path and physical capabilities, while the movement of people modifies the architectural state (e.g., door position), hence fire development and smoke spread (O'Connor et al., 2019). Nevertheless, at this initial stage of model development, coupling between smoke and evacuation will not be implemented as an automatic feature. In fact, life safety assessments will be performed under the conservative assumption that injury will occur as soon as the smoke layer falls below head height (despite people might still be able to self-evacuate in a real emergency), therefore it is not necessary to modify occupants' behaviour based on smoke characteristics. This simplification is useful when working in a probabilistic environment, where coupling hundreds of fire scenarios with hundreds of evacuation scenarios may be a challenging task. Moreover, in a probabilistic framework, fire modelling is likely to be implemented with analytical or zone models which only provide average smoke characteristics; hence the prediction of toxicity would still be affected by large uncertainties.

As for the theoretical development of the model, there will be no efforts in trying to formulate new theories for the analysis of occupants' movement and human behaviour. The evacuation model will be developed through the implementation of existing methodologies into a probabilistic environment.

Lastly, fictitious but realistic input values will be used to test the tool. The scope of the case study will be to illustrate the potential of the model and perform a pseudo validation and verification, rather than producing a fire safety design of the analysed building.

2 Risk-informed fire safety engineering

2.1 Approaches to fire risk management

Fire is one of the risks that originate from the built environment, having the potential of causing undesired consequences on something valuable, such as loss of life or health of occupants, property and goods, the environment, the continuity of production or critical societal functions, or cultural heritage. Fire safety engineers work to reduce fire risk through its identification, evaluation against acceptance criteria, and eventually reduction it by means of elimination of some hazards (preventive measures) and mitigation of likelihood or consequences (active and passive protection). This risk management process can be undertaken through alternative approaches, which differ by the treatment of the three essential information that describe risk, namely 1) what could happen i.e. risk scenarios, 2) the adverse consequences on something valued by stakeholders, and 3) the likelihood of occurrence (Kaplan & Garrick, 1981).

1) Prescriptive design. In most ordinary situations, safety experts implement a set of fire protection measures as mandated by relevant regulations. Designers only need to estimate ‘what can go wrong’ through a qualitative analysis of the facility and its fire hazards. Likelihood and consequences do not need to be calculated explicitly because it is assumed that deemed-to-satisfy measures will reduce fire-related risks to acceptable levels.

2) Performance-based design (PBD). When buildings do not comply entirely with prescriptive regulations due to project constraints or extraordinary characteristics, or when an optimisation of fire safety measures is desired, engineers can implement fire safety with a performance-based approach. Many PBD codes worldwide (e.g., in Sweden, Italy, UK, USA, Canada, Australia, New Zealand, Japan) specify the expected building performance without imposing how the objective should be met (Hadjisophocleous & Benichou, 2000). A consolidated way of verifying the adequacy of the alternative design is to predict the response of the physical sub-system of interest with engineering calculations about fire growth, smoke spread, evacuation, effect of active protection systems, structural response, or a combination of those. The physical quantities can be treated further to express loss in terms of injury to health. In this case, also the second component of the risk ‘How bad are the consequences of a scenario’ is addressed. In order to perform the consequence analysis, engineers need to select a manageable number of ‘design scenarios’ among the infinite ways in which the fire risk can manifest itself. This task can be done with two approaches: deterministic or probabilistic. The treatment of the last component of risk – likelihood – changes according to the chosen methodology.

2a) In **deterministic PBD** a limited number of scenarios is selected for the quantitative analysis. To guarantee that they are representative of the infinite range of fire incidents, the ‘worst credible case’ is typically used (Hurley & Rosenbaum, 2015). Hence, design scenarios are built upon conservative assumptions for many input parameters, leading to the worst sequence of events that can be reasonably expected. Often it is possible to imagine worse circumstances, but it is estimated that their likelihood is so low that worse scenarios are meaningless. Therefore, probabilities are only considered implicitly. If the consequences of few quasi-worst design scenarios are acceptable, it is assumed that the design can mitigate the effects of any (reasonable) fire that can potentially occur in the facility. Also in this case, risk is not quantified explicitly.

2b) With **probabilistic PBD** the large range of possible fires is discretized into a manageable set that covers the whole spectrum of potential outcomes. This is typically done with event trees i.e., systematic logical models that help engineers to identify all the important combinations of elementary events, where each branch represents one design scenario (s_i). Next, the consequences (c_i) and the likelihood (p_i) of each scenario are estimated using qualitative, semi-quantitative or quantitative methods. In a quantitative risk analysis (QRA), consequences are calculated through engineering models, while likelihoods are determined by multiplication of the frequency of the initiating event with the conditional probabilities of the following basic events. Finally, the total risk can be presented in the form of a single indicator (e.g., average societal risk, individual risk) or through frequency-consequences distributions (e.g., FN curves). The acceptance criterion of the design solution is risk itself, which is now described quantitatively in all the components of the triplet (s_i, p_i, c_i). Typically, the primary objective is to reduce risk below a tolerable threshold for society and the secondary objective is to lessen it further ‘as low as reasonably practicable’ (ALARP).

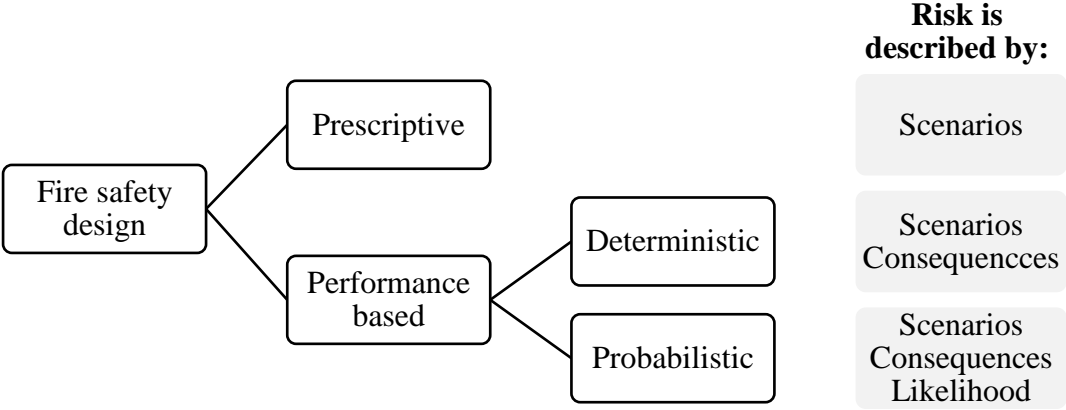


Figure 1 – Approaches to fire risk management

2.2 Advantages of probabilistic evacuation modelling

Despite few designs are based on a formal quantitative fire risk assessment due to the complexity of the task, understanding of risk through its explicit quantification represents the optimal way to inform fire safety decisions (Frantzich, 1998). In fact, the probabilistic approach brings relevant advantages to performance-based design, in particular when it involves evacuation modelling of large crowds. This section highlights why.

The prescriptive approach to fire risk management is practical for designing standard types of buildings for which the codes were derived. However, prescriptive regulations may prove themselves quite inflexible when applied to non-ordinary architectures, such as innovative structures or assemblies with challenging occupant densities.

Even though in some circumstances those buildings may comply with prescriptive rules, designers should reflect on how well deemed-to-satisfy strategies perform in complex design situations. In fact, as highlighted by (Spinardi, Bisby & Torero, 2016), code requirements often originate from a stratification of construction traditions, common-sense, and experience of past incidents rather than on scientific understanding of fire risk.

Hence, on one hand, the mere implementation of prescriptions may not necessarily guarantee the expected level of fire safety, especially when code updates do not keep the pace with innovations in the built environment. For example, can we confidently assume that prescriptive provisions calibrated for standard multi-room compartments guarantee adequate safety in an open-space architecture with densely populated areas?

On the other hand, large margins of safety may be incorporated in prescriptive design values to compensate for the variability of building types and occupancy. For instance, a wide-scale survey conducted in Switzerland demonstrated that codified values for occupant loads of retail stores are usually very high and do not reflect realistic conditions (De Sanctis, Moos & Aumayer, 2019). Therefore, conservativeness represents another limit of prescriptive design, as it can lead to redundant fire protection provisions and sub-optimal investment of resources.

In any case, since the building performance is not measured, designers and code officials have no means to know how the ‘off-the-shelf’ fire safety strategy fits the building of interest and its specific risks. This may be critical when the safety of many people is involved.

Performance-based design and engineered ‘made-to-measure’ fire safety strategies represent an opportunity to overcome projects constraints, support innovation in the built environment, optimise the use of resources invested in fire protection, and gain confidence in the design of non-ordinary facilities. Nevertheless, deterministic PBD leads to few challenges too, mainly originating from the uncertainties that characterise several steps of the design process (Magnusson, Frantzich & Harada, 1995).

First, worst credible scenarios need to be defined on a project basis, and expert judgment is often needed to decide which conditions are to be considered too unlikely. For example, if a prescriptive occupant load is deemed unrealistic, which evacuation scenario should be represented in a deterministic PBD? Should engineers consider the largest number of occupants expected over one year? Should they use some percentile of the probability distribution? Which percentile? Answering these questions is not trivial, and stakeholders with different objectives

and perceptions may define differently what is ‘satisfactory’. As a result, the level of safety may vary according to the parts involved in the design process (Spinardi, Bisby & Torero, 2016).

Furthermore, input parameters are likely to be affected by 1) epistemic uncertainty that originates from a lack of knowledge about some characteristics of the analysed system, and/or 2) aleatory uncertainty due to variability and randomness of real-world phenomena (Notarianni & Parry, 2016). Although the first can be reduced through the collection of additional knowledge, the latter cannot be eliminated. This can produce a large scatter in engineering calculations (Rein et al., 2009), in particular when engineers need to predict human behaviour (Averill, 2011).

A common way of counterbalancing the uncertainties in a deterministic analysis is to use precautionary principles (i.e., conservative design values, safety margins, safety factors, etc.) so that fire safety engineering (FSE) calculations are verified under conservative assumptions. Nevertheless, as in prescriptive design, it is not possible to determine if these precautions are conservative enough, nor if the subsequent extra costs are justified by a proportional reduction of risk. In fact, as highlighted in (Hopkin, Van Coile & Lange, 2017), FSE is a relatively young field of science and not enough feedback has yet been gained from low-probability fires in non-ordinary designs, where PBD is typically applied. Thus, it is not possible to assess if commonly agreed deterministic criteria and safety factors are sufficiently stringent to reduce risk to acceptable levels.

All these difficulties may be overcome with quantitative risk analysis. The first advantage of using the probabilistic approach is that designers can measure risk, hence verify objectively the effectiveness of fire protection measures. This also allows to find the most cost-effective fire safety strategy and guide investments of resources that are scarce so that a balanced level of safety is guaranteed in all domains of society (e.g., deriving from natural disasters, man-made technologies, diseases, conflicts, etc.). For instance, using ‘de minimis criterion’, resources are spent on fire safety measures until fire-related risks fall below the societal threshold; when this goal is reached, further resources are allocated to the reduction of other sources of risk.

The second benefit of QRA is that also uncertainty can be treated explicitly. On one hand, uncertainty about design scenarios is resolved using event trees. On the other hand, uncertainty about stochastic parameters can be investigated with sensitivity studies, where model inputs are represented by statistical distributions rather than single values. It is even possible to treat branch probabilities as uncertain parameters using the ‘extended QRA’ method described in (Frantzych, 1998). Therefore, probabilistic PBD is particularly useful to analyse design situations characterised by large uncertainties that may have a relevant impact on engineering calculations. For example, this is of particular importance in the prediction of evacuation modelling, where the variability of human behaviour plays an important role in the prediction of the egress performance (Ronchi, Reneke & Peacock, 2014; Tavares & Ronchi, 2015).

Given the background provided so far, this study aims to promote the use of quantitative risk assessment methods in the context of evacuation modelling. Furthermore, this work will focus specifically on large facilities where the total number of occupants can vary greatly over opening hours. This is because uncertainty about the initial conditions of an emergency scenario and the specificities of modelling large crowds add complexity to the problem and will highlight the advantages of using a probabilistic approach to egress calculations.

2.3 General probabilistic framework

The design method proposed in this study is intended to be used for probabilistic performance-based designs that address life safety of people exposed to building fires. The suggested approach is to combine the of mesoscopic evacuation modelling with QRA methods to 1) analyse a wide range of evacuation scenarios in large gatherings (consequence analysis) and 2) quantify uncertainty in engineering predictions (uncertainty/sensitivity analysis). The general probabilistic framework is described in this section.

The first step of the process consists in the creation of an event tree that includes a complete set of fire and evacuation scenarios that may occur in a facility, also considering the effect of fire protection systems and their potential failure. Next, likelihoods and unwanted consequences are calculated for each scenario. The final goal is to present the fire risk of the facility in the form of a FN curve which represents the frequency F of having N or more persons exposed to untenable conditions generated by a fire in the building (Tehler, 2015).

The current study focuses on consequences analysis i.e., the calculation of N for every scenario of the event tree. This is done by comparing the time necessary to evacuate a specified area in the building (Required Safe Egress Time – RSET [s]) with the time at which untenable conditions occur (Available Safe Egress Time – ASET [s]). The condition $RSET = ASET$ is taken as the limit state function (Frantzich, 1998). If $ASET < RSET$ the enclosure becomes untenable before evacuation is completed, hence the fire safety strategy fails. When this occurs, the unwanted consequences of the risk scenario are quantified by calculating the number of occupants N that are still in the enclosure when ASET is reached.

The tenability criterion used in this study is the zero-exposure method, which assumes that occupants escape in undisturbed air below the hot smoke layer without being directly exposed to combustion products and heat (ISO/TR 16738 : 2009). As a consequence, it is assumed that smoke does not have an impact on human behaviour i.e. it neither affects people walking speed nor route choice (Purser, 2010). Hence, fire and evacuation calculations are decoupled.

ASET is defined as the time when the smoke layer reaches 2 m above floor level or a threshold temperature of 200 °C that can cause dangerous radiative heat fluxes (Poh, 2010). These conditions can be calculated with a fire model. Although the fire component is characterised by uncertainty (e.g., related to ignition sources, fire growth rate, type of combustion, yields of byproducts, etc.), in this study fire characteristics will be treated deterministically as the main focus is probabilistic modelling of evacuation.

RSET and N are calculated with the proposed evacuation model. Since the prediction of the egress of large crowds may be affected by the variability associated with the stochastic nature of human behaviour, the model integrates a microscopic representation of the crowd. This allows to account for individual attributes through parameter distributions (e.g., individual walking speed, pre-evacuation time, exit choice, etc.). Using a probabilistic approach, the evacuation model samples the attributes of every occupant, calculates their individual evacuation time, and generates the evacuation curve that represents the egress process of the population. Since quasi-random sampling methods may produce a different result at every run, the calculation is repeated iteratively for the same model setup (i.e., scenario) until convergence is reached. Then, inferential statistics are used to derive a design curve i.e., a conservative curve among the spectrum of results generated before convergence is achieved.

This process is repeated for every scenario of the event tree, and finally, the ensemble of triplets of scenarios, likelihood and consequences is used to produce the FN curve that represents the fire-related risk to which people in the facility are exposed.

Further analysis can address the effect of uncertainties on the final FN curve. So far, both the likelihood of tree branches and the model inputs used in the consequence analysis are deterministic. However, the calculation of likelihoods and consequences can be repeated multiple times for the same fire scenario using input parameter distributions (uncertainty/sensitivity analysis). When this is extended to the whole event tree, each iteration will produce a new FN curve, and the ensemble of curves expresses the confidence in the QRA prediction (Figure 2) as described in (Frantzich, 1998).

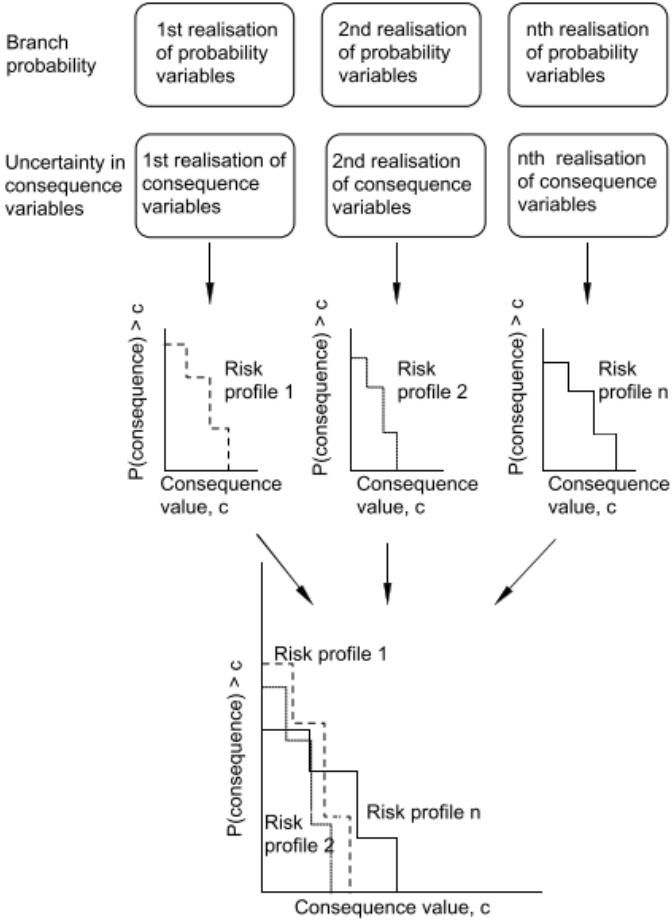


Figure 2 – Example of uncertainty analysis of a QRA from (Frantzich, 1998)

3 Mesoscopic evacuation modelling of large gatherings

3.1 Advantages of mesoscopic evacuation modelling

The general probabilistic framework presented earlier suggests two essential features required to an evacuation model for integration in QRAs of large gatherings.

The first one is computational efficiency for probabilistic analysis. In fact, the proposed approach requires to perform hundreds or thousands of repeated runs of the model to 1) reach the convergence of results for each scenario towards an average predicted output value 2) perform the consequence analysis for many branches of the event tree, and 3) perform the uncertainty analysis for uncertain parameters (for a single scenario or for the whole event tree).

The second feature is accuracy of egress calculations in a wide spectrum of representative occupancy conditions. In fact, given the probabilistic framework, the model should be used to investigate wide ranges of evacuation scenarios e.g., from low to high occupant densities.

Two families of tools are commonly used to predict building evacuation (O'Connor et al., 2019).

- 1) Hand-based engineering calculations or computer models that treat building occupants at a **macroscopic** level. In this case, people are represented collectively through average attributes and move as a homogeneous and continuous flow along a sequence of egress components. At the nodes, empirical rules apply and the flow is modified according to the components' characteristics, just like what occurs to a fluid moving through a hydraulic network (Gwynne & Rosenbaum, 2016; Predtechenskii & Milinskii, 1978).
- 2) Computer simulation tools that treat building occupants at a **microscopic** level. With this approach people are represented as autonomous agents that move independently throughout the geometry according to individual physical and behavioural characteristics (Kuligowski, 2016).

However, neither of the two approaches covers both the aforementioned features required for probabilistic modelling of large gatherings.

On one hand, engineering calculations are performed with a set of empirical equations that can be easily integrated in a probabilistic framework, as for example in (Chen & Mao, 2018). Nonetheless, the simplified representation the evacuation process mostly ignores the variability people attributes and in turn may lead to error in the outcome prediction (Kuligowski, 2016). Purser and Gwynne proposed a method to account indirectly for pre-evacuation time distributions while working with a macroscopic approach, and suggested to determine RSET as the worse evacuation time in two extremes conditions: 1) when the building is sparsely populated, hence egress is governed by the free flow of the last few occupants responding to the emergency, and 2) when the building is densely proposed, thus congestion dominates the evacuation process since the early stages of movement (Purser & Gwynne, 2007). As a consequence, this conservative method leads to gross predictions when an average occupant density is expected i.e., the flow is not entirely unconstrained nor exit-controlled. Therefore, using the macroscopic approach is not ideal in probabilistic studies where risk analysts want to investigate many evacuation scenarios and predict accurately the formation of queues.

On the other hand, microscopic models are suitable for the analysis of complex evacuation patterns and congestion, as the formation of queues and occupant flows are not parameters imposed by the engineer prior to the calculation but rather emergent outcomes i.e., an output of the model. Moreover, computerised evacuation models can be coupled dynamically with fire models to account for the effect of fire-induced conditions on evacuees' performance (O'Connor et al., 2019). The downside of advanced simulation tools is that often they are computationally expensive for probabilistic applications (Lord et al., 2005). In fact, tracking every agent while accounting for interactions between people and the environment (e.g., speed adjustment, collision avoidance, lane formation, bottlenecks, etc.) may come at the cost of greater simulation time, which adds up to the increased time for the construction of the simulation domain and for post-processing output data. Moreover, when microscopic are used, the same scenario must be simulated multiple times to cover the behavioural uncertainty that stems from the pseudo-random sampling of the individual characteristics of the agents.

A number of probabilistic methodologies using microscopic models have been developed in previous research where the computational cost is reduced using surface modelling (Van Weyenberge et al., 2016) or fine grid evacuation models are used in combination with fuzzy modelling (Kong et al., 2014). However, unless specific tools are developed for this purpose, the use of these techniques requires modellers to have a robust background in the fields of probability theory and numerical analysis, and it might be not viable to integrate these approaches it in fire safety engineering practice.

Since the aim of this study is to develop a probabilistic evacuation model that 1) can be easily implemented by fire safety engineers in quantitative risk analyses, and 2) predicts accurately the evacuation dynamics in many density conditions, the best features of macroscopic and microscopic approaches are combined in a mesoscopic model i.e., a hybrid tool that covers both scales, integrating individual diversity into crowd movement.

3.2 Review of existing mesoscopic models

The combination of macroscopic and microscopic approaches is common in the field of traffic analysis, where the movement of vehicles in large-scale applications is represented in terms of hydraulic flows, but the vehicles are tracked independently and characterised by individual behavioural rules (Ronchi et al., 2017). Few research efforts have extended the mesoscopic approach to pedestrian dynamics and building evacuation. A review of the main research efforts in this field is given in this section.

Hanisch, Tolujew et al. developed a mesoscopic model to predict pedestrian flows in public facilities (e.g. train stations, airports and shopping centres) and monitor the building performance in real-time. Individuals are represented by groups of pedestrians with their own characteristics (i.e., travel path and walking speed) that flow as a fluid through a coarse network representation of space. Since the model is developed for ordinary usage of buildings, it is assumed that free movement occurs independent of population density. The model is implemented with VBA (Visual Basic for Application) in Microsoft Excel and produces plots of the number of occupants in a part of the network as a function of time (Hanisch et al., 2003; Tolujew & Alcalá, 2004).

Teknomo and Gerilla proposed a mesoscopic model where the space is represented as an ensemble of large cells that can contain multiple agents, in contrast with typical microscopic

models where each person occupies a single cell. This reduces the computational time to track persons inside the grid. In each cell, occupants are still tracked individually, and a probabilistic approach is used to determine their next move. Interactions are represented by speed-density correlations instead of common collision algorithms. The output is a coarse spatial representation of the crowd while it navigates the floor plan (Teknomo & Gerilla, 2008). Shi, Lee and Ma adopted a similar technique with small cells close to the exits and large cells further away. To optimise computations, they treat the crowd as a continuum: instead of tracking individual agents, the model computes density flows between cells (Shi, Lee & Ma, 2018).

Dressler et al. combined macroscopic network flow approaches with a microscopic cellular automata system. The macroscopic algorithm is used to generate an ideal evacuation plan that directs evacuees along the exit path that minimises the total evacuation time. The optimal routing strategy is then used as an input of the microscopic algorithm. This calculates local crowd conditions, and then updates each agent's movement based on a set of transition rules that reflect individual behaviour. If the first step was not done, agents would only move according to locally optimal decisions (e.g. based on a potential field) instead of overall knowledge, and the microscopic model would provide sub-optimal evacuation times (Dressler et al., 2010).

A number of studies extended the previous approach by implementing bidirectional coupling between the two algorithms. Thanks to an iterative calculation cycle, the outputs of the macroscopic model become the input of the microscopic model, and vice versa. Hence, the results of the macroscopic calculation are used to correct route choice of the agents in the microscopic simulation; next, the results of the latter are used to adjust movement in the macroscopic network. The iteration is repeated until the gap between the two predictions is narrow and steady. Borrmann et al. combined a network model with a grid-based model (Borrmann et al., 2012). Xiong, Tang, and Zhao used a continuum model where crowd movement is governed by a typical Navier-Stokes equation, in combination with a cellular automata (CA) model i.e. where individuals move as particles across small cells (Xiong, Tang & Zhao, 2013). Similarly, Zambrano et al. developed an iterative approach where microscopic modelling is performed with a discrete-event simulation technique (Zambrano et al., 2020).

3.3 Proposed mesoscopic model

The review highlights that in most of the existing hybrid models the macroscopic and microscopic algorithms are layered. This means that each of the two is run in parallel to the other throughout the whole building domain in order to refine the prediction or reduce computational time. This technique is useful when designers seek the optimal evacuation strategy in deterministic scenarios but may bring limited advantages to probabilistic performance-based design where the aim is to quantify the evacuation curve in realistic conditions that do not necessarily represent the fastest evacuation process. Moreover, in many existing mesoscopic models the microscopic component is based on a grid-representation of the geometry, which comes with several limitations in terms of density predictions. This is because many fine network models typically presuppose that each cell of the grid is occupied by one person, therefore density and flow conditions are strongly driven by user assumptions about the grid structure (O'Connor et al., 2019).

The idea behind the mesoscopic model proposed in this study is to execute microscopic and macroscopic calculations in series rather than in parallel. Instead of applying the two approaches

to the whole geometry, each of them is applied to a different region of the building. In particular, occupants are represented as single agents with individual characteristics in the fire enclosure (microscopic approach), while they are treated as a uniform stream of occupants with homogeneous characteristics along the other parts of the egress route (macroscopic approach). This technique will provide accurate predictions of the initial outflow and the formation of queues in the parts of the building characterised by the largest number of occupants and the presence of hazardous conditions. In the following parts of the building, where no direct threat to life is foreseen (e.g., protected corridors, staircases, unaffected fire compartments, etc.), a coarser level of detail will reduce computational time.

Since the aim is getting a realistic prediction of the evacuation process, which might be sub-optimal, there is no need to use a grid model that accounts for dynamic behaviours (e.g., re-routing) to find the minimum evacuation time. Exit choice remains a deterministic input and it is assumed that occupants wait in a queue even if other exits are free.

This allows to minimize complexity and develop a model which is fully analytical and relies exclusively on a coarse network representation of the building. The microscopic representation of the occupants is achieved using distributions of initial conditions and individual characteristics for the agents that move throughout the network, similar to the approach by (Tolujew & Alcalá, 2004) which is expanded to represent key features of emergency situations such as pre-evacuation delays or density-speed correlations. The result is a model that captures all the significant quantities that characterise the evacuation process in the crucial parts of the building, but demands negligible time to run.

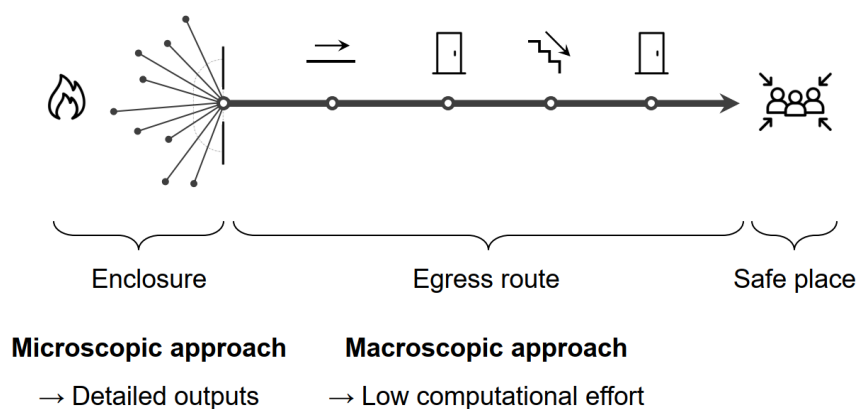


Figure 3 – Conceptual representation of the proposed mesoscopic approach

3.3.1 Microscopic representation

As anticipated, movement in the enclosure where occupants are initially located at the start of the fire emergency is represented with a microscopic approach.

The RSET timeline model (ISO/TR 16738 : 2009) is at the basis of egress calculations, where the evacuation process is represented by four key phases: 1) the time t_d [s] from fire ignition to detection by an automatic system or an occupant, 2) the time t_n [s] from detection to notification

of the occupants, 3) the time t_{pre} [s] from notification until the start evacuation, and 4) the time t_e [s] from the start of evacuation until the first egress component is reached.

$$RSET = t_d + t_n + t_{pre} + t_e \quad \text{Equation 1 (ISO/TR 16738 : 2009)}$$

Furthermore, the evacuation time t_e can be broken down in two components: the time spent to travel along the exit route t_{trav} [s] and the time spent in congestions that arise where restrictions limit the flow of occupants t_{flow} [s].

In real evacuations each person has unique physical abilities and reacts differently to the fire emergency depending on the available information, on the individual risk aversion, and on the subsequent psychological process (Tong & Canter, 1985). Initial conditions at the start of the emergency will also vary for every occupant of the building. Therefore, Equation 1 is modified to calculate the ‘presentation time’ t_{pres} [s] of every occupant j . This is defined as the period between fire ignition and the time at which they reach the first egress component (e.g., exit door of the compartment on fire). Here it is assumed that t_{pres} only accounts for the time t_{trav} required to reach the egress component, but not for the time t_{flow} required to traverse it.

$$t_{pres,j} = t_{d,j} + t_{n,j} + t_{pre,j} + t_{trav,j} \quad \text{Equation 2}$$

Through this notation, each occupant is represented by a set of individual attributes, that are sampled from user-defined statistical distributions. Some of the input parameters affected by variability are addressed in more detail below.

3.3.1.1 Detection time

When an automatic detection system (or a sprinkler system) is installed, engineers can use a fire model to calculate the time it takes for smoke or heat to trigger detectors. The model can be either an analytical correlation such as the one proposed in (Alpert, 2016) or a sub-model in a computational fluid dynamics (CFD) tool such as the Fire Dynamics Simulator (FDS) (McGrattan et al., 2020).

If a building is only equipped with a manually activated alarm system, detection occurs when occupants receive a direct cue (e.g., see/smell/hear flames or smoke) or an indirect cue (e.g., interruption of building services, glass breakage, presence of firefighters). In this case, the detection time can be considered as the period needed for the fire cues to manifest to the occupants e.g. the time required for the fire to reach a certain heat release rate (HRR) or for the ceiling jet to traverse the enclosure (New Zealand C/VM2, 2017). Individual pre-evacuation time may vary greatly according to the enclosure geometry (e.g., single open-plan versus multi-room enclosure), the occupants status and their proximity to fire.

In both cases, the calculation of detection time depends upon the fire scenario and the characteristics of the fire detection system. This topic is out of the scope of this thesis, but further guidance can be found in (PD 7974-1, PD 7974-4, Hurley et al., 2016). The distribution of t_d can be constructed through expert judgement or probabilistic uncertainty analyses considering distributions of fire growth rates and detectors/people responsiveness.

3.3.1.2 Notification time

When a building is equipped with an automatic alarm system (or a sprinkler system) and a standard simultaneous evacuation strategy is implemented, notification immediately follows detection. If siren horns are installed t_n is zero. When a voice alarm is present a value of $t_n = 30$ s is often used to account for the emergency message to be spoken. If a non-standard evacuation strategy is foreseen (e.g., phased evacuation, pre-warning to trained staff, progressive horizontal evacuation, etc.) a delay should be included according to the fire safety management procedures. In these circumstances it is reasonable to use a deterministic design value for t_n .

If a building is only equipped with a manually activated alarm system, the time required for an occupant to search/reach a manual push-button must be included. If a building does not have an alarm system at all, the notification time can be modelled as the period required for the occupant who detects the fire to reach other people in the premise and communicate the information. In these cases, designers should use distributions that express uncertainty about human behaviour.

3.3.1.3 Pre-evacuation time

Pre-evacuation time is the period required for occupants to receive a cue (e.g., hear a voice message), recognize the cue (e.g., realise the message is an alarm), interpret the cue (e.g., realise the alarm refers to fire in the building) and validate a cue (e.g., investigate for more cues). It also includes the time required for decision making (e.g., determine the appropriate actions, wayfinding, etc.) and to perform preparatory actions (e.g., getting dressed, stopping machinery, gathering group members or personal belongings, alerting others, etc.). The pre-evacuation phase may also include firefighting actions or incorrect activities due to misleading information. (Canter, Breaux & Sime, 1980).

Efforts have been made to formulate a conceptual model to simulate human behaviour in fire (HBiF) through inclusion of 'behavioural statements' (Gwynne, Hulse & Kinsey, 2016; Kuligowski et al., 2017) or employing Random Utility Theory to predict behavioural choices (Lovreglio, Ronchi & Nilsson, 2015). Nevertheless, current evacuation models focus more on simulating physical movement rather than decision-making during fire emergencies. It is common practice among fire safety engineers to simplify human behaviour through a time delay or predefined itineraries to particular locations within the building (Ronchi et al., 2017).

To predict realistic pre-evacuation times, engineers should refer to fire incidents or unannounced drills in facilities similar to the scenario being modelled. A useful collection of data is compiled in (Gwynne & Boyce, 2016; Lovreglio et al., 2019). Moreover, some performance-based codes suggest design values for the pre-evacuation time based on the characteristics of the building (e.g., occupancy type, building layout, type of detection and alarm system, fire safety management strategy, presence of focused activities, etc.) and its occupants (e.g., alertness, familiarity, proximity to fire, need for preparation, training, etc.). For example, the British PD 7974-6 provides data in the form of log-normal distributions, where the skewed shape shifted towards small values indirectly represents social influence. In fact, it has been demonstrated that the response of occupants confronted with fire cues may be inhibited by the presence of bystanders due to informational social influence (i.e., people observe others to collect information) or normative social influence (i.e. people tend to conform to the norm of the group)

(Latané & Darley, 1970). Therefore, as soon as the most reactive occupants start evacuating, a large portion of the population moves soon after (Nilsson & Johansson, 2009).

3.3.1.4 Travel time

The travel time is calculated according to the method proposed by (Gwynne & Rosenbaum, 2016), currently included in the SFPE Handbook of Fire Protection Engineering.

$$t_{\text{trav}} = L_{\text{trav}} / S \quad \text{Equation 3 (Gwynne \& Rosenbaum, 2016)}$$

where L_{trav} is the travel distance [m] and S is the walking speed [m/s]. In a population, the individual travel time $t_{\text{trav},j}$ depends on individual walking speed S_j and travel distance $L_{\text{trav},j}$.

3.3.1.5 Unimpeded walking speed

The SFPE hydraulic model assumes that when the population density D is lower than 0.54 pers/m², people move at their unimpeded walking speed $S_{\text{max},j}$. On horizontal surfaces S_{max} is on average 1.19 m/s. At a microscopic level it varies according to occupants' characteristics, such as age and physical/cognitive abilities.

It is further affected by the type of egress component which is traversed e.g., horizontal versus vertical components such as ramps, stairs, escalators, etc. (O'Connor et al., 2019). Engineering data can be found in (Gwynne & Boyce, 2016).

When occupant density increases, the ability to move decreases. The SFPE model assumes that movement ceases at a density of 3.77 pers/m², while between 0.54 and 3.77 pers/m² the walking speed decreases linearly as the population density increases, according to the following function:

$$S = k - akD \quad \text{Equation 4 (Gwynne \& Rosenbaum, 2016)}$$

where k relates to the type of egress component (e.g., $k = 1.4$ for horizontal travel) and $a = 0.266$.

Although movement at densities greater than 3.77 pers/m² can occur, this is not contemplated by the hydraulic model as it represents a dangerous condition for life safety that should be avoided during egress. In fact, at densities of 4 ÷ 5 pers/m², the interpersonal distance between people in a crowd reduces to zero, and direct contact between bodies causes individuals to lose the ability to move independently. This generates a transmission of forces that produce crowd turbulence and crush conditions (Gwynne & Rosenbaum, 2016).

3.3.1.6 Travel distance

The individual travel distance is related to occupants' initial location and individual route choice.

In a rectangular enclosure, the initial location can be attributed to each occupant by sampling two random coordinates from uniform distributions of length in two orthogonal directions.

With regards to exit choice, the model is developed under the assumption that this is a user-specified input. This allows modellers to investigate alternative scenarios, including sub-optimal egress paths. In fact, route choice may be affected by the building design and occupants' individual behaviour. On one hand, poor affordances may prevent people from noticing an escape route (Hartson, 2003); on the other hand, affiliation may induce them to evacuate from the most familiar area of the building or to move towards familiar people (Sime, 1985).

Fire-induced environmental conditions that may prevent occupants from using escape routes can be modelled by discarding some egress components from the model, thus reducing the total exit capacity.

3.3.1.7 Presentation flow and outflow

The aggregation of all the individual presentation times provides the distribution of t_{pres} among the population. As a result, the flow of people reaching an exit – that will be further called ‘presentation flow’ F_{pres} [pers/s] – varies over time.

After the presentation flow has been calculated, the effective outflow from the first enclosure is adjusted based on egress component capacity.

If the maximum flow that can be sustained through the exit F_c [pers/s] is greater than the presentation flow, occupants evacuate freely. The evacuation time coincides with the travel time since no queue occurs and occupants flow out of the enclosure as soon as they reach the exit ($t_{flow} = 0$ s). This typically the case when the number of occupants is low in comparison with the exit capacity, or when the presentation time has a large scatter among the population.

If the presentation flow exceeds the exit capacity, a queue will form at the exit. From the moment at which the queue occurs $t_{q,on}$ [s], the egress flow is controlled by the component capacity and occupants presenting at the exit will add to the queue. Since F_{pres} varies with time, also the queue size evolves according to the instantaneous difference between F_{pres} and F_c .

3.3.2 Macroscopic representation

From the first egress component onwards, the macroscopic approach is implemented, and the model treats occupants as a homogeneous group of people with average characteristics. The SFPE hydraulic model is used to calculate movement until a place of safety.

The flow time t_{flow} [s] through an egress component is calculated as:

$$t_{flow} = P / F_c \quad \text{Equation 5 (Gwynne \& Rosenbaum, 2016)}$$

where P is the population size in front of the component [pers] and F_c is the calculated flow of persons passing through it [pers/s]. It can be derived with the following equations:

$$F_c = F_s W_e \quad \text{Equation 6 (Gwynne \& Rosenbaum, 2016)}$$

$$F_s = S D \quad \text{Equation 7 (Gwynne \& Rosenbaum, 2016)}$$

$$W_e = W - BL \quad \text{Equation 8 (Gwynne \& Rosenbaum, 2016)}$$

where F_s is the specific flow [pers/(s m)] and W_e is the effective width of the component being traversed [m]. The latter is calculated as the component measured width W [m] minus the boundary layer clearance used by people to accommodate lateral body sway [m].

When Equation 4 is combined into Equation 7 the specific flow is described by the parabolic function $F_s = kD - akD^2$. On horizontal surfaces, the maximum specific flow of 1.32 per/(s m) occurs at a population density of 1.88 pers/m².

3.4 Application field

The overview provided so far on risk-informed FSE and evacuation modelling has outlined the intended use and the main features of the mesoscopic model. This section further defines the range of emergency scenarios that can be treated with the tool.

First, the model is formulated for ASET/RSET analyses, hence for the use in the context of evacuation from building fires. Potentially, the tool could be adapted to assess the risk related to natural hazards (e.g., earthquake, flooding, hurricane, wildland fire, etc.), man-induced hazards (e.g., gas leakages, explosions, vehicle crashes, terroristic attacks, etc.), or to other contexts (e.g., tunnels, outdoors gatherings, ships, etc.). Nevertheless, the extension of the model to those scenarios will not be explored in this study.

Next, the model is conceived for the analysis of buildings with a simple geometry and internal layout. This is because the analytical nature of the tool implies a coarse-network representation of the building. For design situations where complex geometries and layout are foreseen, a sophisticated model should be preferred (e.g., continuous representation of space).

Moreover, the model is not suitable where complex occupant flows are expected. In fact, it is not possible to represent in detail group behaviours, counterflows or complex merging patterns. For instance, the proposed model cannot account for the interaction between agents mixing from bi-directional flows along a corridor; this scenario can only be schematised as two opposite homogeneous lanes of occupants neatly separated. As another example, the model is not yet optimised to predict movement on stairs serving many fire compartments or in facilities such as sports arena, theatres, cinemas etc. where the presence of stands and seat rows affects crowd dynamics (Burghardt, Seyfried & Klingsch, 2013). The ideal use of the tool is for the simulation single-storey buildings where simple escape routes lead horizontally to the exterior, or for multi-storey buildings where a phased evacuation strategy is chosen.

Despite the scope of this thesis is limited to evacuation modelling, it is easy to foresee that the ideal fire sub-model that completes the probabilistic framework is analytical in its nature. This means that the best application field are single open plan enclosures where hand calculations or two-zone models can be implemented also for the calculation of ASET.

Finally, the application area with the greatest potential for probabilistic evacuation modelling are facilities where the population density can be high, but where the total number of occupants varies during opening hours. For instance, an engineer may want to predict the evacuation process of a building accessible to the public at different occupant densities, and weight the consequences with the probability of having a specific occupant load (often proportional to the time of the day).

All these characteristics can be found in facilities such as:

- Exhibition halls hosting trade fairs, art shows, etc.
- Reception halls hosting social events, conferences, public meetings, ceremonies, etc.
- Commercial occupancies with regular open-plan layout such as supermarkets, wholesale shops, furniture stores, malls, etc.
- Large public buildings such as train stations and airports.

In the following chapters, these will be referred as ‘large gatherings’

4 Conceptual and mathematical description of the proposed model

The workflow for the analysis of a single risk scenario is proposed in Figure 4. This is composed of five main phases: 1) definition of risk scenarios through an event tree and selection of the one to be analysed, 2) likelihood analysis, 3) evacuation modelling, 4) fire modelling, and 5) consequences analysis.

The evacuation modelling phase can be further subdivided into three stages:

- 3a) **Model setup**: model users represent the building as a coarse network and define input parameters according to the analysed scenario.
- 3b) **Deterministic run**: the model samples a random realization of the stochastic parameters from input distributions and performs a single evacuation calculation; as a result, the model returns a set of deterministic outputs (e.g., evacuation curve, RSET, flows, queue size, etc.).
- 3c) **Convergence runs**: the model automatically reiterates stage 3b and performs a convergence assessment after every new realization. The iterations end as soon as the outputs converge towards a stable average value with a user-defined accuracy. This is then used by the model to automatically calculate conservative values that can be employed to perform the consequence analysis. Hence, the number of runs is automatically optimised to save computational resources, while delivering stable and conservative results.

This chapter provides the conceptual and mathematical description of the prototype mesoscopic evacuation model for the analysis of phases 3 and 5 mentioned earlier. Stages 3a and 3b are described in detail in section 4.1; stage 3c is described in section 4.2; stage 5 is described in section 4.4.

Performing the whole process represented in Figure 4 leads to the ASET/RSET analysis of a single risk scenario s_i , accounting for behavioural uncertainty. When a quantitative risk assessment is performed, the cycle is repeated for all the risk scenarios of the event tree and a FN curve is built at the completion of the process. This is described in section 4.3 and will be illustrated with a case study in chapter 5. By repeating the cycle multiple times for the same scenario while changing the value of input parameters it is possible to perform uncertainty and parameter analyses.

The model is currently implemented with VBA (Visual Basic for Application) in Microsoft Excel, and a user manual can be found in appendix B.

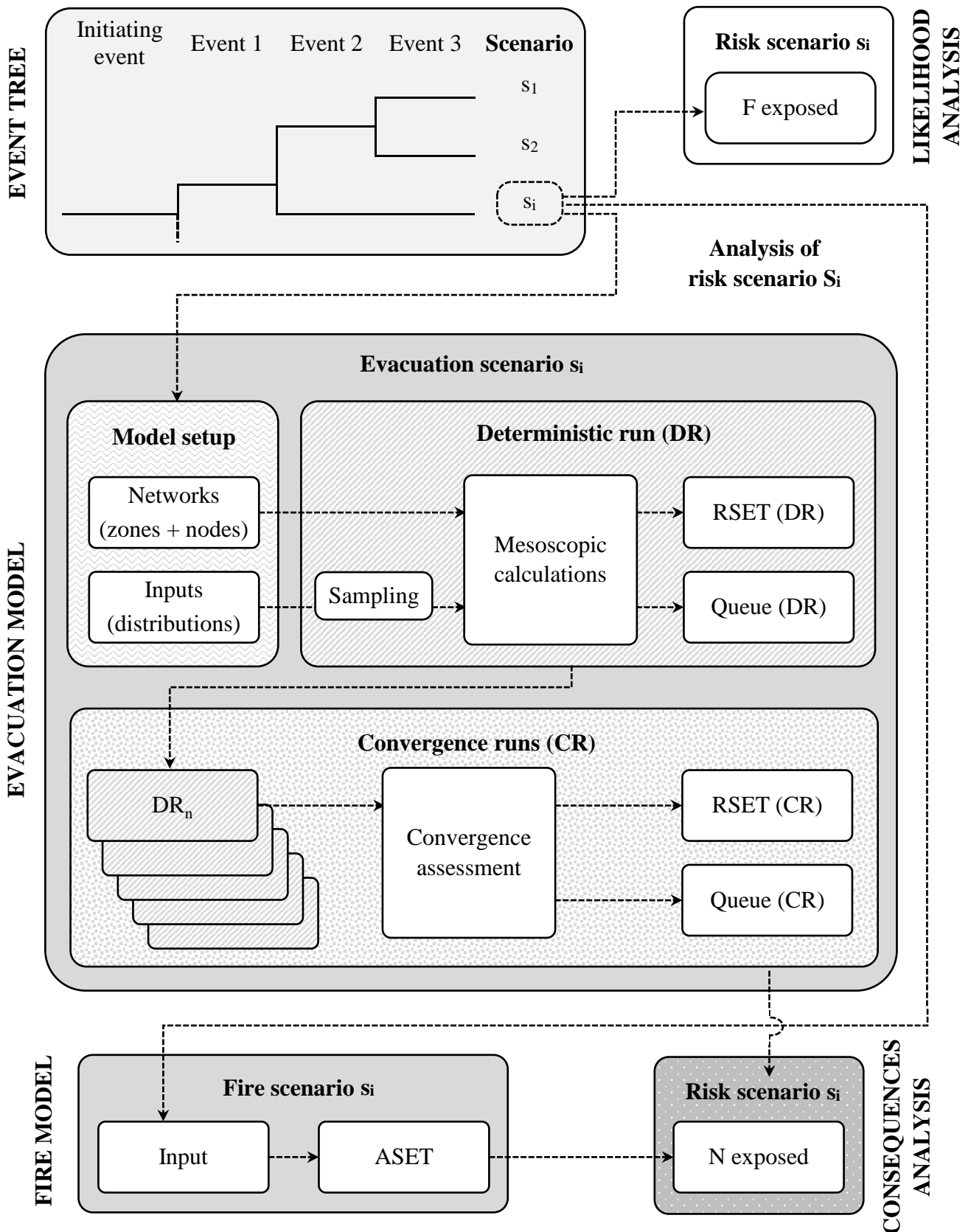


Figure 4 – Workflow for the analysis of a single risk scenario

4.1 Model setup and deterministic run

4.1.1 Networks

The first step of the evacuation modelling process consists in the representation of the building through an abstract coarse network for each egress path from the analysed area of the facility. All the egress components along an egress route should be included in a network as in the second order representation of the SFPE hydraulic model (Gwynne & Rosenbaum, 2016). Therefore, modellers assign to evacuees a predefined route which is maintained throughout the evacuation process i.e., the model does not account for re-routing due to queues or combustion byproducts.

Networks consist of two types of components:

- **Zones** represent building regions where the occupants are located when ignition occurs. In zones the microscopic approach is used: each person is represented by a stochastic set of individual characteristics based on user-defined statistical distributions and moves individually. Therefore, zones are the first component of any network and generate the occupants' flow entering in it.
- **Nodes** represent egress components (e.g., doors, corridors, stairs, etc.) along the path from occupants' initial location to a place of safety. They are also used to represent the locations where there is a change in the dimension of a component (e.g., where a corridor becomes wider/narrower) or where streams of occupants merge/split. Nodes are linked in a logical manner according to the route of evacuees. Here the macroscopic approach is implemented: the model treats persons as a homogeneous group with average characteristics flowing together along the network. Nodes have the ability to modify or delay the flow arriving from the previous part of the network. The last node acts like a sink that removes occupants from the network.

Some examples of building schematization are provided below, while a detailed description of zones and nodes is provided in parts 4.1.2 and 4.1.3 respectively.

The simplest possible network is composed by one zone and one node, representing a room with one exit leading directly to a safe place (e.g., exterior of the building) as represented in Figure 5a. As it is assumed that one zone always leads to one single egress path, Figure 5b shows how to treat enclosures that have more than one exit. In this case the floor area is divided into sub-areas, each one considered as an independent zone that leads to the pertinent egress path. Hence, the modeler generates an independent network for each. The subdivision of an enclosure in smaller areas can also be used to represent an unbalanced usage of egress paths: as the dimensions of the sub-areas are modified, the percentage of occupants using different egress routes changes accordingly. If the exit of the room to be evacuated leads to a corridor and a final door, the network is composed of one zone (room) and three nodes (room door + corridor + final door) as exemplified in Figure 5c. If the corridor serves multiple rooms, each one is represented by a zone and intermediate nodes are introduced in the corridor where the flows of evacuees merge (Figure 6). Figure 7a exemplifies the construction of a network for a stair serving a single floor. Figure 7b shows the network for a stair connecting multiple floors: each of them is represented by a different zone, while the stair is schematised as multiple nodes corresponding to doors, flights, and locations where groups of occupants merge.

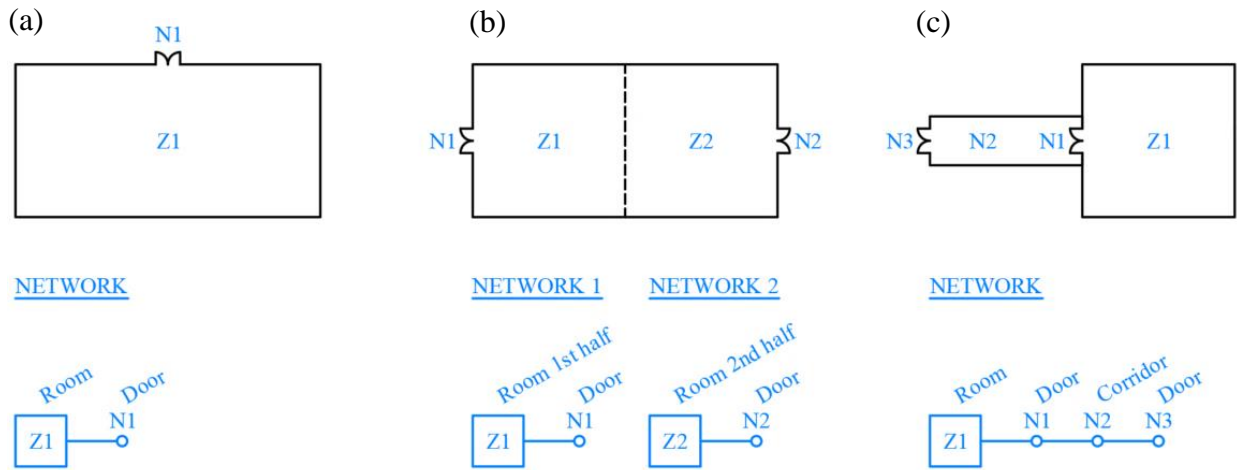


Figure 5 – Examples of networks with a single flow

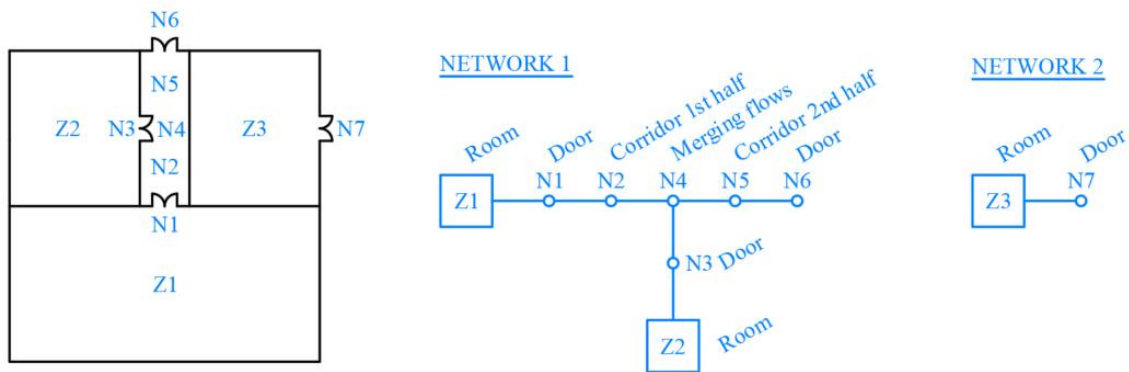


Figure 6 – Example of network with multiple flows

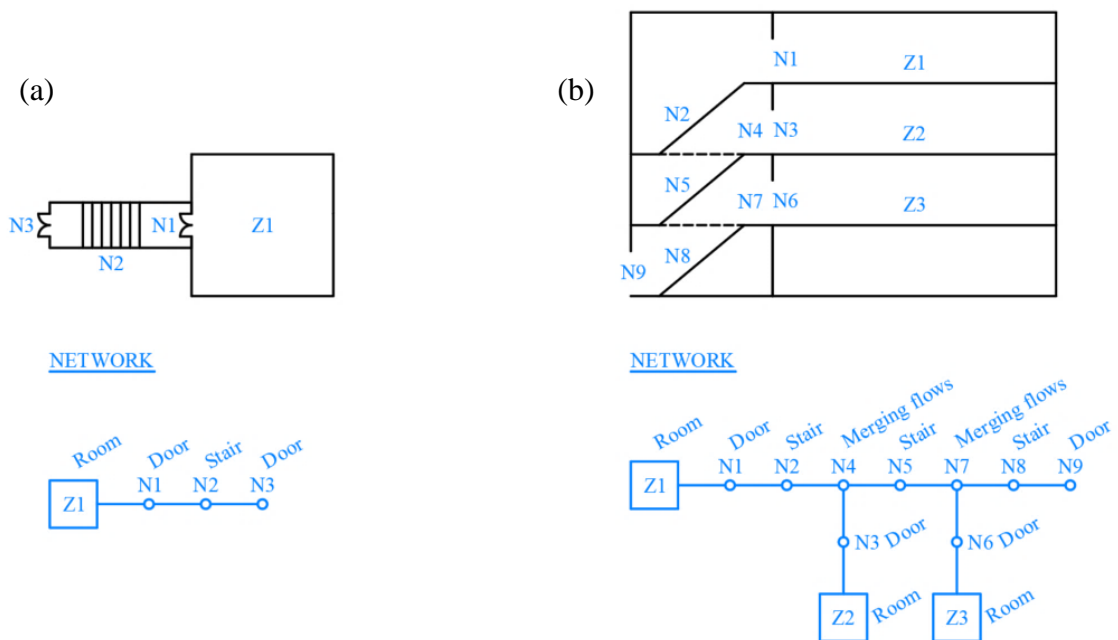


Figure 7 – Example of networks for stairs

4.1.2 Zones

A zone is a rectangular region that represents a room or a portion of it. If a room is not rectangular, the best approximation should be used. Modellers define zones through their geometrical dimensions X and Y [m] and the initial occupant density D [pers/m²]. The door is always assumed to be located at the centre of side X .

The model calculates the floor area $A = X \cdot Y$ [m²] and the initial number of occupants $P_0 = A \cdot D$ [pers]. Next it distributes randomly the occupants across the zone. This is done by assigning to each person two random values x_j and y_j [m] that represent the distance from the door along the two orthogonal directions (Figure 8a). Therefore, x_j is sampled randomly from a uniform distribution ranging between 0 and $X/2$ and y_j from a uniform distribution between 0 and Y . Next, the model calculates the travel distance L_j between each occupant and the exit. If the room is free of obstacles, the travel distance is calculated as $L_j = \sqrt{x_j^2 + y_j^2}$ (Figure 8b). If there are obstacles, the travel distance is calculated as $L_j = x_j + y_j$ (Figure 8c). The user can choose which path shape is the best alternative based on the internal layout of a facility.

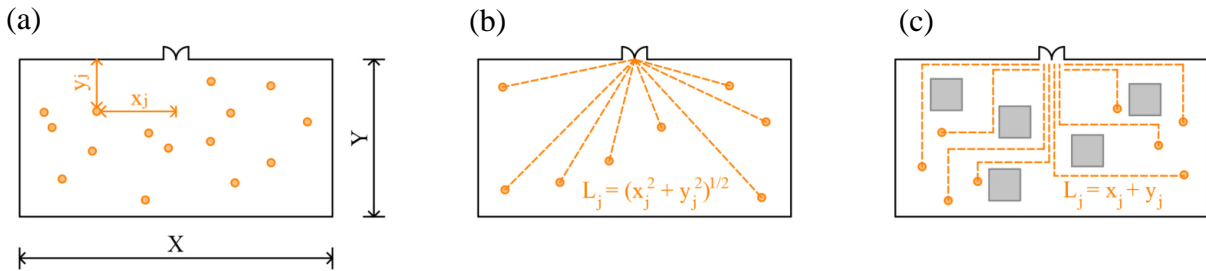


Figure 8 – Example of a zone with its population and travel distances with/without obstacles

The zone is then converted by the model into a set of virtual nodes that compose the first part of the network: for each occupant, one node represents the initial location and another node represents the travel path within the enclosure. These all converge to a virtual node that represents the location of the first egress component, as presented in Figure 9.

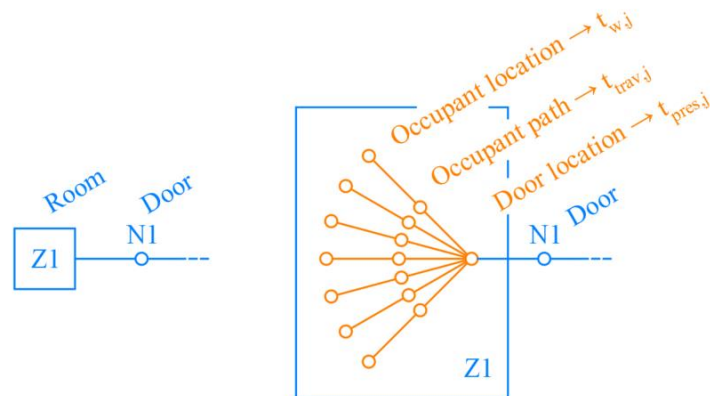


Figure 9 – Example of a zone converted into virtual nodes

Next, users must define design values for detection time, notification time, pre-evacuation time and unimpeded walking speed.

The detection time t_d and the notification time t_n are grouped into a unique deterministic value $t_{d+n} = t_d + t_n$. This is because regulations for the fire safety design of large gatherings often mandate the installation of automatic detection and alarm systems, such as in (Italian Fire Safety Code, 2019). In this case, fire is detected at a precise moment and all the occupants of a fire compartment are notified of the emergency at the same time. Hence, t_d can be calculated with a fire model and t_n can be chosen according to the fire management strategy.

The pre-evacuation time t_{pre} and the unimpeded walking speed S_{max} are treated as distributions to account for variability among individuals. This is done by specifying three distribution parameters: shape, location and scale. By default, t_{pre} follows a lognormal distribution as the majority of occupants will start evacuation soon after the most reactive ones (ISO/TR 16738 : 2009) and S_{max} follows a normal distribution to account for mixed populations which include children, elderly persons, people with functional limitations, etc. (Gwynne & Boyce, 2016).

The user-specified distribution of unimpeded walking speed is then automatically adjusted to account for the initial population density. This is done assuming that Equation 4 is representative of the average value of the distribution. Therefore, if the initial density of a zone is below 0.54 pers/m² the input distribution remains unchanged. Between 0.54 and 3.77 pers/m², the average walking speed reduces linearly as the occupant density increases. The standard deviation is reduced accordingly by a factor S / S_{max} as shown in Figure 10. This represents the fact that as the interpersonal distance increases, individuals will tend to adapt their speed to the one of those surrounding them, hence variability reduces. At densities close to 3.77 pers/m², the distribution of walking speed collapses around the average value. In fact, such high densities can cause direct contact between the body of occupants and a transfer of forces which may induce ‘crowd turbulence’. This is the extreme unwanted situation where the occupants cease to move as individuals and are forced to move as a uniform crowd (standard deviation tends to zero).

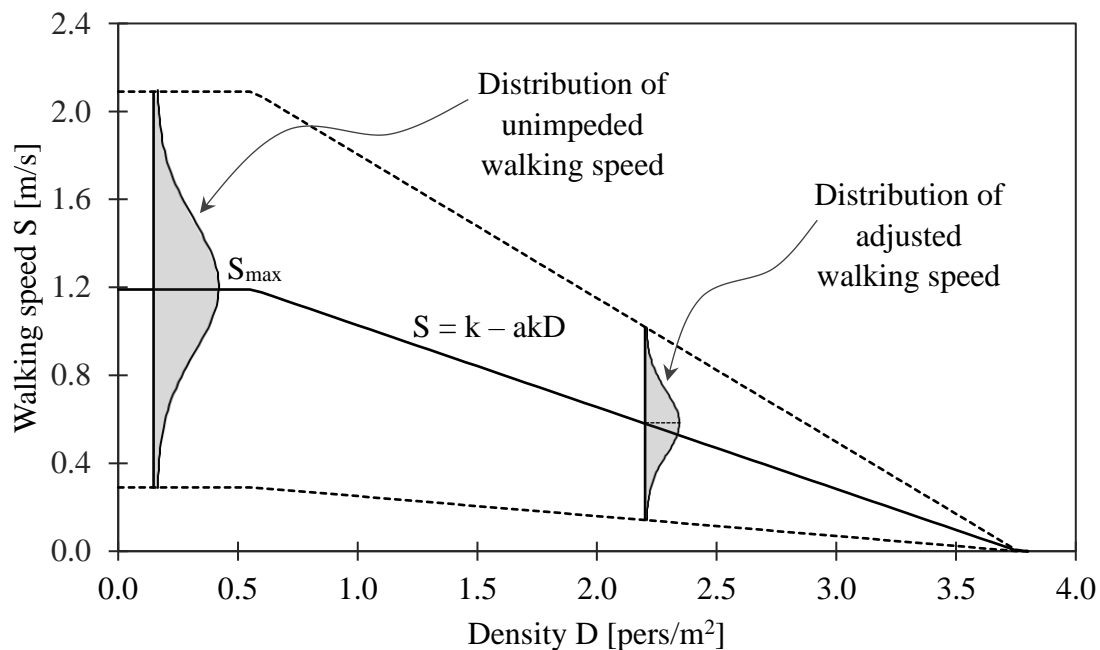


Figure 10 – Adjustment of walking speed as a function of density

The values of t_{d+n} and t_{pre} can be differentiated for each zone to account for phased evacuation or for the coexistence of different activities that generate different pre-evacuation times. S_{max} is specified at building level, since it is assumed that the population is similar throughout the same fire compartment (this might not be the case in occupancies such as hospitals, elderly care houses, or schools, which are not addressed in this study).

Once input parameters are defined, the model generates a random set of attributes for each occupant ($x_j, y_j, t_{pre,j}, S_j$). Next, the model calculates L_j and two individual time periods:

- The waiting time $t_{w,j}$ [s] that each occupant spends at his/her initial virtual node without evacuating, calculated as $t_{w,j} = t_{d+n} + t_{pre,j}$. Note that in reality occupants will not necessarily remain static during t_{pre} as they might perform pre-evacuation activities that involve movement. Nevertheless, x_j and y_j can be seen as the location of the occupants once they have completed their pre-evacuation activities, independently of their previous itineraries.
- The travel time $t_{trav,j} = L_j / S_j$ [s] that each occupant takes to move along his/her travel path from (x_j, y_j) to the exit of the zone (second virtual node).

Now the model determines the individual presentation time $t_{pres,j} = t_{w,j} + t_{trav,j}$ [s] which is the period between ignition until when an occupant reaches the exit location (third virtual node). Note that here the presentation time does not incorporate t_{flow} as defined in Equation 5. In fact, the presentation time coincides with the evacuation time that would occur if there was no further egress component constraining the flow of occupants (e.g., a door). The zone can be seen a horizontal surface with no boundary walls: occupants can flow out from its perimeter without restrictions. Another way of seeing a zone is to imagine it as a room with an infinitely wide exit (and component capacity F_c) that cannot cause the formation of queues. Hence, occupants will traverse it as soon as they reach it. The set of individual presentation times $t_{pres,j}$ provides the distribution of t_{pres} among the population.

The number of persons reaching the exit location is recorded at discrete time steps. For this purpose, the simulation time is divided into time intervals $\Delta t = 5$ s (Figure 11). At every time step t , the presentation flow $F_{pres}(t)$ [pers/s] is calculated by dividing the number of persons reaching the exit location $p_{pres}(t)$ by the time interval Δt . An example of presentation flow curve is provided in Figure 12a.

Finally, the model calculates the cumulative number of occupants that have evacuated the zone at every time step $P_{evacuated}(t)$ [pers]. Since the consequence analysis requires the prediction of the number of people potentially exposed to combustion products when ASET is reached, the curve is reversed to represent the number of occupants that are still located inside the zone as a function of time $P_{remaining}(t) = P_0 - P_{evacuated}(t)$ [pers]. This will be further referred as ‘evacuation curve’ for conciseness and indicated with the simpler notation $P(t)$. At this stage the curve represents the evacuation process in free flow conditions, as no constraints to the flow have been considered yet. Its typical shape is represented in Figure 12b.

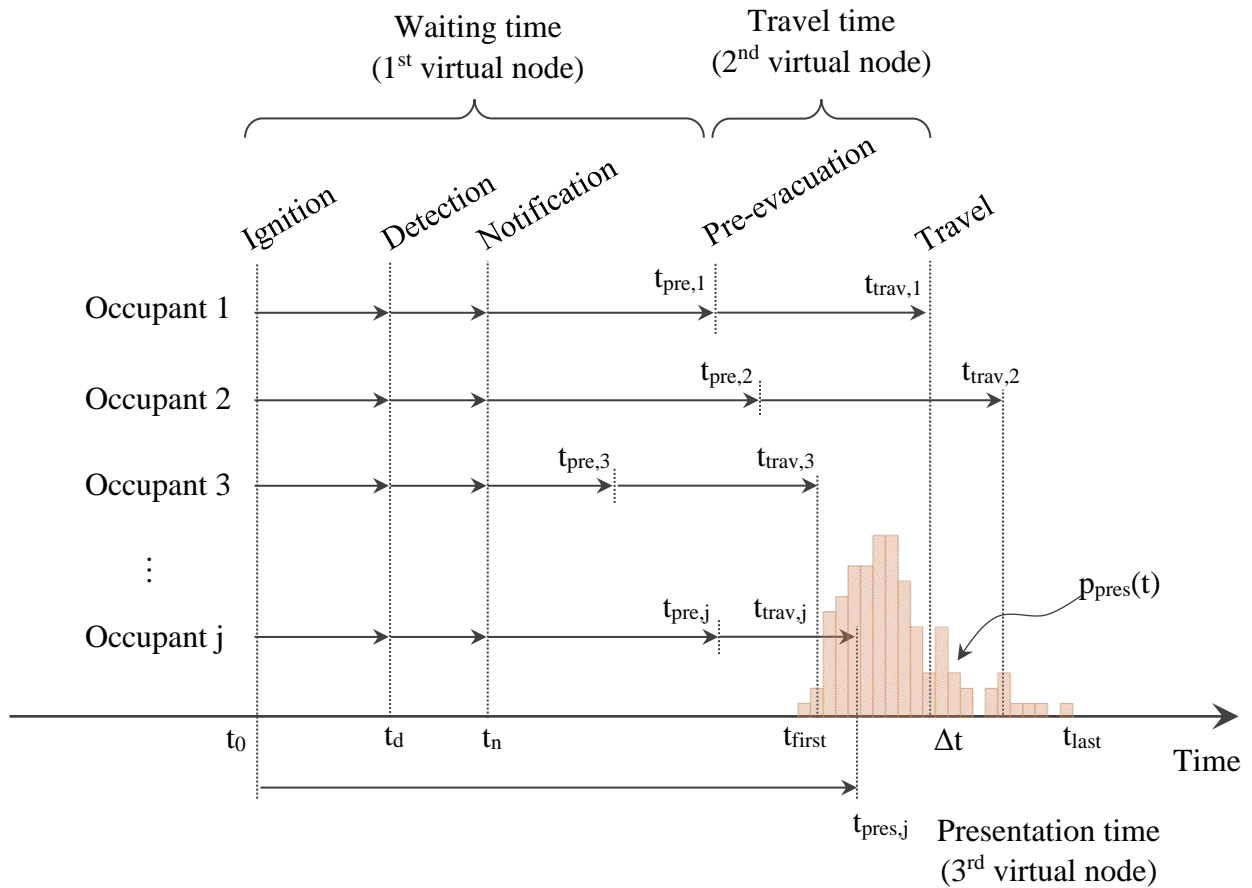


Figure 11 – Representation of individual presentation time $t_{pres,j}$ in an enclosure with automatic fire detection and notification systems

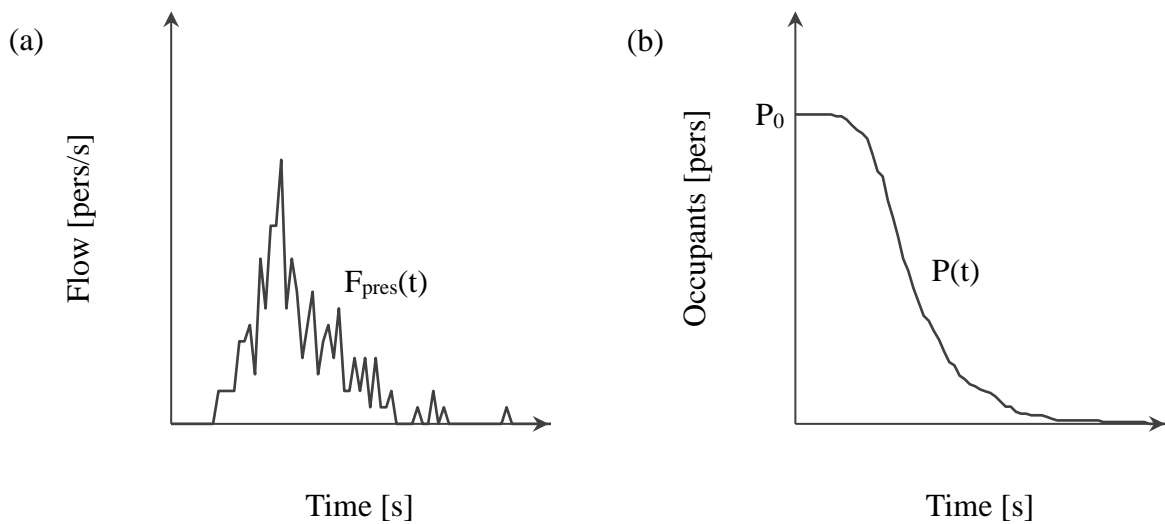


Figure 12 – Example of presentation flow $F_{pres}(t)$ at the door location (a) and evacuation curve $P(t)$ from a zone (b) in free flow conditions

4.1.3 Nodes

The main purpose of the evacuation model is to determine the distribution of the occupants throughout the building as time evolves i.e., the number of persons at every node at every time step. The calculations that are performed at different node types are described below.

4.1.3.1 Doorways

Doorways are egress components characterised by a maximum capacity $F_{c,max}$ that is automatically calculated by the model according to Equation 6 once the user has specified the measured width W , the boundary layer clearance BL and the maximum specific flow $F_{s,max}$. Based on (Gwynne & Rosenbaum, 2016) the value of BL for doors is assumed as $2 \cdot 15 \text{ cm} = 30 \text{ cm}$. The standard $F_{s,max}$ is assumed as $1.32 \text{ pers}/(\text{m s})$. The length of doorways is null.

At every time step t , the model compares the maximum flow allowed by the analysed node k $F_{c,k,max}$ with the flow arriving from the previous node of the network $F_{c,k-1}(t)$.

If $F_{c,k-1}(t) \leq F_{c,k,max}$ the doorway is sufficiently wide to allow all the approaching persons to flow freely through it, at a rate $F_{c,k}(t) = F_{c,k-1}(t)$. Because of this, the evacuation curve representing the passage through the analysed node $P_k(t)$ coincides with the curve obtained at the previous node $P_{k-1}(t)$, as exemplified in Figure 13.

If $F_{c,k-1}(t) > F_{c,k,max}$ the doorway capacity limits the number of occupants that can flow through it. Hence, the node outflow is capped to $F_{c,k,max}$ and the rest of the persons add up in a virtual node that represents the queue forming in front of the doorway (Figure 14). This grows at a rate:

$$F_{q,k,in}(t) = F_{c,k-1}(t) - F_{c,k,max} \quad \text{Equation 9}$$

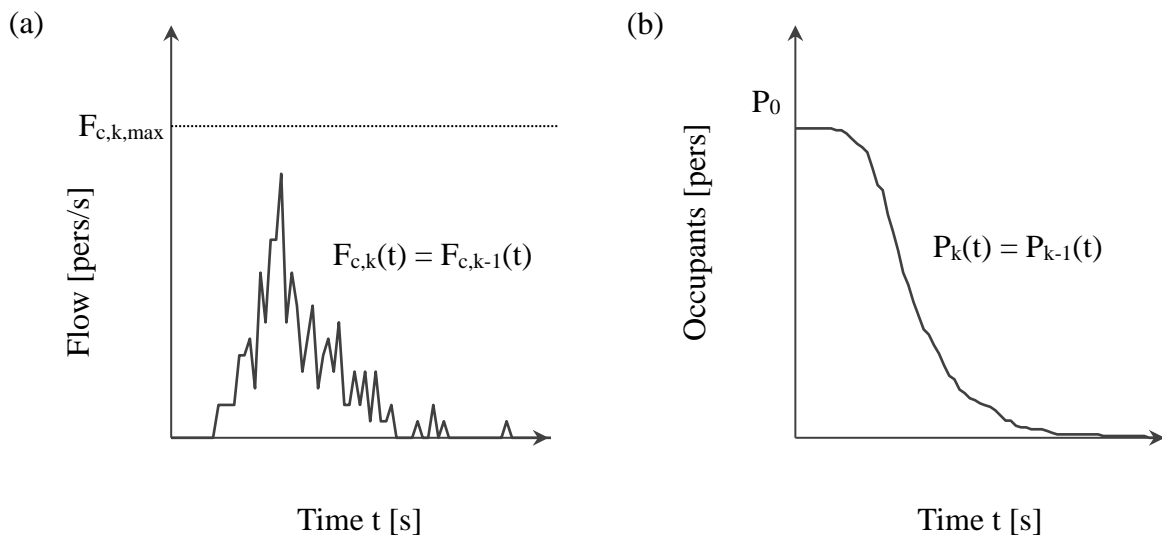


Figure 13 – Example of component flow $F_{c,k}(t)$ (a) and evacuation curve $P_k(t)$ (b) at a node k in free flow conditions ($F_{c,k-1}(t) \leq F_{c,k,max}$)

Conceptually the virtual node is like a buffer in the network: it absorbs as many occupants as necessary to maintain the equilibrium $F_{c,k}(t) = F_{c,k,max}$. When $F_{c,k-1}(t)$ drops below the doorway capacity $F_{c,k,max}$, the occupants accumulated in the queue node are released again into the network at a rate $F_{q,k,out}(t) = F_{c,k,max} - F_{c,k-1}(t)$.

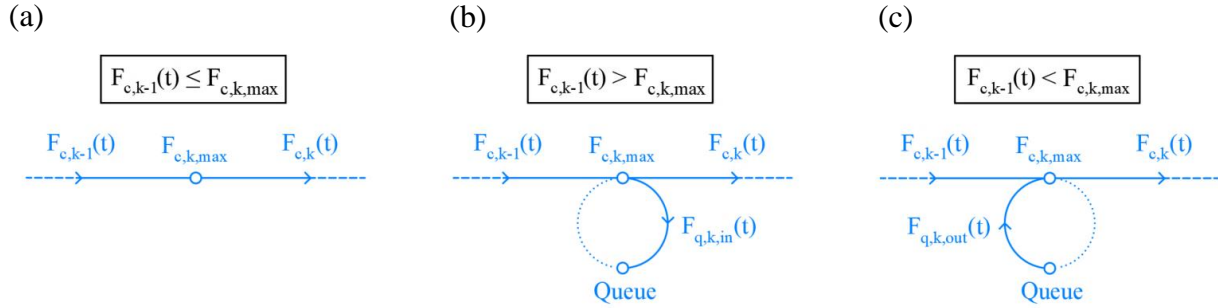


Figure 14 – Network representation of a node where $F_{c,k-1}(t) > F_{c,k,max}$ before queue (a), during queue formation (b) and during queue reduction (c)

As long as there are sufficient occupants approaching from node $k-1$ or waiting in the queue at node k , the flow out of the analysed node proceeds at the maximum rate $F_{c,k} = F_{c,k,max}$. Once $F_{c,k-1}(t) + F_{q,k,out}(t) < F_{c,k,max}$ the outflow decreases until zero when all the persons in the network have traversed node k . The time when this occurs is further called $t_{k,last}$. Similarly, the time when the first occupant traverses the node is called $t_{k,first}$ while the times when the queue forms and dissolves are called respectively $t_{k,q,on}$ and $t_{k,q,off}$.

Two alternative situations are possible when the queue reduces (De Sanctis, 2015):

- the queue dissolves before all the occupants have reached the node ($t_{k,q,off} < t_{k,last}$), or
- the queue lasts until the end of the flow through the node ($t_{k,q,off} = t_{k,last}$).

The two conditions are represented qualitatively in Figure 15 and Figure 16. The one occurring depends on the evacuation scenario, and more specifically on the ratio between the inflow of occupants from the previous node $F_{c,k-1}(t)$ and the component capacity $F_{c,k,max}$.

The difference between the evacuation curves $P_k(t) - P_{k-1}(t)$ provides the ‘queue curve’ $Q_k(t)$ which represents the number of occupants waiting in the queue at node k as a function of time (Figure 17).

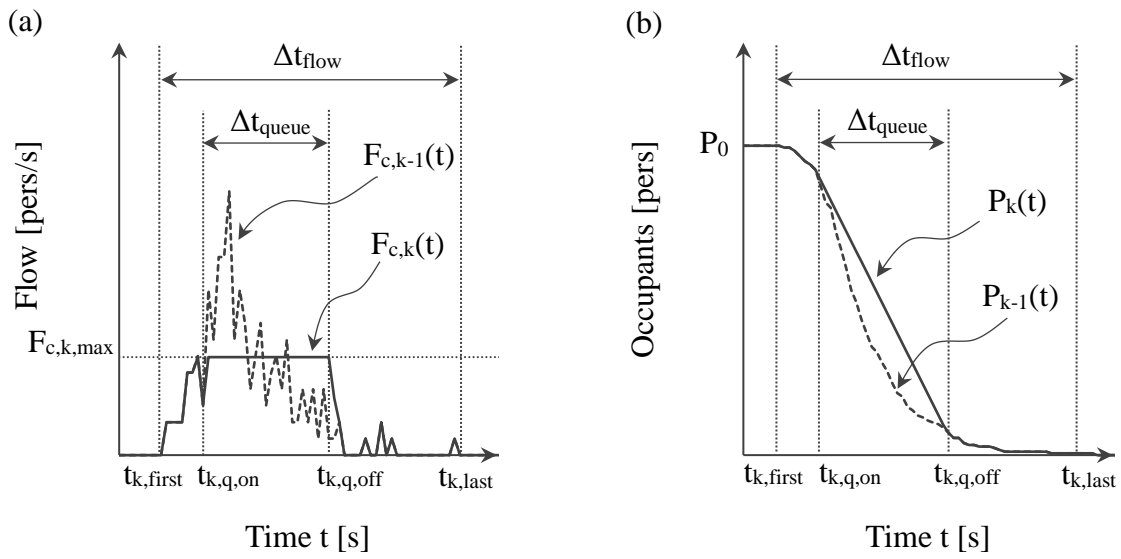


Figure 15 – Example of outflow $F_{c,k}(t)$ (a) and evacuation curve $P_k(t)$ (b) at a node k when a queue forms ($F_{c,k-1}(t) > F_{c,k,max}$) which dissolves before the end of the flow ($t_{k,q,off} < t_{k,last}$)

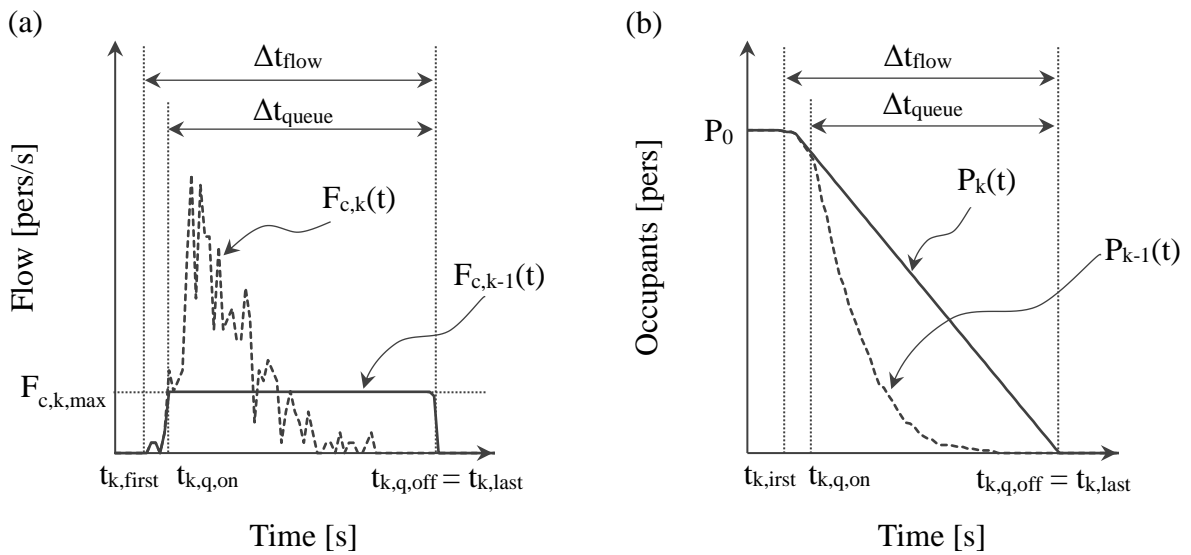


Figure 16 – Example of outflow $F_{c,k}(t)$ (a) and evacuation curve $P_k(t)$ (b) at a node k when a queue forms ($F_{c,k-1}(t) > F_{c,k,max}$) which dissolves at the end of the flow ($t_{k,q,off} = t_{k,last}$)

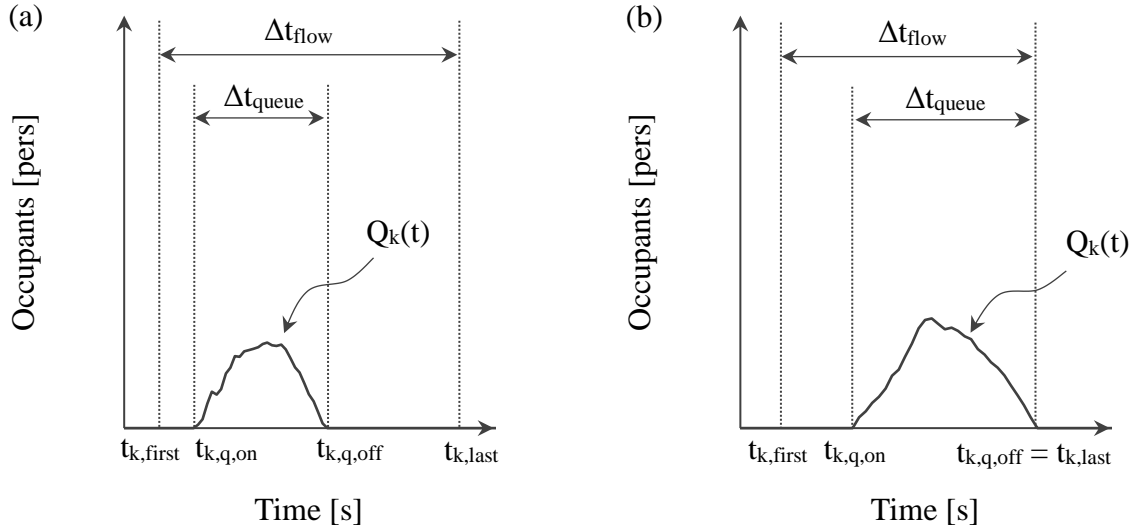


Figure 17 – Examples of queue curve $Q_k(t)$ at a node k which dissolves before the end of the flow ($t_{k,q,off} < t_{k,last}$) (a) or at the end of the flow ($t_{k,q,off} = t_{k,last}$) (b)

As further calculations along the network require the use of macroscopic quantities, the model also calculates the average density D_k and walking speed S_k of the population flowing through node k . This is done starting from the outflow $F_{c,k}(t)$ according to the following steps:

1. The specific flow is calculated as $F_{s,k}(t) = F_{c,k}(t) / W_{e,k}$. This varies between 0 and 1.32 pers/(s m) because $F_{c,k}(t)$ has been already capped at $F_{c,k,max} = F_{s,k,max} \cdot W_{e,k}$.
2. The average specific flow $F_{s,k}$ is calculated by averaging $F_{s,k}(t)$ between $t_{k,first}$ and $t_{k,last}$.
3. The average population density is calculated solving Equation 4 combined with Equation 7:
 - If $F_{s,k} = 1.32$ pers/(s m), then $D_k = 1.88$ pers/m².
 - If $F_{s,k} < 1.32$ pers/(s m), the quadratic equation produces two solutions $D_k = \frac{k \pm \sqrt{k^2 - 4akF_s}}{2ak}$. The lower value is used, since densities larger than 1.88 pers/m² would imply that the occupant flow rate rises and falls during the transition between egress components, which is not reasonable (Gwynne & Rosenbaum, 2016).
4. The average walking speed is calculated as $S_k = F_{s,k} / D_k$. Due to the ranges of $F_{s,k}$ and D_k the value of S_k falls between 0.70 and 1.19 m/s.

This calculation procedure is represented in Figure 18.

Notice that the current version of the proposed mesoscopic model implements the equations from the SFPE hydraulic model, but users can potentially customize it if other fundamental diagrams are deemed more representative of specific evacuation conditions (Vanumu, Ramachandra Rao & Tiwari, 2017).

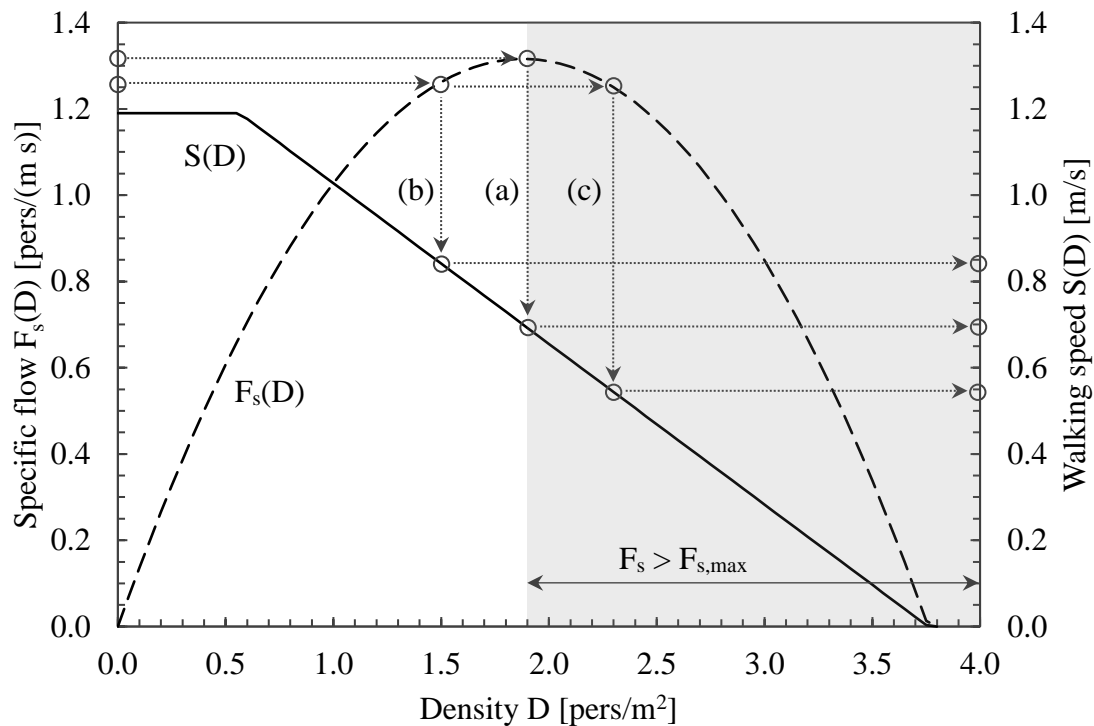


Figure 18 – Combined representation of SFPE fundamental diagrams of $F_s(D)$ and $S(D)$ for horizontal movement. The dotted lines represent the graphical derivation of S from F_s . Line (a) represents the upper boundary when $F_s = F_{s,max}$. Line (b) exemplifies one solution for $F_s < F_{s,max}$. Line (c) represents the alternative solution which is discarded because the component specific capacity $F_{s,max}$ is exceeded (shaded region)

4.1.3.2 Corridors

Corridors are sections of the egress path where occupants travel along a horizontal distance while being constrained by lateral walls that affect the movement of the crowd. Therefore, corridor nodes are described through a length L [m] and a component capacity $F_{c,max} = F_{s,max} \cdot (W - BL)$, where $F_{s,max} = 1.32$ pers/(m s) and $BL = 2 \cdot 20 = 40$ cm (Gwynne & Rosenbaum, 2016).

When a corridor node k is considered, $F_{c,k,max}$ potentially causes a modification of the occupant flow (hence of the average density and walking speed) while the length L_k prolongs the evacuation process because occupants need to traverse the corridor. The model calculates these two effects separately. This is first illustrated in the case where a room is followed by a corridor without doors (Figure 19a). The passageway that connects the room with the corridor acts like a doorway where the flow is calculated as previously: at every time step the model compares the presentation flow with the maximum corridor capacity, and caps the flow in case $F_{c,k-1}(t) > F_{c,k,max}$ i.e., a queue forms at the corridor entrance. Next, it is assumed that the occupants that have entered the corridor traverse it at the uniform average speed S_k resulting from the flow $F_{c,k}(t)$. Hence, the stream of occupants reaches the end of the corridor after a period $t_k = L_k / S_k$ [s]. Since the passageway at the end of the corridor is as wide as the entrance, occupants leave the component at the same rate at which they got into it. As a result, the evacuation curve is shifted in time by t_k (Figure 19b).

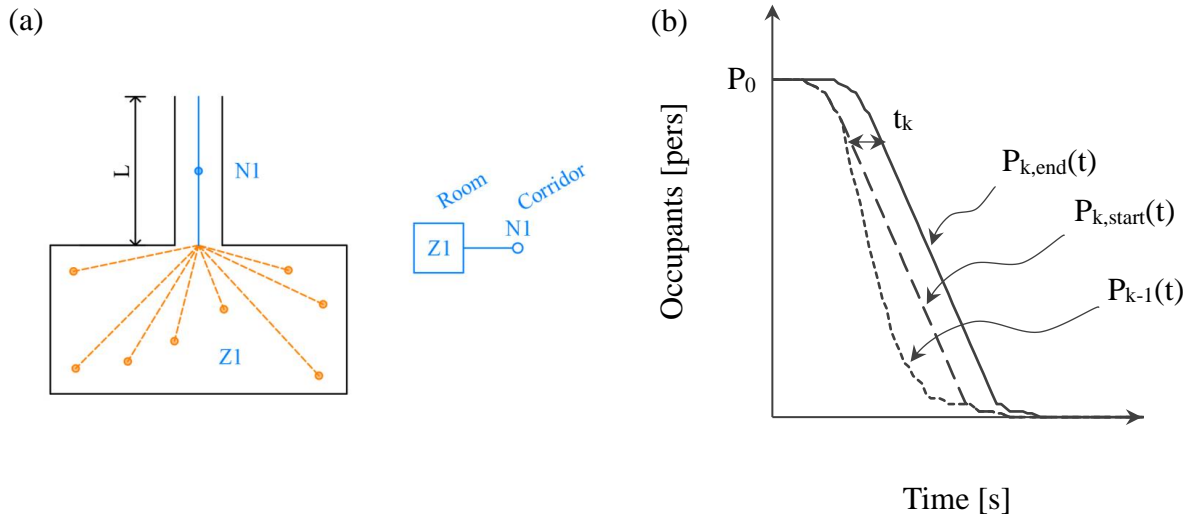


Figure 19 – Example of corridor without doors (a) and evacuation curve through it (b). $P_{k-1}(t)$ represents the presentation flow from the zone, $P_{k,start}(t)$ represents the evacuation curve at the entrance of the corridor and $P_{k,end}(t)$ represents the evacuation curve at the exit

A more common situation is depicted in Figure 20, where a corridor is bounded by two doors. These must be included in the building network as additional nodes. Following the SFPE approach, it is assumed that the flow F_c is conserved along the network, but F_s , D and S change at every node along the path according to the changes in the effective width W_e . The updated values are calculated with the conservation equations presented below, using the notations of Figure 20.

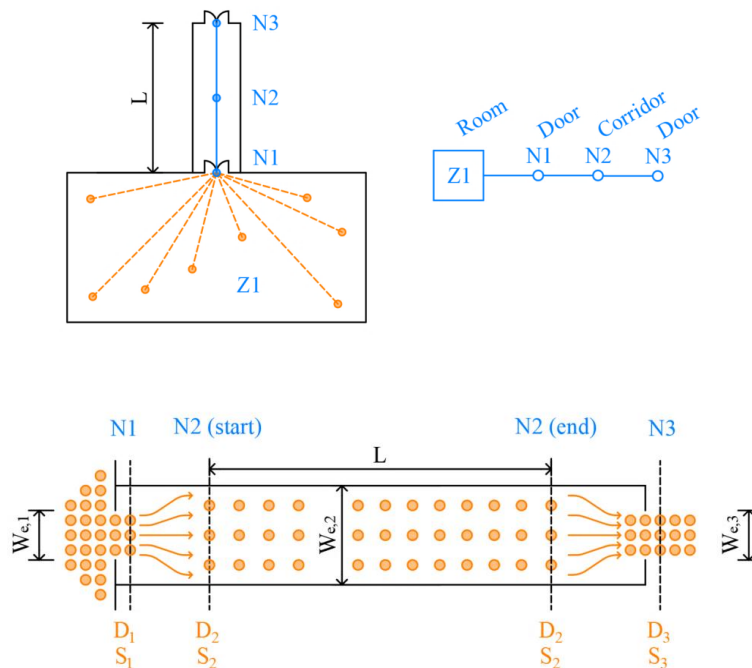


Figure 20 – Example of corridor with doors

At the transition from the entrance door (node 1) to the corridor (node 2) the model calculates the occupant flows according to the following steps:

1. At the entrance door the flow $F_{c,1}(t)$ and the average quantities $F_{s,1}$, D_1 and S_1 are calculated as described in part 4.1.3.1.
2. The conservation equation $F_{c,1}(t) = F_{c,2}(t)$ is applied (Gwynne & Rosenbaum, 2016). The occupant flow through the corridor is always equal to the flow coming from the door because the corridor capacity is always greater than or equal to the door capacity ($F_{c,2,max} \geq F_{c,1,max}$). In fact, the maximum specific flow of doors and corridors is the same $F_{s,1,max} = F_{s,2,max} = 1.32$ pers/(s m) while the geometrical width of the egress route becomes wider ($W_{e,2} \geq W_{e,1}$). Hence the flow in the corridor is never capped ($F_{c,2} \leq F_{c,2,max}$).
3. The average specific flow in the corridor is calculated as $F_{s,2} = (W_{e,1} / W_{e,2}) \cdot F_{s,1}$.
4. The average density in the corridor is calculated as $D_2 = \frac{k_2 - \sqrt{k_2^2 - 4ak_2F_{s,2}}}{2ak_2}$.
5. The average walking speed in the corridor is calculated as $S_2 = k_2 - ak_2D_2$.

Provided that the exit route becomes wider ($W_{e,1} / W_{e,2} \leq 1$) and that the component constant is the same for doors and corridors ($k_1 = k_2 = 1.40$), the following transformations occur:

- The specific flow in the corridor reduces ($F_{s,2} \leq F_{s,1}$).
- The density in the corridor reduces ($D_2 \leq D_1$).
- The walking speed in the corridor increases ($S_2 \geq S_1$).

At the transition from the corridor (node 2) to the exit door (node 3) the model calculates the occupant flows in the same manner, but the reversed process occurs when the exit route narrows (Figure 21). If the width of the exit door is such that $F_{c,3,max} < F_{c,2}(t)$ the outflow is capped and a second queue forms at the end of the corridor.

The evacuation curve at each node of the network is shown in Figure 22. The same transformations occur when egress components change in width (e.g., a corridor getting wider/narrower).

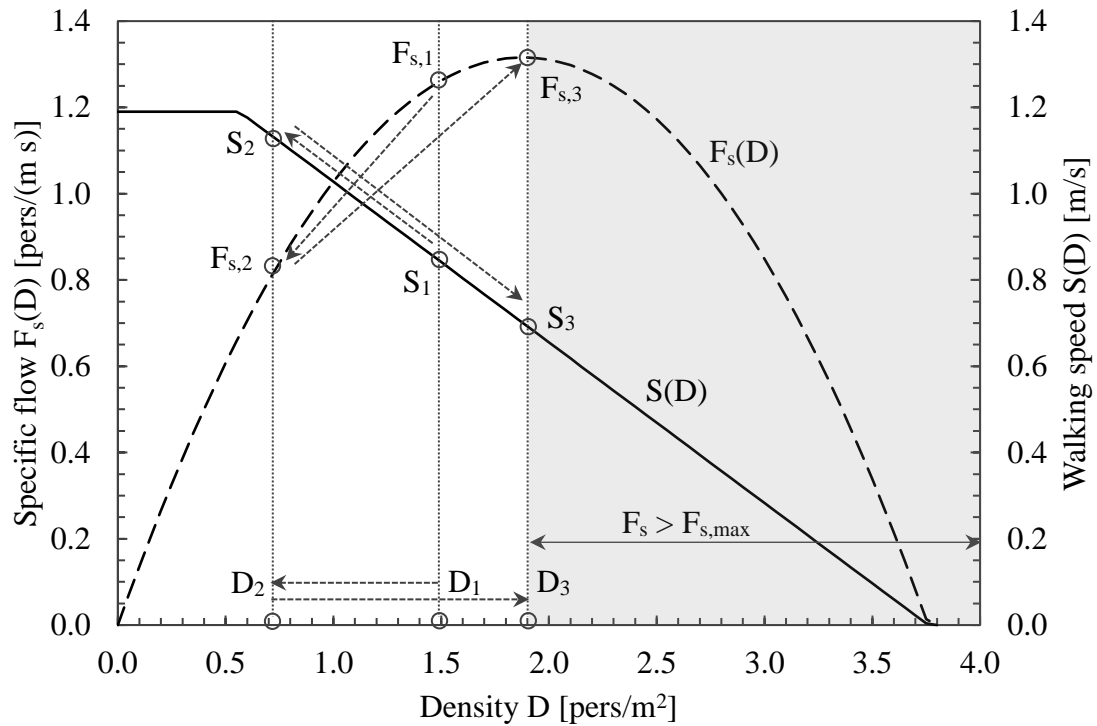


Figure 21 – Example of transition from a door to a corridor (node 1 → node 2) and from a corridor to a door (node 2 → node 3) where the maximum capacity of the latter is reached

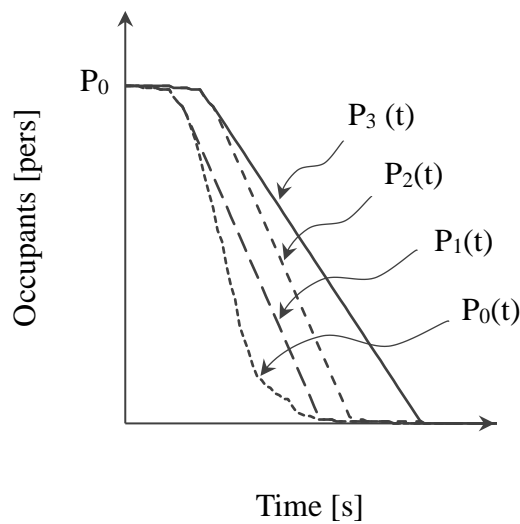


Figure 22 – Example of evacuation curve at different locations along a corridor with two doors, where the exit is narrower than the entrance.

$P_0(t)$ represents the presentation flow from the zone, $P_1(t)$ the entrance door, $P_2(t)$ the end of the end of the corridor and $P_3(t)$ the exit door

4.1.3.3 Transits

In this study, the sections of the egress path where occupants travel horizontally without being constrained laterally by physical boundaries are called ‘transits’. For example, this is the case when evacuees traverse a wide enclosure such as a room adjacent to the initial zone (still located in the same fire compartment).

Therefore, transit nodes are characterised by a virtually infinite capacity F_c and a user-specified distance L . Since the capacity of any transit k is greater than the one of the previous node $k-1$, transits do not modify the occupant flow $F_{c,k-1}(t)$ nor the evacuation curve $P_{k-1}(t)$. Their only effect is to prolong evacuation and shift the curve by a time delay $t_k = L_k / S_k$, where L_k and S_k are the travel distance and the walking speed within the transit area.

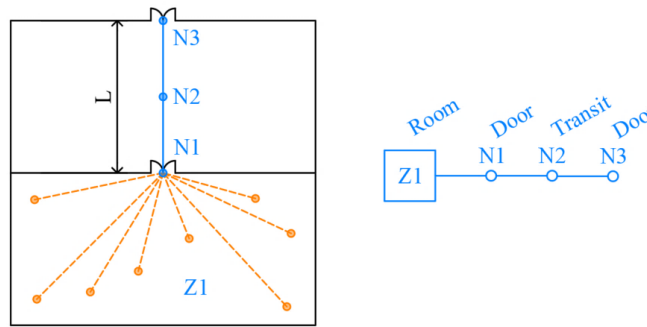


Figure 23 – Example of a zone followed by a transit

L_k can be regarded as the length of the path connecting the entrance and the exit of the transit region. Despite in reality agents may take slightly different trajectories, the travel distance can be reasonably approximated to a constant value for all the occupants. If fixed obstacles are foreseen in the traversed space users should account for their presence by inputting the length of the deviated path around them. S_k is the average unimpeded walking speed of the population, as it is assumed that occupants have enough space to take a distance from each other and move at their ideal speed.

In this case the transformation of the evacuation curve is similar to what is represented in Figure 19b, where $P_{k-1}(t)$ represents the presentation flow from the zone, $P_{k,start}(t)$ represents the evacuation curve at the entrance of the transit area and $P_{k,end}(t)$ represents the evacuation curve at the exit.

4.1.3.4 Merging points

Like in the SFPE hydraulic model, if more than one stream of occupants merge into a node, the model calculates the outflow as shown in Equation 10. The opposite is done when flows split, after the modeller has decided the proportion of occupants flowing in each of the output streams.

$$F_{s,out} = \frac{F_{s,in,1} W_{e,in,1} + F_{s,in,2} W_{e,in,2}}{W_{e,out}} \quad \text{Equation 10 (Gwynne \& Rosenbaum, 2016)}$$

4.1.3.5 Stairs

Stairs are components similar to corridors. However, the maximum specific flow $F_{s,max}$, the maximum unimpeded walking speed S_{max} and the constant k for stairs are always smaller than for other types of components (Table 1). Therefore, the same calculations presented in part 4.1.3.2 apply, but the occupant flow may be modified right after the first door in the network. Eventually, a queue can form along the stair itself (e.g., at the transition from horizontal to vertical movement). An example is provided in Figure 24.

Also in this case, the characteristics of stairs implemented in the proposed model correspond to default values from the SFPE model; nevertheless, these parameters are potentially customisable according to other literature sources, for example to model movement through spiral staircases (Gustafsson, 2016).

Table 1 – Maximum specific flow $F_{s,max}$, unimpeded walking speed S_{max} and constant k for different types of egress components from (Gwynne & Rosenbaum, 2016)

Egress component	$F_{s,max}$ [pers/(m s)]	S_{max} [m/s]	k [-]
Corridor, aisle, ramp, doorway	1.32	1.19	1.40
Stairs (riser 19.1 cm, tread 25.4 cm)	0.94	0.85	1.00
Stairs (riser 17.8 cm, tread 27.9 cm)	1.01	0.95	1.08
Stairs (riser 16.5 cm, tread 30.5 cm)	1.09	1.00	1.16
Stairs (riser 16.5 cm, tread 33.0 cm)	1.16	1.05	1.23

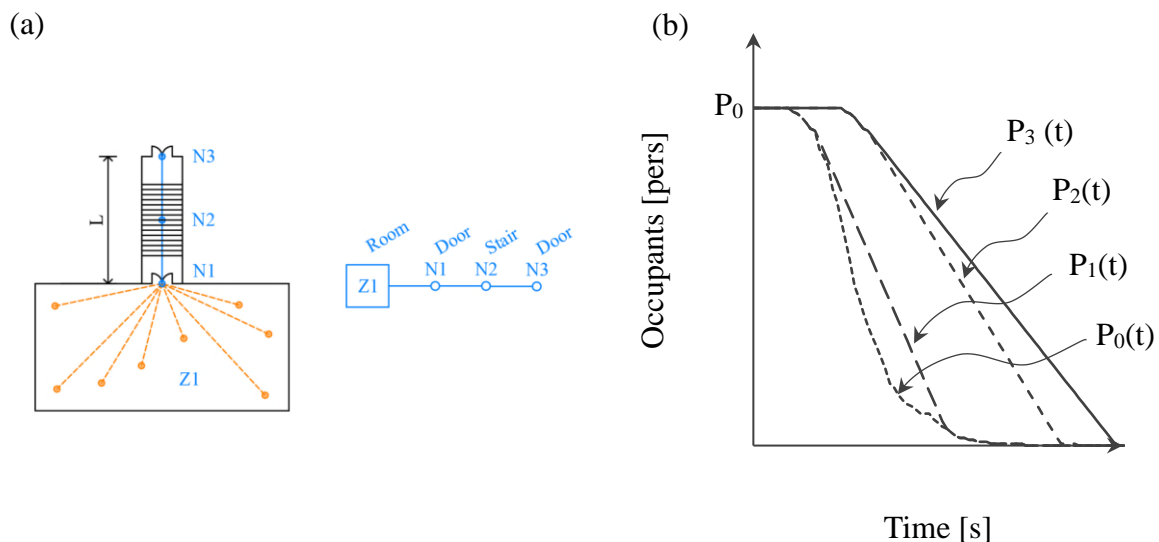


Figure 24 – Example of a stair with two doors (a) and evacuation curve through it (b) where the exit is narrower than the entrance.

$P_0(t)$ represents the presentation flow from the zone, $P_1(t)$ the entrance door, $P_2(t)$ the end of the stair and $P_3(t)$ the exit door

4.2 Iterative runs for convergence

The proposed mesoscopic model is based on probabilistic approaches, with many of the input parameters being defined as distributions. As a result, the predicted evacuation curve for one evacuation scenario may differ every time the model is run. Since fire safety engineers are interested in representative and conservative results, pseudo-random sampling from input distributions is used to explore the impact of variability and uncertainty on model outputs. This allows to obtain a distribution of numerical results (e.g., an ensemble of evacuation curves) that are then treated statistically to derive design values to be used for consequences analysis (e.g., for comparison with ASET).

One difficulty of utilising pseudo-random sampling approaches is to determine the number of repeated simulations that is sufficient to get a representative prediction of the scenario outcome. Since it is unlikely for end users to know this a priori, a dynamic assessment criterion is implemented within the tool so that the iteration process halts automatically as soon as convergence is reached.

In the current implementation, the variable that is monitored for the convergence assessment is the average time required for the occupants to evacuate the initial zone of a network, which will be further called Zone Evacuation Time (ZET). Further development could expand the convergence assessment to other variables such as the standard deviation of ZET, the maximum queue size, occupant flows, etc.

The routine proceeds as follows:

1. The user sets up the model, defines a convergence criterion (described below) and launches the iteration process.

At every new run:

2. The model draws a random realization of the stochastic variables from user-specified distributions (e.g., location, walking speed or pre-evacuation time of each occupant).
3. The model calculates and records a set of deterministic outputs (e.g., evacuation curve, RSET, maximum queue size, etc.).
4. The new outputs are analysed together with the ones produced from previous runs; if the convergence criterion is not met, steps 2, 3 and 4 are repeated in order to generate a larger sample of stochastic outputs; if the convergence criterion is satisfied, the sample of outputs is deemed stable and representative of the analysed scenario. Thus, no additional runs are necessary and the iterative process stops.

The convergence criterion implemented in the mesoscopic model is based on inferential statistics and confidence intervals as proposed in (Tinaburri, 2022). It utilises error estimations to assess the convergence of model results, based on the theoretical background synthesised in appendix A. The method is based on the idea that the error in the prediction a stochastic model decreases as the number of repeated simulations increases, due to the law of large numbers. Therefore, to achieve an optimum balance between accuracy and computational cost, designers should define a desired confidence level and an acceptable error for their analysis, and generate repeated simulations just until when the desired accuracy is achieved. For instance, fire safety engineers may deem adequate for the scope of their analysis to run a number of simulations sufficient to predict RSET with an error of ± 10 s and a 95% degree of confidence.

In this study, the approach proposed by (Tinaburri, 2022) is slightly modified so that the convergence assessment is performed after every new model iteration instead of using clusters of simulations. Consequently, the number of repeated runs is optimised and the computational cost is reduced to the minimum. Moreover, the dynamic assessment is fully automated so that evacuation modellers can be confident about the reliability of the results without necessarily having extensive expertise in statistical analysis.

The convergence criterion works as follows:

1. A desired accuracy is specified by means of design standard error Δ_d .
2. A desired reliability is specified by means of a design confidence level $CL = 100(1 - \alpha) \%$. The associated values of α and $z_{\alpha/2}$ are calculated automatically.
3. An initial set of $n = 50$ egress simulations is generated so that z statistics are applicable regardless of the distribution of the model outcomes. An evacuation curve for every node of the network is obtained from each model run. The curve associated with the initial zone is monitored, as this is the part of the network where occupants are treated microscopically.
4. The model calculates the mean \overline{ZET} and standard deviation S_{ZET} of the sample of ZETs.
5. The model calculates the standard error Δ (half-width of the confidence interval) as:

$$\Delta = z_{\alpha/2} \frac{S_{ZET}}{\sqrt{n}} \quad \text{Equation 11 (Tinaburri, 2022)}$$

6. If $\Delta \leq \Delta_d$ convergence is achieved and the iteration process stops; if $\Delta > \Delta_d$ a new simulation is generated and steps 4, 5, 6 are repeated iteratively. Since $z_{\alpha/2}$ is constant (function of the desired confidence level) and n increases after every new run, the error Δ reduces progressively. Thus, the process is repeated until $\Delta = \Delta_d$.

A visual representation of this process is exemplified in the figures below, which has been calculated for evacuation scenario T1 presented in section 5.1.1.

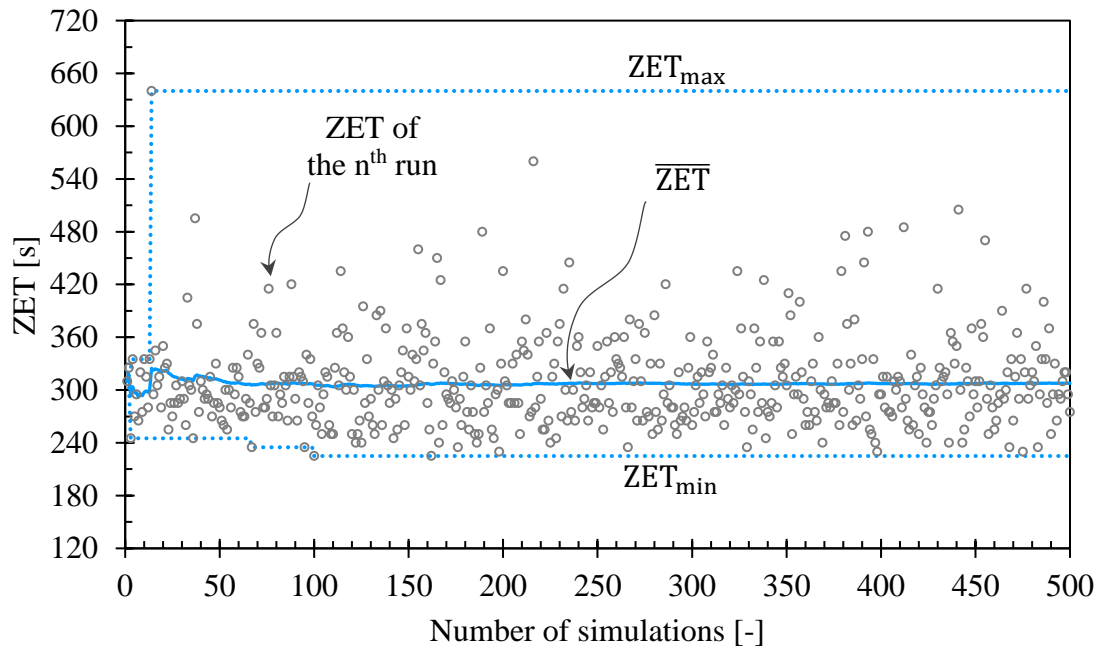


Figure 25 – Example of a sample of ZETs obtained from 500 repeated runs of the evacuation model for a single scenario. The continuous line represents the evolution of the sample mean \overline{ZET} calculated after every model run. The dotted lines represent the evolution of the max and min values of ZET

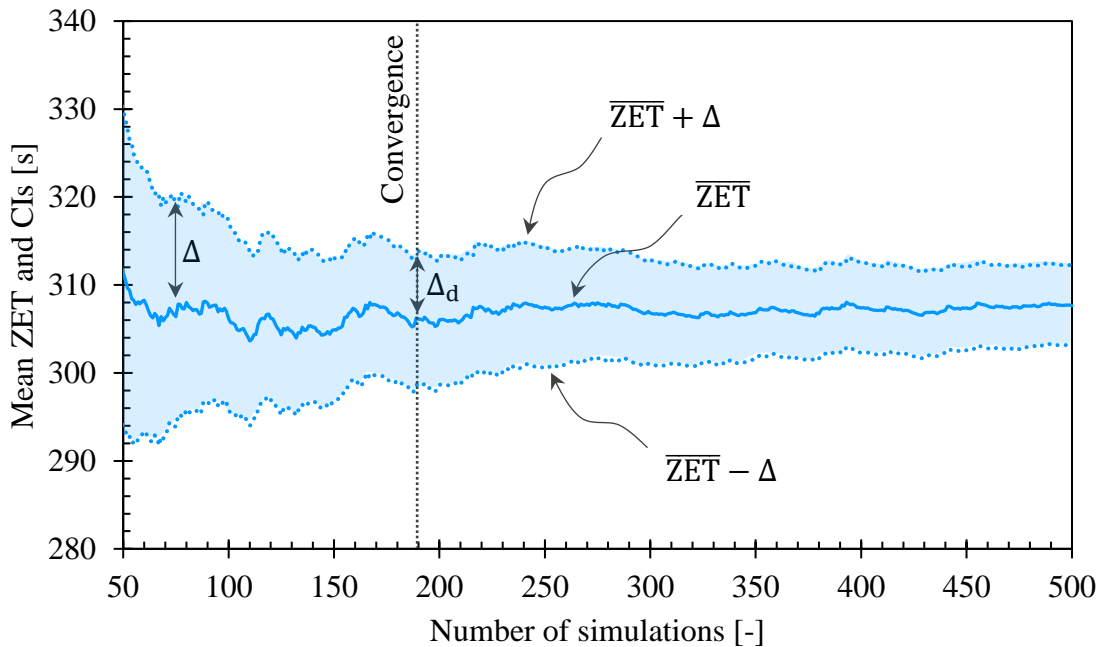


Figure 26 – Example the evolution of the sample mean \overline{ZET} (continuous line) and of the 95% confidence interval (dotted lines) calculated after every model run. The confidence interval gets narrower since the standard error Δ decreases as the number of simulations n increases. Convergence is reached when Δ falls below the design value Δ_d

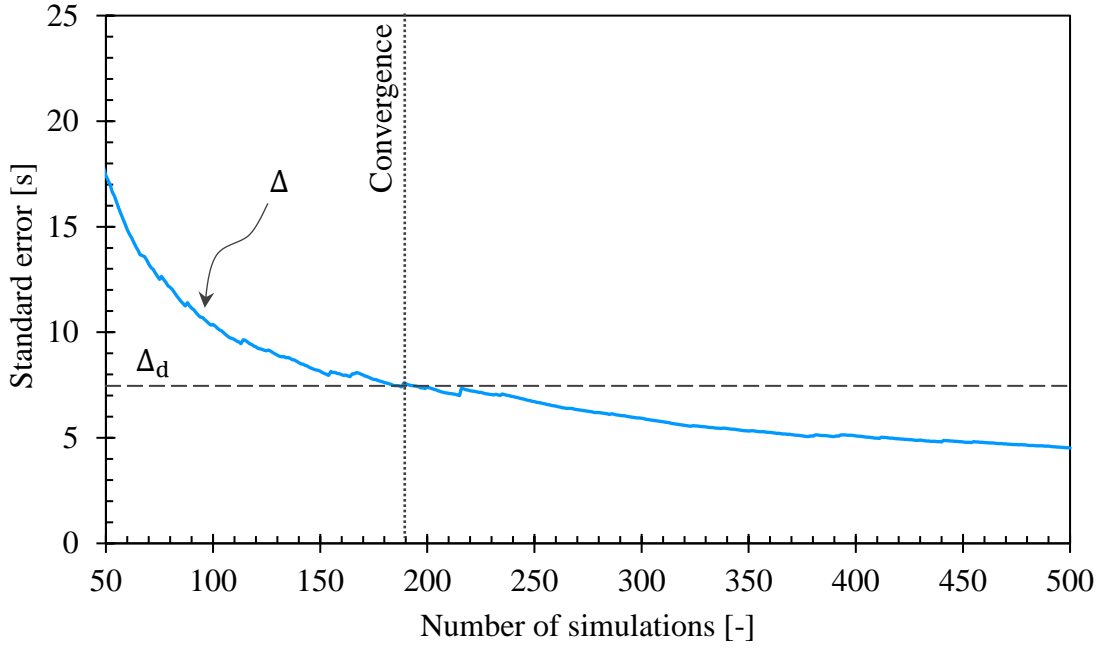


Figure 27 – Example the evolution of the standard error Δ which decreases as the number of simulations n increases. Convergence is reached when Δ falls below the design acceptable value Δ_d

When the model is run iteratively as described so far, a family of tens or hundreds of evacuation curves is generated for every node of the network before convergence is reached. However, to perform the consequences analysis in a performance-based design, modellers need to select one representative (conservative) curve.

Inferential statistics theory is used again to derive a design evacuation curve for the initial zone of the network, which will in turn produce a set of design evacuation curves for every other node. The method proposed by (Tinaburri, 2022) for the calculation of a design value of TET is applied here to derive the whole design evacuation curve.

The following process is implemented in the proposed model:

1. The set of n evacuation curves generated for the initial zone of the network is considered and the degrees of freedom $\nu = 1 - n$ are calculated. At every time step, the model calculates the mean number of occupants \bar{N} , the standard deviation s_N and the variance s_N^2 .
2. A desired reliability is specified by means of design confidence level $CL = 100(1 - \alpha) \%$. The associated values of α , $z_{\alpha/2}$, $\chi^2_{1-\alpha/2,\nu}$, $\chi^2_{\alpha/2,\nu}$, are calculated automatically.
3. At every time step, the model calculates the confidence interval for μ_N ; the upper limit is:

$$\mu_{N,\max} = \bar{N} + z_{\alpha/2} \frac{s_N}{\sqrt{n}} \quad \text{Equation 12 (Tinaburri, 2022)}$$

4. Provided that N has a normal distribution at every time step, the model calculates the confidence interval for σ_N ; the upper limit is.

$$\sigma_{N,\max} = \sqrt{\frac{(n-1)s^2}{\chi^2_{1-\alpha/2, n}}} \quad \text{Equation 13 (Tinaburri, 2022)}$$

5. A desired percentile is specified by the user, and the corresponding z score is calculated automatically by the model. Commonly used values are reported in Table 2.
6. At every time step, the model calculates the design number of occupants N_d that are still within the initial zone. These provide the design evacuation curve from the initial zone of the network, which is further used to calculate the evacuation curves at every other node and perform the consequence analysis. An example is shown in Figure 28.

$$N_d = \mu_{N,\max} + z \sigma_{N,\max} \quad \text{Equation 14 (Tinaburri, 2022)}$$

Table 2 – Values of z for commonly used percentiles

Percentile	z	Percentile	z
84.1 th	1.000	97.7 th	2.000
90.0 th	1.282	99.0 th	2.326
95.0 th	1.645	99.9 th	3.000

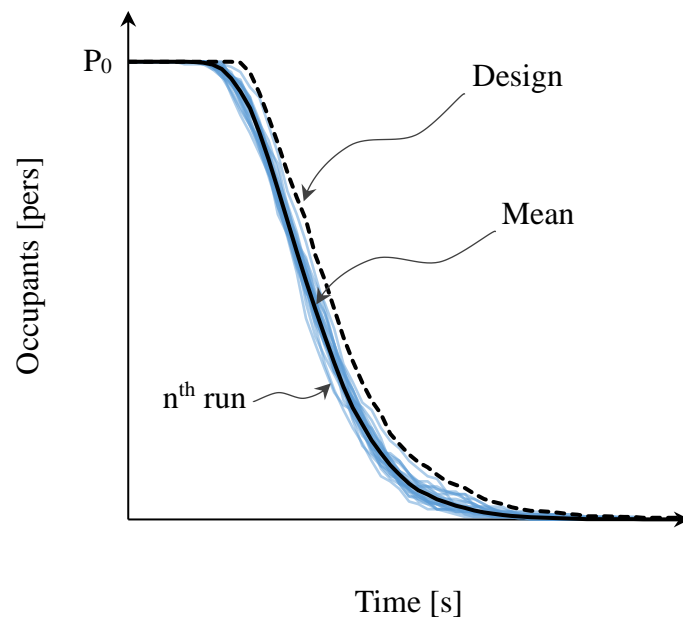


Figure 28 – Example of a sample of evacuation curves obtained from 50 repeated runs of the evacuation model for a single scenario (continuous thin lines), mean evacuation curve (continuous thick line), and the design evacuation curve for the 99th percentile (dashed line).

If the percentile is reduced, the design curve moves towards the mean curve

4.3 Iterative runs for the analysis of multiple scenarios

When fire safety engineers need to perform a consequence analysis, the iterative process presented in section 4.2 should be repeated for each of the evacuation scenarios in the event tree. The same is valid for uncertainty analyses, where the evacuation scenario is fixed but a spectrum of input parameters variations needs to be investigated.

In order to optimise this task, an automated routine is implemented within the proposed tool. The modelling process works as follows:

1. Users setup the mesoscopic network as presented in section 4.1.
2. Users generate a matrix of parameter combinations for each evacuation scenario variation. Every column of the matrix represents one of the input parameters and every row an evacuation scenario. This will be used by the model as a scenario generator.
3. Once the routine for the calculation of multiple scenarios is run, the model automatically draws one combination of parameters from the matrix, inputs them into the network, performs iterative calculations until convergence, generates and records the design evacuation curves for each node of a network. Next, a new set of input parameters is selected, and the process is repeated until all the evacuation scenarios have been modelled.

As a result, modellers get a group of evacuation curve for every node of the network, each representing a different evacuation scenario. For instance, Figure 29 shows a family of curves where ten different values for the initial number of occupants are considered.

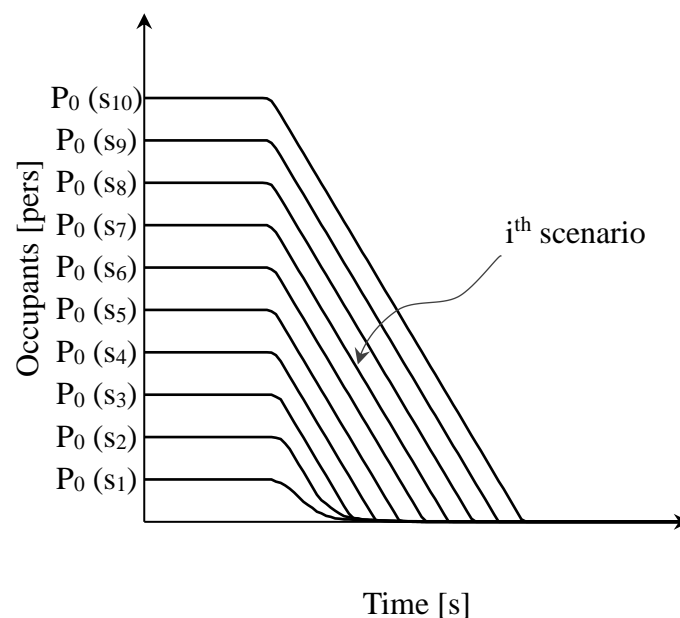


Figure 29 – Example of a group of evacuation curves obtained for the same node of a network from 10 different evacuation scenarios with variable initial occupant density

4.4 Consequence analysis

The ensemble of evacuation curves calculated at the nodes of a network informs modellers about the distribution of the occupants throughout the analysed egress path as time evolves i.e., number of persons before every node at every time step $P_k(t)$. With regards to one evacuation path, RSET corresponds the time when the evacuation curve of the last node gets to 0.

Once ASET is determined with a fire model, the consequences analysis can be performed by drawing a vertical line on the evacuation graph (Figure 30). If $ASET > RSET$ all the occupants that choose route evacuate safely. When the ASET line crosses the evacuation curves, the intersections provide the number of persons exposed to untenable conditions at every node $P_k(ASET)$. If combustion products can reach every node location, the consequences of the risk scenario along the analysed egress path can be calculated as $N = \sum P_k(ASET)$. When this analysis is performed simultaneously for multiple egress paths, the overall consequences of the fire incident can be calculated as the sum of N calculated along each network. If it is foreseen that combustion products only reach some of the network nodes (e.g., a part of the egress path is protected through fire rated walls/doors) the overall consequences N can be calculated as the sum of the occupants at the exposed nodes only.

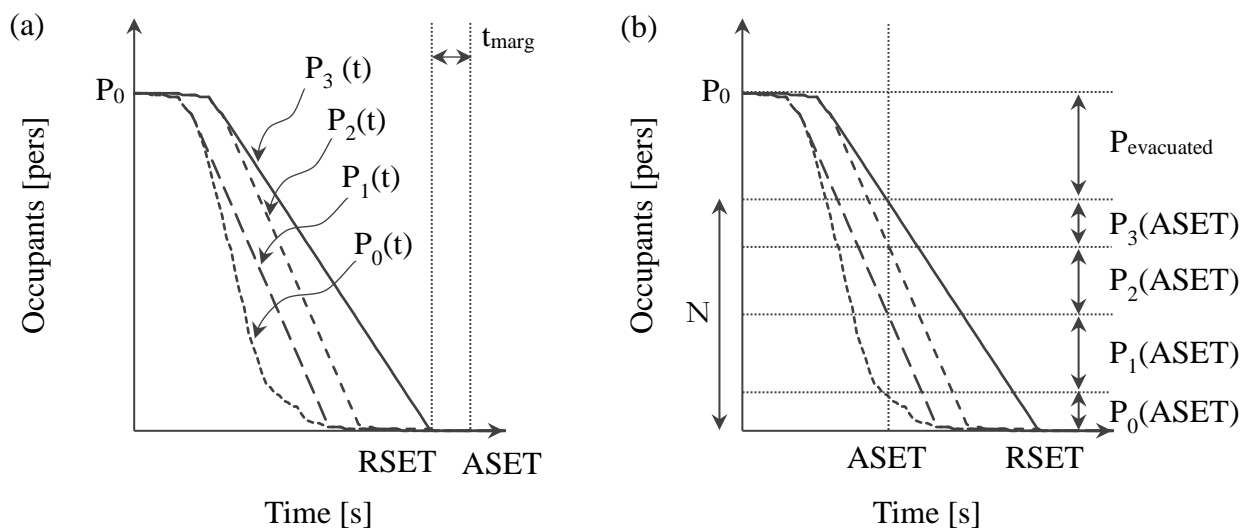


Figure 30 – Example of evacuation curve at different locations along an egress path in case of zero consequences (a) and undesired consequences (b)

5 Application of the proposed model and discussion of the results

This chapter presents the results of the proposed model when it is applied to a variety of evacuation scenarios. First, the mesoscopic model is tested with five basic scenarios characterised by simple geometries and sequences of egress components. Next, the proposed model is applied to an existing building to illustrate how networks can be constructed to represent complex facilities and test how the model performs in typical design circumstances. In the second application, the whole QRA process is performed.

The results of the proposed model are also benchmarked against the outputs produced for the same scenarios with an agent-based egress simulator, to assess how the mesoscopic simplification performs in contrast with microscopic calculations. Pathfinder version 2020.4 developed by Thunderhead Engineering is chosen for this purpose since, in addition to steering behaviours, it also implements the hydraulic model of the SFPE Handbook of Fire Protection Engineering (Thunderhead Engineering, 2021). Therefore, when simulations are run in ‘SFPE mode’, the same speed-density correlations are applied by both models, with the following main differences:

- In Pathfinder space is represented as continuous bidimensional mesh where agents can navigate autonomously around obstacles, while in the proposed mesoscopic model space is represented by a coarse network and the path around obstacles can only be considered by specifying a priori the length of nodes.
- In Pathfinder occupants are represented individually throughout the whole simulation domain, while in the proposed mesoscopic model occupants possess individual characteristics only in the initial zone, after which they are treated as a homogeneous crowd.
- In Pathfinder occupants plan autonomously and dynamically their egress path based on the distance to exits and queue conditions at the doors, while in the proposed mesoscopic model the egress path is defined a priori by the user and occupants wait in queues without rerouting.

5.1 Test scenarios

The mesoscopic model described so far is tested here in five basic scenarios, where a rectangular enclosure is followed by 1) a single exit, 2) a corridor, 3) a large room (transit), 4) a stair, and 5) a large room where multiple streams of occupants merge before the final exit.

Multiple variations of each basic scenario are also considered to account for different initial conditions (e.g., occupant density) or different configurations of egress components (e.g., door width, stair slope, etc.). These variations are useful to test the model in both free-flow and queue-controlled conditions and ensure that it is reliable over a wide range of scenarios.

For every scenario variation, the calculation is repeated for 100 runs with both the mesoscopic model and Pathfinder. This is to ensure that convergence is achieved and that the results of the two models are comparable. The mean evacuation curve is used as a benchmark for comparison.

As the mesoscopic model is developed primarily for the simulation of large gatherings, the basic scenarios are constructed to be representative of this kind of facilities.

The initial zone consists of a rectangular enclosure measuring 30 x 15 m with the exit located at the centre of the longer wall. This may represent a portion of a large open-space enclosure where the longest travel distance is between 30 and 40 m, in agreement with several regulations concerning assembly halls, such as (Italian Fire Safety Code, 2019) or (BS 9999 : 2019).

The shape of the individual travel path is chosen to be diagonal to reduce the differences in simulation results within the microscopic section of the network i.e., initial zones. This means that the differences between the outputs of the two models will arise mainly from the macroscopic/microscopic treatment of the second part of the network.

The occupant density is set to 0.5 pers/m². This is a reasonable value representing ordinary usage of facilities open to the public, which also requires short computational time (this is proportional to the number of agents in the simulation domain). Nonetheless, in the single-exit scenario, initial densities of 1 pers/m² and 2 pers/m² are also investigated. In all the other basic scenarios different flow conditions are explored by varying the dimension of egress components.

Fire regulations often prescribe automatic detection and notification systems in facilities that accommodate large crowds. In the basic test cases, the detection and notification time is set to 0 s to save computational resources without affecting the quality of the results. In fact, non-zero values only shift the evacuation curve later the timeline without modifying its shape (this only occurs when t_{d+n} is treated as a distribution which affects individual presentation times).

The unimpeded walking speed on horizontal surfaces is treated as a normal distribution with a mean $\mu = 1.19$ m/s and a standard deviation $\sigma = 0.3$ m/s. The interval from which the models sample random values is within $\mu \pm 3 \sigma$, hence includes 99.7% of the values. Therefore, the minimum and maximum value for S_{max} are respectively 0.29 and 2.09 m/s. This is in agreement with the measurements of travel speed in public places, theatres, educational centres, transport terminals, etc. reported in (ISO TR 16738 : 2009).

The pre-evacuation time is treated as a lognormal distribution. The value of the 1st and 99th percentiles are taken as 30 and 150 s in accordance to (ISO TR 16738 : 2009) for occupants that are awake and unfamiliar with the building; the use of these values also implies that the enclosure has a simple geometry and layout, automatic detection and alarm systems, and a well-developed safety management plan (B-M1-B1-A1/A2). Hence the lognormal distribution is characterised by a location value of 4.21 and a scale of 0.27.

The input parameters used to set-up the models are summarised in Table 3 and Table 4. Slight variations are described in the next sections for specific scenarios. Ultimately, the input parameters related to egress components are taken from (Gwynne & Rosenbaum, 2016) as summarised in Table 1 and Table 5.

Table 3 – Input point values for test scenarios

Parameter	Symbol	Unit	Value
Enclosure length	X	m	30
Enclosure width	Y	m	15
Path shape	PS	-	Diagonal
Occupant density	D	pers/m ²	0.5
Detection + notification time	t _{d+n}	s	0

Table 4 – Input distributions for test scenarios

Parameter	Symbol	Unit	Shape	Location	Scale	Min	Max
Unimpeded walking speed (horizontal)	S _{max}	m/s	Normal	1.19	0.30	0.29	2.09
Pre-evacuation time	t _{pre}	s	Lognormal	4.21	0.27	30	150

Table 5 – Boundary layer clearance from (Gwynne & Rosenbaum, 2016)

Egress component	Boundary layer BL [cm]
Stairways (wall or side of tread)	15
Railings, handrails	9
Theatre chairs, stadium benches	0
Corridor, ramp walls	20
Obstacles	10
Wide concourses, passageways	46
Doors, archways	15

5.1.1 Scenario T1: Doorway

First, a rectangular enclosure leading to a single exit door is analysed. In Pathfinder, the navigation mesh is composed of a single room, with an exit door on the exterior boundary (Figure 34a). When used in the SFPE mode, the agents' walking speed and door flow rates are adjusted according to the occupant density (considered uniform throughout each room). Pathfinder automatically assigns a maximum flow rate to doors, which behave as flow limiters: agents are queued or removed from the simulation domain at according to SFPE hydraulic rules (Thunderhead Engineering, 2021). In the proposed mesoscopic model, the geometry is simplified as a network composed of one zone and one node (Figure 34b).

Multiple variations of this scenario are investigated considering three different occupant densities and two alternative door sizes, combined as shown in Figure 35. A boundary layer of 15 cm is deducted from each side of the door.

After running the simulations, an initial check of the realizations of the stochastic variables is performed. The distributions of the occupants' individual coordinates (Figure 31), walking speed (Figure 32) and pre-evacuation time (Figure 33) taken from a scenario simulation show qualitatively that the proposed model assigns correctly the individual characteristics in accordance with user-specified input distributions.

The evacuation curves produced with the two models match in every variation of the scenario (Figure 35). This is because only the microscopic algorithm is invoked for the calculation of the evacuation curve. In fact, in this specific case, occupants leave the network right after the initial zone. Hence, the test demonstrates that the microscopic algorithms have been implemented correctly and produce exact results in both free-flow and queue-controlled conditions.

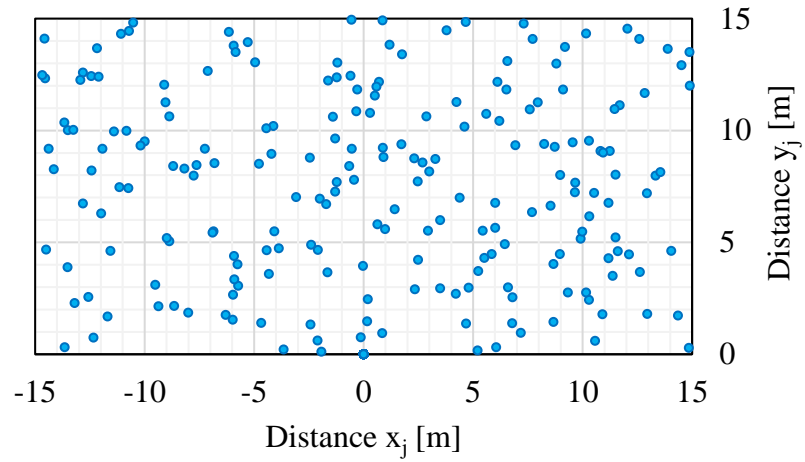


Figure 31 – Scenario T1 – Spatial distribution of occupants within the zone ($D = 0.5 \text{ pers/m}^2$)

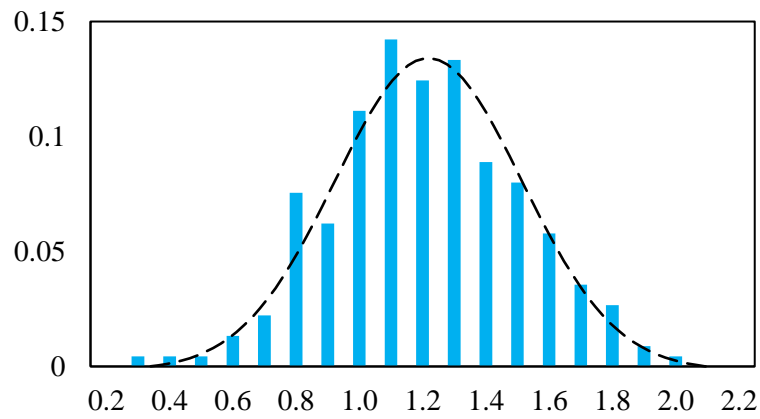


Figure 32 – Scenario T1 – Uniform distribution of individual walking speed S_j [m/s].
The dashed line is the input distribution and the histogram is the random realisation

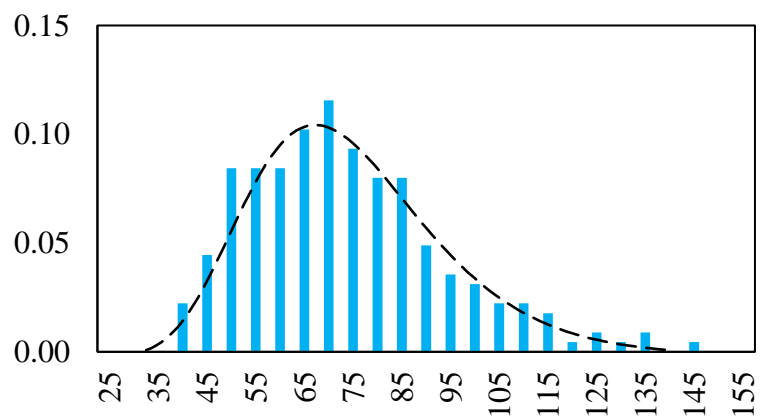


Figure 33 – Scenario T1 – Log-normal distribution of individual pre-evacuation time $t_{pre,j}$ [s].
The dashed line is the input distribution and the histogram is the random realisation

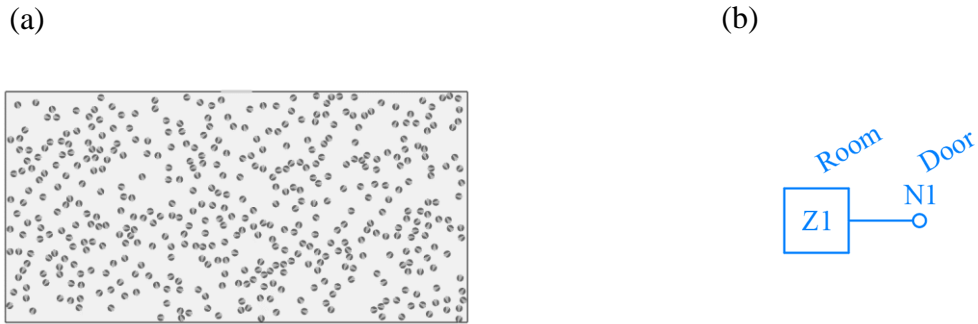


Figure 34 – Scenario T1 – Pathfinder geometry (a) and mesoscopic network (b)

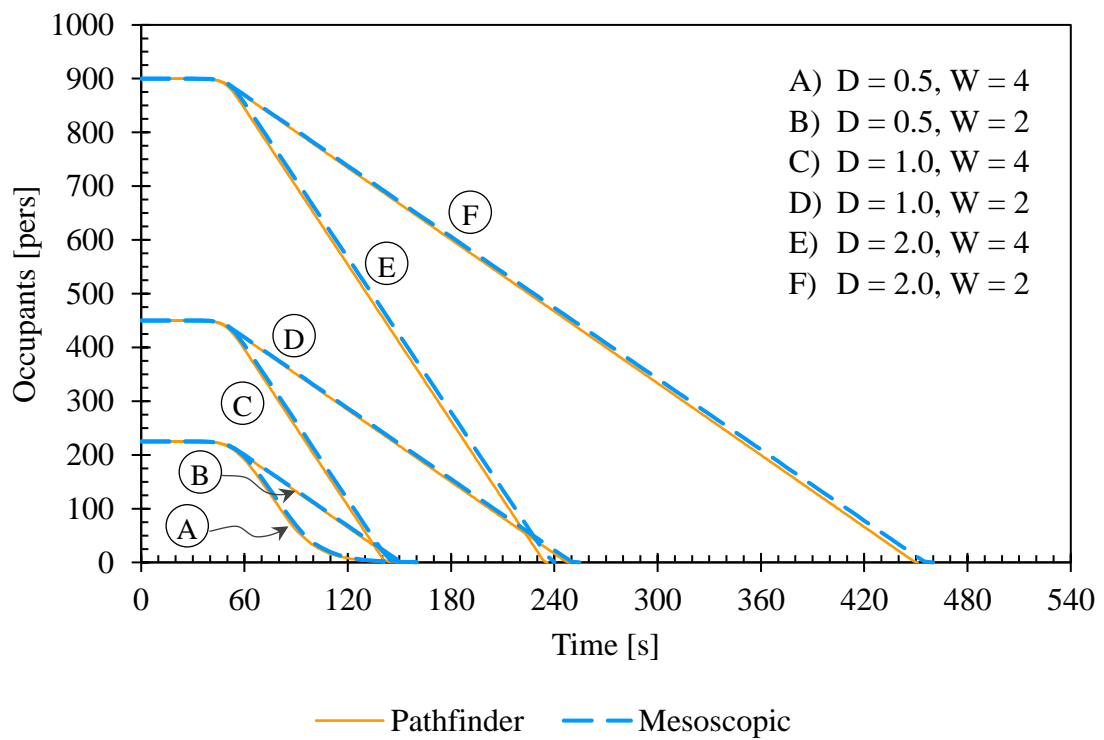


Figure 35 – Scenario T1 – Evacuation curves obtained with the proposed mesoscopic model and Pathfinder, for six combinations of occupant density D [pers/m²] and door width W [m]

5.1.2 Scenario T2: Corridor

The second test scenario is composed of one room and a corridor with two doors at its ends. Pathfinder does not include any specialized element as in the SFPE methodology, hence the corridor is modelled as a narrow room (Figure 36a). In the proposed mesoscopic model, the geometry is simplified as a network composed of one zone and three nodes (Figure 36b).

The length of the corridor is chosen as 30 m. Two alternative widths are investigated: 2 and 4 m. In both cases, 20 cm are deducted from each side of the corridor to account for the boundary layer clearance. The width of the two doors is also varied as shown in Figure 37.

The comparison of the evacuation curves T2_A and T2_B highlights good agreement of the two models (Figure 37). In fact, in these scenarios evacuation occurs in free flow conditions in every part of the network and occupants always proceed at their unimpeded walking speed. Therefore, the average value of 1.19 m/s used in node 2 of the mesoscopic model is effectively the mean of the individual unimpeded walking speeds attributed to agents in Pathfinder. In scenario T2_C and T2_D the proposed model provides a slight overprediction of $P(t)$ compared to the microscopic calculation. In fact, when Pathfinder is used, a complex density-velocity evolution emerges as follows:

1. Agents evacuate the initial zone as in scenario T1. At the first door, the flow rate of occupants is capped, and a constant stream of occupants enters the corridor (Figure 38).
2. Agents proceed at their unimpeded walking speed along the corridor, therefore they take different periods to traverse it, and they reach the exit door at different times. For example, if 10 occupants enter corridor at 0 s, some of them will reach the exit door after 20 s, some after 30 s, and others at 40 s. This means that the flow of occupants approaching the second door is different than the outflow from the first door, and varies with time as shown in Figure 39 (it would be constant as assumed by the SFPE hydraulic approach only if the occupant's velocity was constant throughout the population). As a result, since the two corridor doors have the same size, at some moments the flow is smaller than the capacity of the second door, and at some moments it is larger. In the second case, the outflow is capped and a queue of occupants forms in the corridor in front of the second door. At initial stages of the evacuation the queue grows and vanishes cyclically according to 'waves' of occupants approaching the door. At later stages the queue is steadier.
3. As the queue grows in the corridor, Pathfinder interprets it as an increase of the density (Figure 40). Therefore, occupants' walking speed is reduced accordingly (Figure 41) and the emerging corridor specific flow varies with time.

This explains why the evacuation curves T2_C and T2_D do not have a steady slope in the queue-controlled phase of the evacuation, and the discrepancies from mesoscopic results. In fact, the proposed model only accounts for an average density and walking speed along the corridor, therefore it is not able to represent the mentioned phenomena. Nevertheless, it is possible to notice that in this test case the average values used for mesoscopic calculations coincide with the time-averaged results of Pathfinder. Consequently, the final point of the curves coincides, while at previous stages of the egress process the mesoscopic model produces conservative estimates.

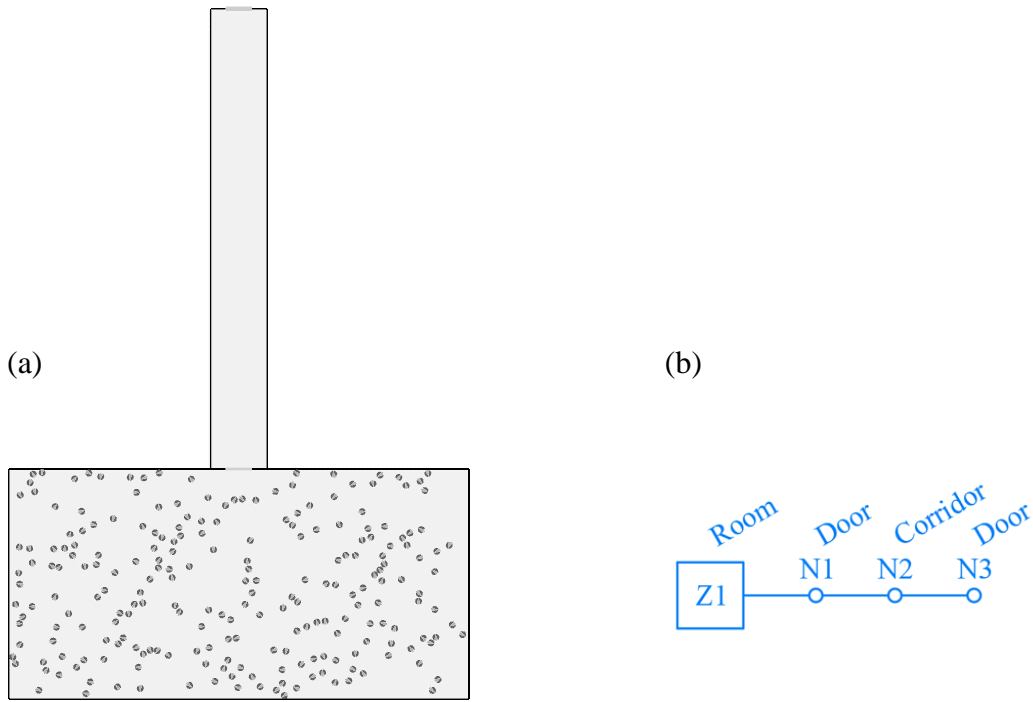


Figure 36 – Scenario T2 – Pathfinder geometry (a) and mesoscopic network (b)

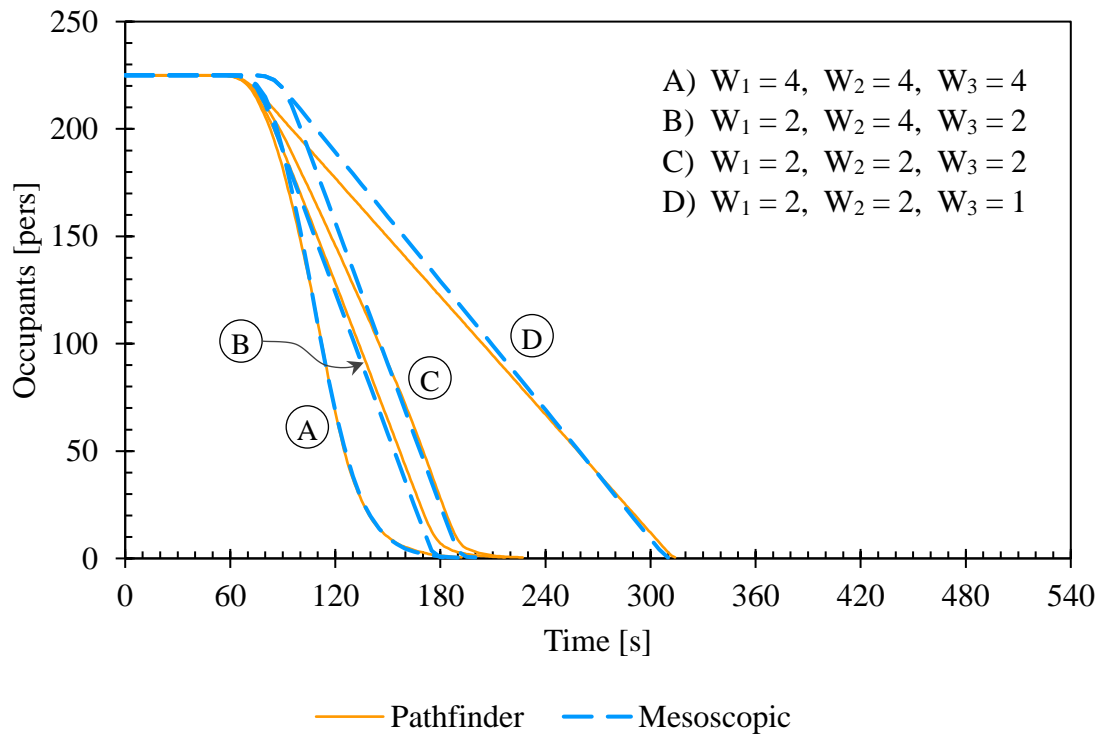


Figure 37 – Scenario T2 – Evacuation curves obtained with the proposed mesoscopic model and Pathfinder, for four combinations of door and corridor width. W_1, W_2, W_3 are respectively the width of the first door, of the corridor, and of the final exit [m]

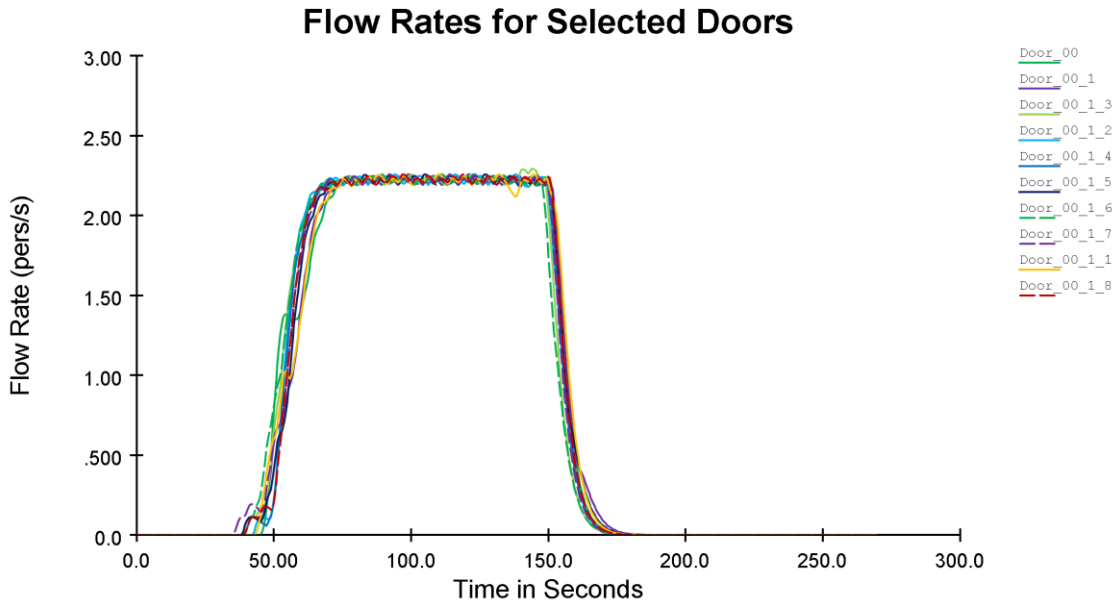


Figure 38 – Scenario T2 – Results from 10 randomly-chosen Pathfinder simulations representing the flow rate of occupants through the first door

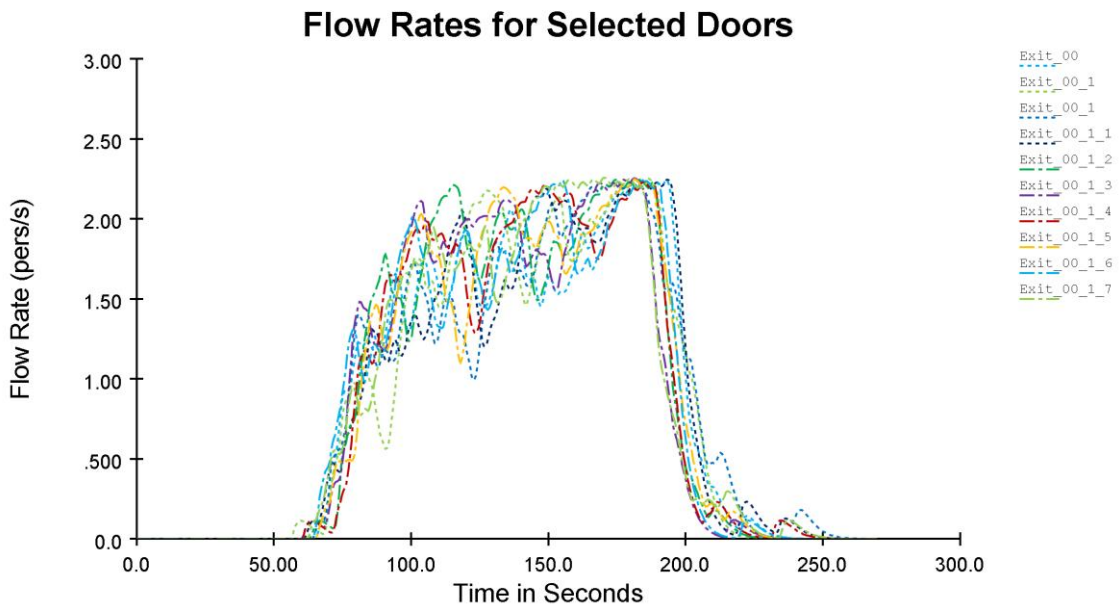


Figure 39 – Scenario T2 – Results from 10 randomly-chosen Pathfinder simulations representing the flow rate of occupants through the second door

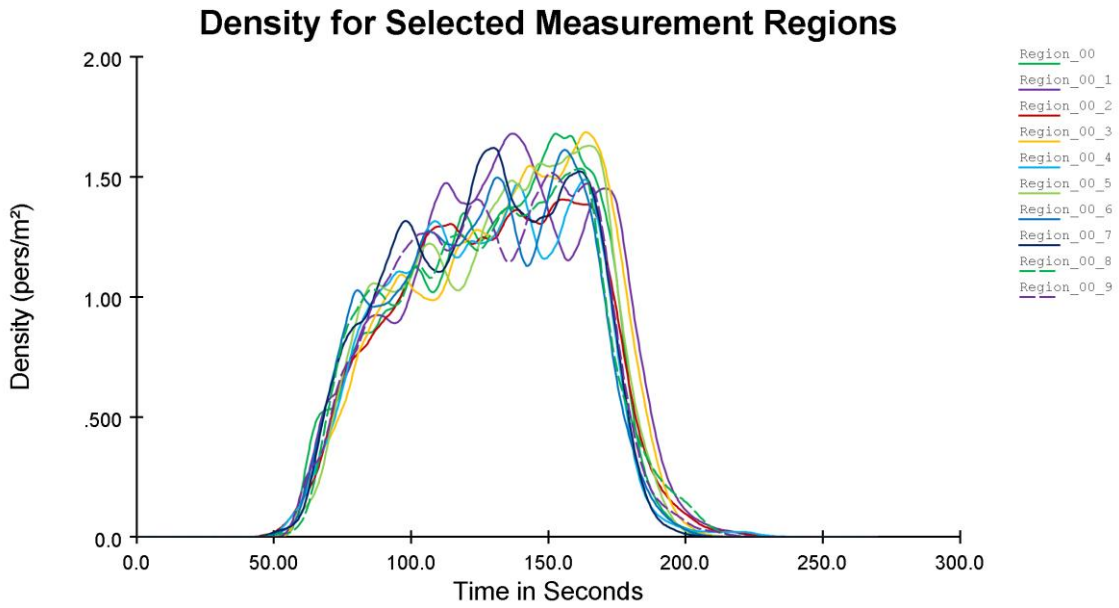


Figure 40 – Scenario T2 – Results from 10 randomly-chosen Pathfinder simulations representing the occupant density in the corridor

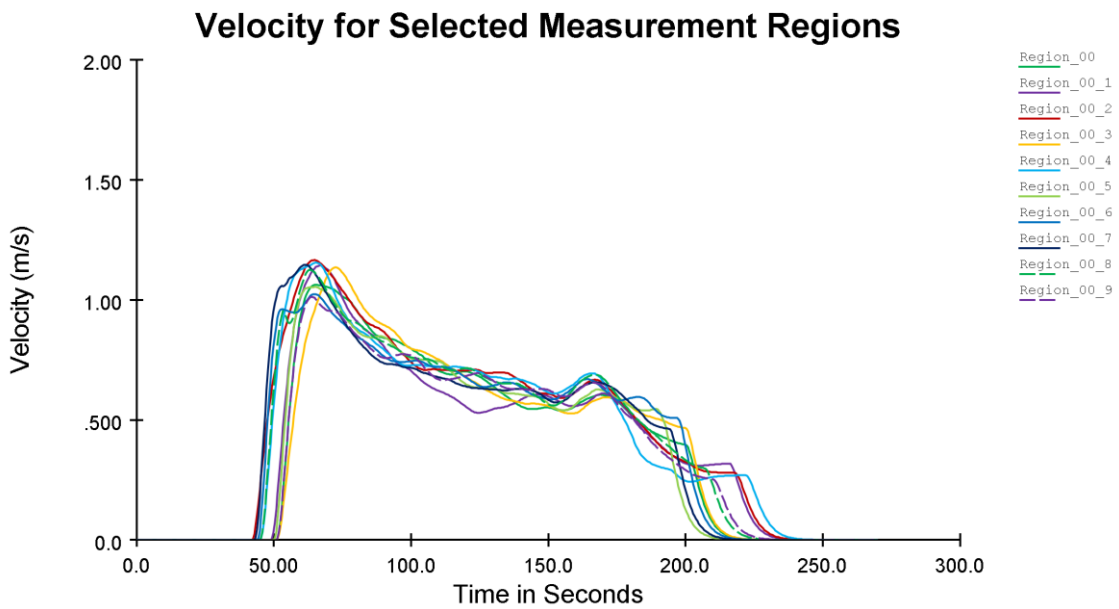


Figure 41 – Scenario T2 – Results from 10 randomly-chosen Pathfinder simulations representing the average walking speed in the corridor

5.1.3 Scenario T3: Transit

The third test scenario is composed of two adjacent enclosures connected by a door. Occupants are initially located in one of the two enclosures and need to traverse the second one to reach the final exit. In Pathfinder the geometry is constructed via two rooms and two doors (Figure 42a). In the proposed mesoscopic model, the first room is set as the initial zone, while the second room is represented as a transit node; the doors are nodes as well. (Figure 42b).

Also in this case, the resulting evacuation curves match precisely (Figure 43) since the occupants traverse the transit area in free-flow conditions.

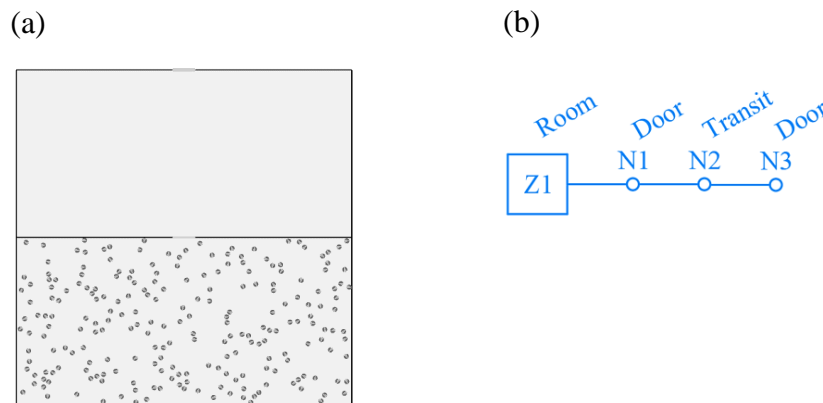


Figure 42 – Scenario T3 – Pathfinder geometry (a) and mesoscopic network (b)

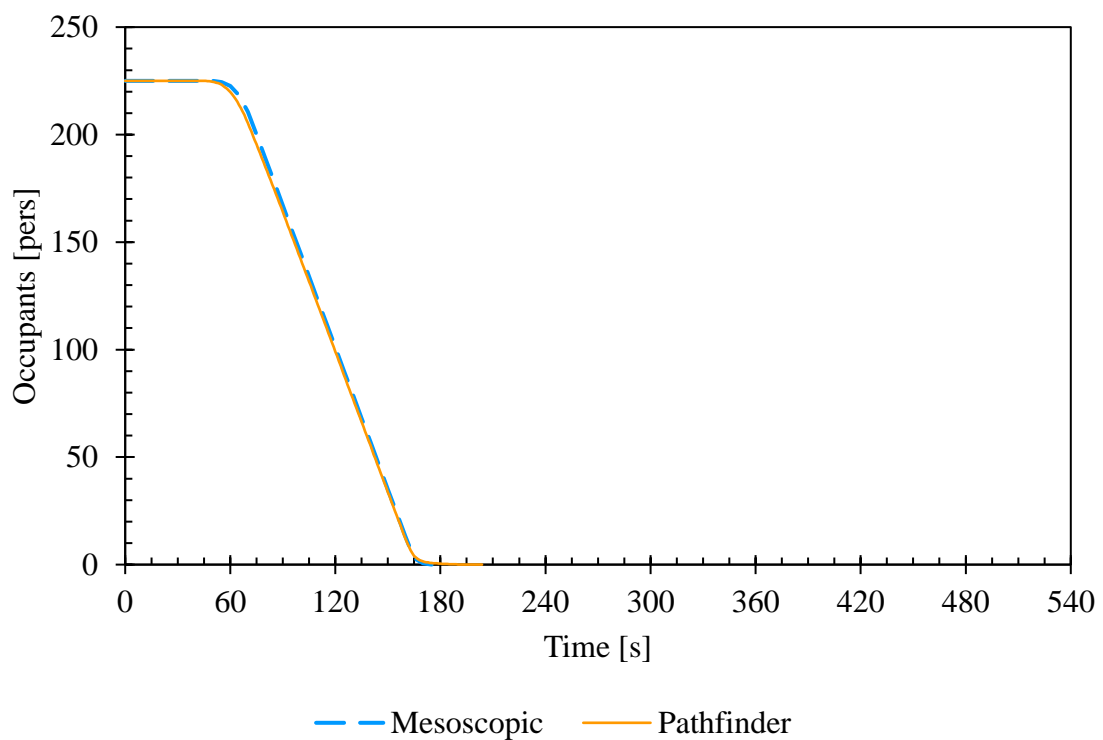


Figure 43 – Scenario T3 – Evacuation curve obtained with the proposed mesoscopic model and Pathfinder, for a transit

5.1.4 Scenario T4: Stair

Scenario T4 is designed to test the prediction of movement on stairs, in a modified version of the Test 11 from ISO 20414 (International Organisation for Standardization, 2020). In Pathfinder, stairs behave like specialised rooms where the flow of occupants is limited by the stair slope (defined through its riser and tread dimensions). Density on the stairs limits both occupants' flow and walking speed along that component (Thunderhead Engineering, 2021). The model for this test is composed of the initial room, a door, a lower landing, a stair, an upper landing, and the final exit (Figure 44a). The same sequence of nodes is modelled with the proposed mesoscopic model (Figure 44b).

The elevation of the stair is chosen as 3.3 m. The diagonal length is about 7 m and varies according to the riser and tread geometry. Two alternative slopes are investigated: a stair with 19.1 cm (7.5 in) risers and 25.4 cm (10 in) treads, and a stair with 16.5 cm (6.5 in) risers and 33 cm (13 in) treads. Two alternative stair widths of 2 and 4 m are also investigated, considering a 15 cm boundary layer on each side. It is assumed that the doors and the landings have the same width W of the stair.

As in the corridor case, the mesoscopic/microscopic representation of the crowd produces discrepancies between the two models' outputs (Figure 45 and Figure 46). The difference is due to complex speed-density evolutions that emerge when Pathfinder keeps track of individual speed of occupants. In fact, when Pathfinder simulations are repeated by setting a walking speed $S_{\max} = 1.19$ m/s constant across the population, the discrepancies between the two models reduce considerably.

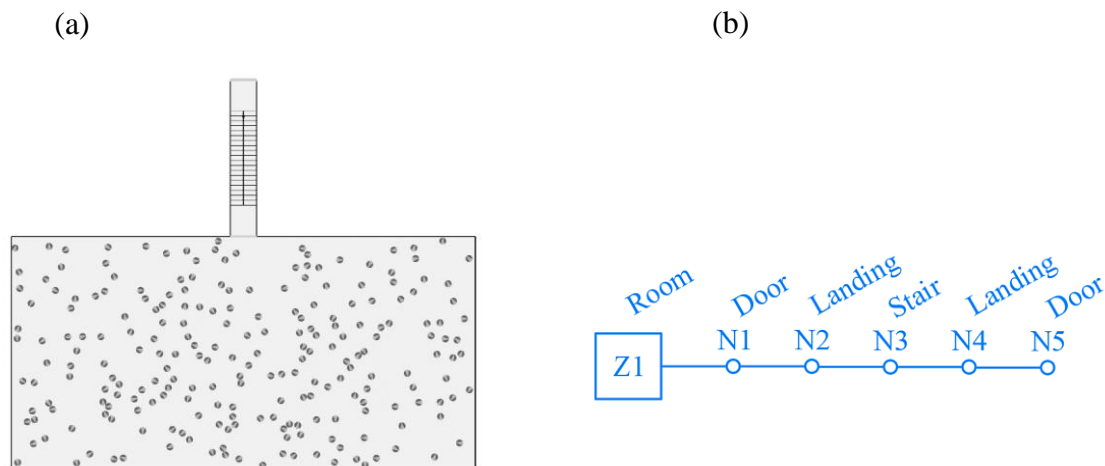


Figure 44 – Scenario T4 – Pathfinder geometry (a) and mesoscopic network (b)

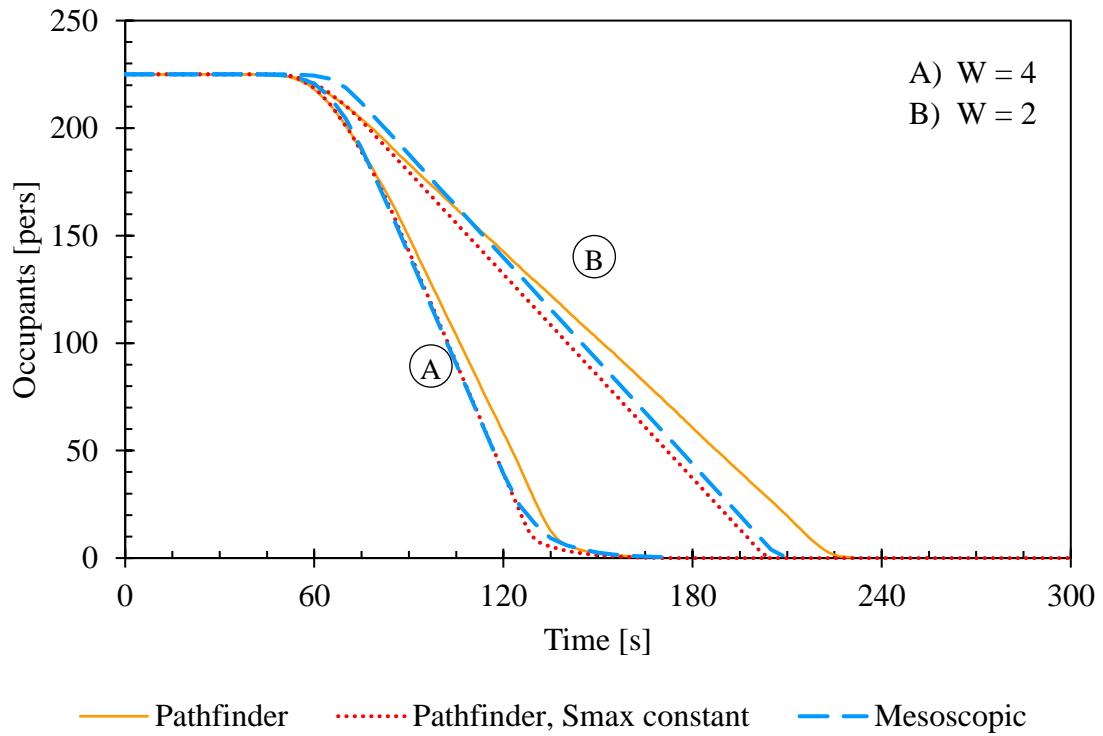


Figure 45 – Scenario T4 – Evacuation curves obtained with the proposed mesoscopic model and Pathfinder, for a stair with 19.1 cm (7.5 in) risers and 25.4 cm (10 in) treads

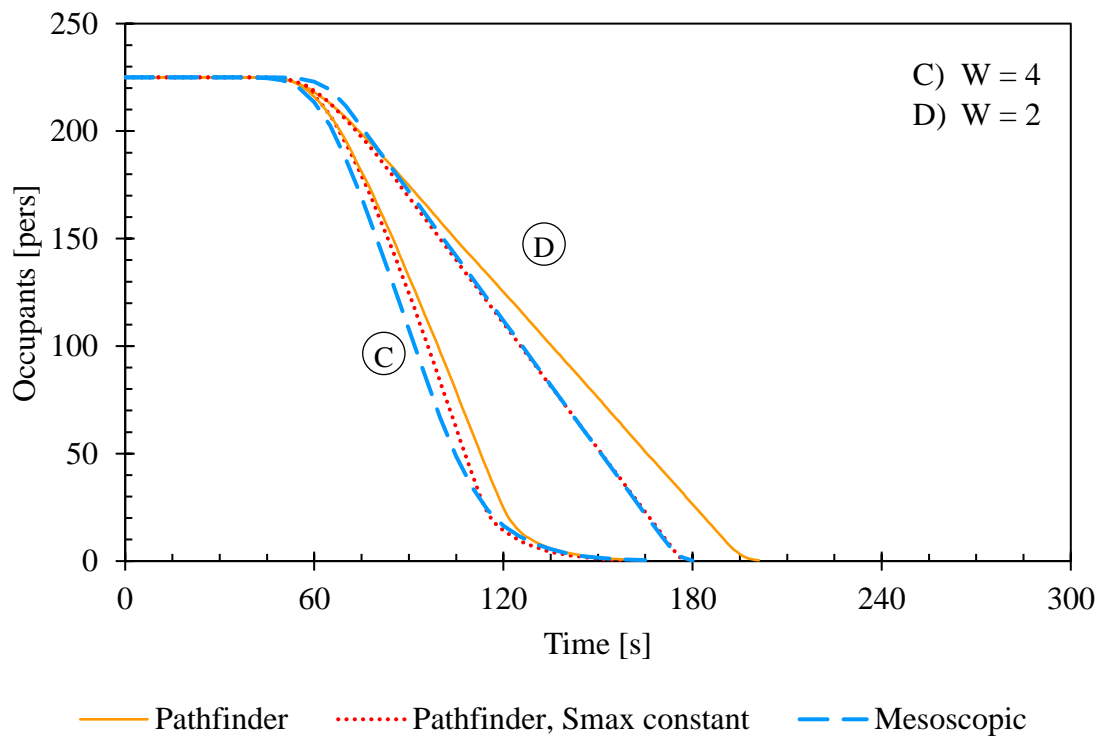


Figure 46 – Scenario T4 – Evacuation curves obtained with the proposed mesoscopic model and Pathfinder, for a stair with 16.5 cm (6.5 in) risers and 33 cm (13 in) treads

5.1.5 Scenario T5: Merging point

In the fifth test scenario, two groups of occupants are initially located in two different enclosures and will need to traverse a third during evacuation. Consequently, two streams of occupants will merge before the final exit. In Pathfinder the geometry is composed of three rooms, two internal doors, and a final exit (Figure 47a). In the proposed mesoscopic model, the initial part of the network is composed of two parallel branches with an initial zone, a door node and a transit node; next, a virtual node represents the location in the common room where the flows add up, followed by the final exit node (Figure 47b).

Two variations of the scenario are analysed. In the first one, a simultaneous evacuation is modelled, with both groups of occupants having the same pre-evacuation time distribution. In the second case, the same distributions are used, but the movement of one of the two groups is delayed in order to simulate a phased evacuation. A delay $\Delta t = 90$ s is chosen so that the second group of occupants starts to evacuate before the first group has completed evacuation.

Figure 48 shows that the evacuation curves produced by the two models match.

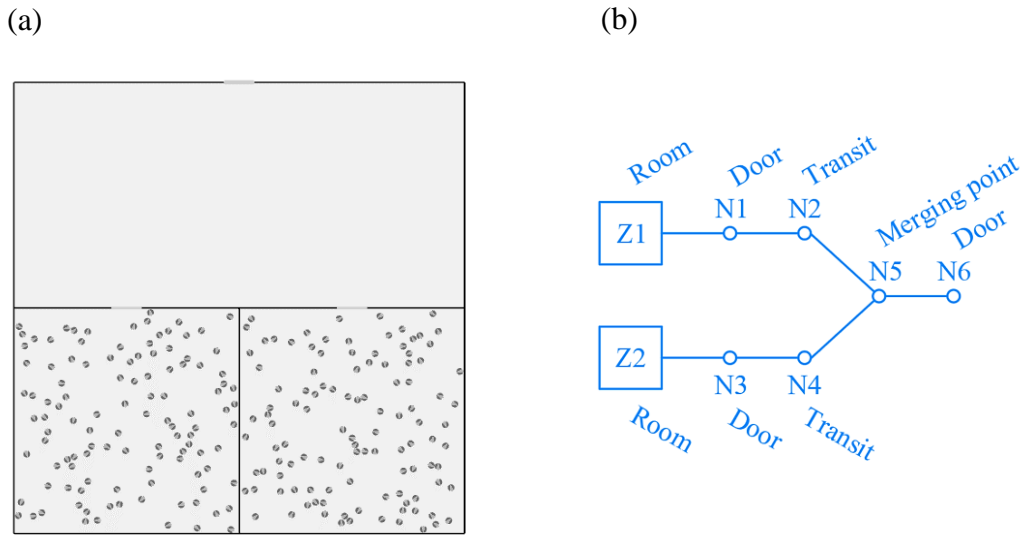


Figure 47 – Scenario T5 – Pathfinder geometry (a) and mesoscopic network (b)

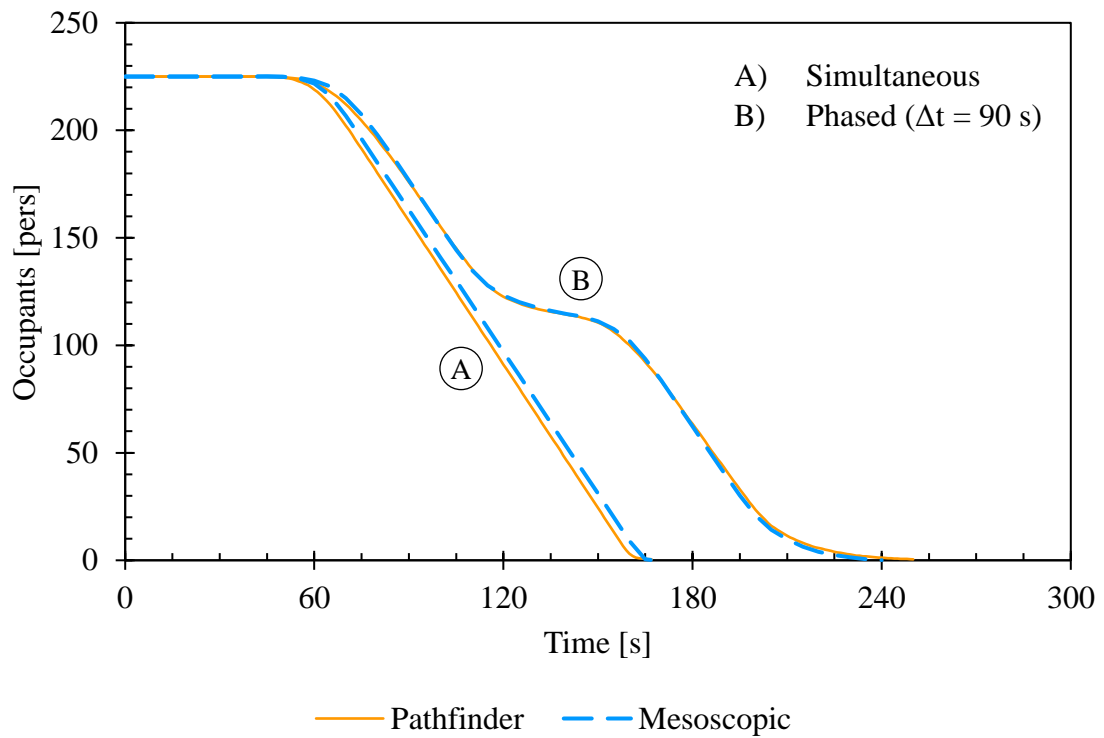


Figure 48 – Scenario T5 – Evacuation curve obtained with the proposed mesoscopic model and Pathfinder, for two groups of occupants merging for simultaneous and phased evacuation.

5.2 Case study

In this chapter the proposed model is applied to a real case study which consists of a food court located within an Italian train station. A performance-based approach to fire safety design is necessary to support the renovation of this portion of the train station since the egress routes do not fully comply with prescriptive regulations. Therefore, the scope of the analysis is to demonstrate that the facility is safe despite the non-conformities. For this purpose, a quantitative risk assessment is carried out to calculate the risk for the building occupants of being exposed to combustion products due to a lack of protected egress routes. An ASET/RSET analysis is performed using the proposed model to determine the consequences of various risk scenarios.

The calculations presented in this chapter should only be intended as a demonstration of the capabilities of the proposed evacuation model when it is used for the fire safety design of an existing building. Although realistic, some design assumptions and model inputs do not necessarily reflect the real characteristics of the facility or the actual fire risk.

5.2.1 Description of the facility

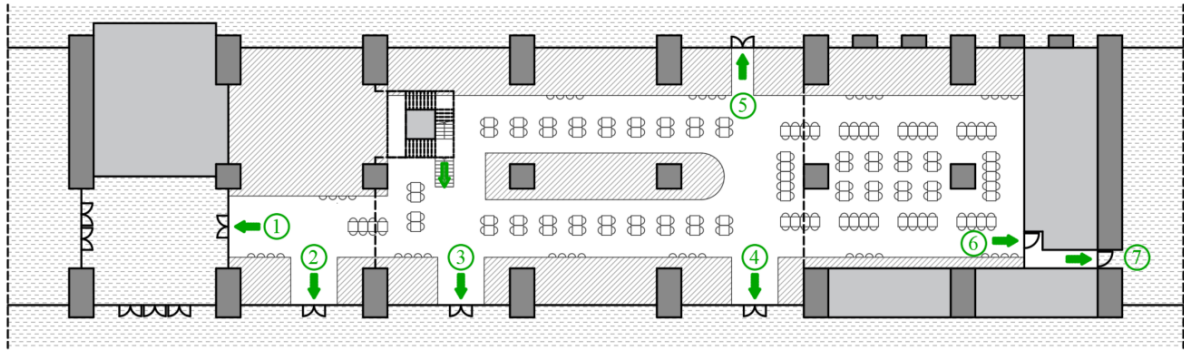
The analysed food court consists of three levels: a ground floor of about 1200 m², a first floor of about 360 m² and a second floor with a surface of about 250 m² (Figure 49). Every floor has a simple open-plan layout. Multiple vendors cook and sell food along the perimeter of every floor. Clients can then consume the meals directly at the counter or in common dining areas equipped with tables and chairs. Most of the kitchens of the food vendors are open towards food consumption and circulation areas.

The three floors are open towards each other and connected by an open stair, therefore they are all comprised in the same fire compartment. This is separated from the adjacent areas of the train station, hence only the food court is analysed in this study. The food court enclosure can be schematised by a bigger volume (47 x 20 x 14.2 m) comprising the majority of the ground floor and the two upper floors, and a smaller volume (18 x 17 x 4.5 m) which includes the remaining part of the ground floor.

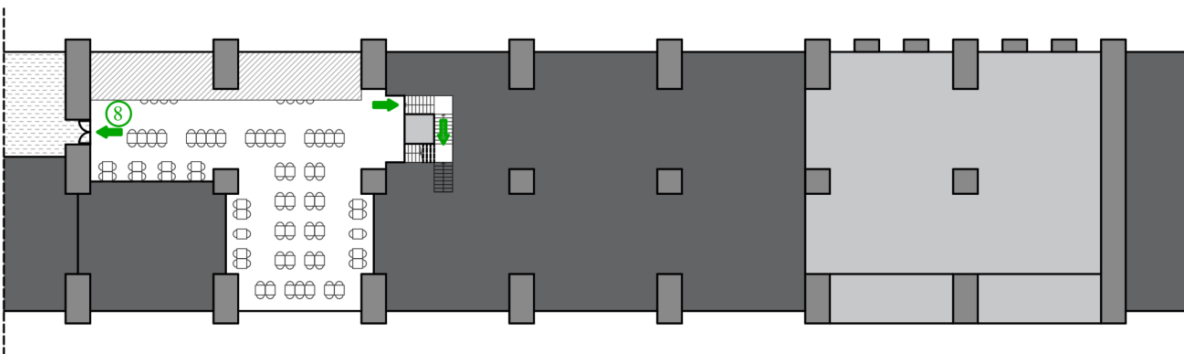
Evacuation from the second floor occurs through the open stair, while the occupants located at the first floor have two alternatives: the open stair or an exit which leads to an adjacent fire compartment. At ground level evacuation occurs through six exits that are uniformly distributed across the area. Occupants are considered safe as soon as they have left the food court.

The entire compartment is equipped with an automatic smoke detection and notification system (SDN) and mechanical smoke and heat control systems (SHC). An automatic fire suppression (FS) system is installed in the kitchens only.

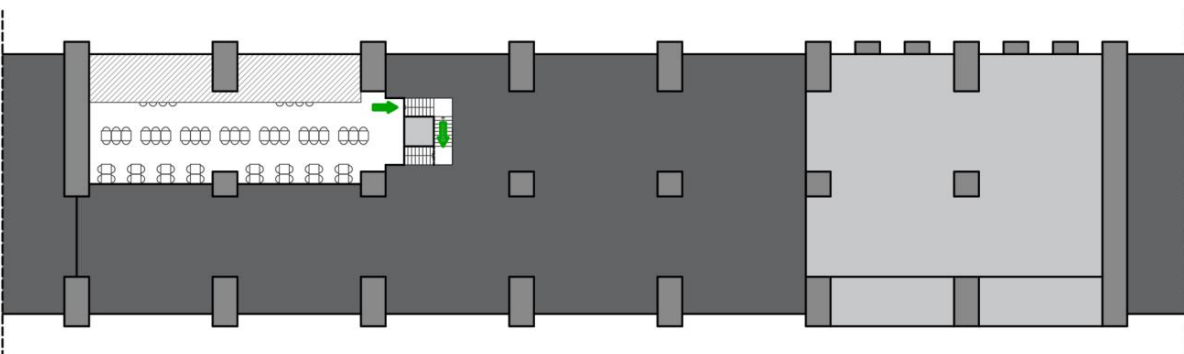
The food court is open to the public and most of the occupants are the visitors in transit through the train station. Therefore, it is expected that the majority of them is unfamiliar with the facility. The occupant density is expected to vary greatly throughout the opening hours and to be affected by the train time schedule. A limited number of vendors and employees is also present, which are familiar with the facility and trained for emergency procedures. Occasional presence of occupants with sensory, cognitive, or physical impairments is possible. However, these are not explicitly included in the evacuation simulations as it is assumed that specific procedures are in place for the evacuation of these occupants.



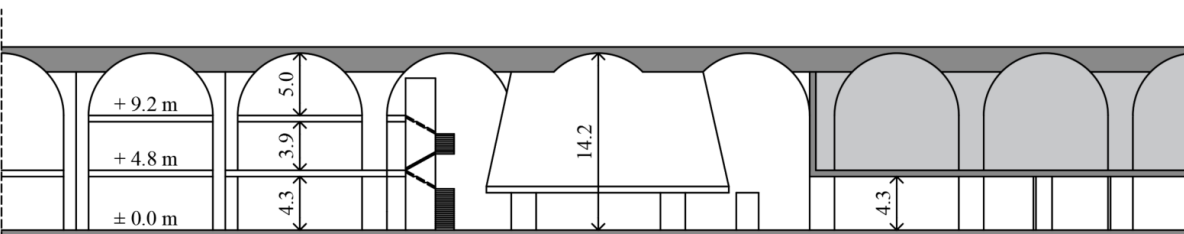
GROUND FLOOR (± 0 m)



FIRST FLOOR (+ 4.8 m)



SECOND FLOOR (+ 9.2 m)



SECTION

- | | | | |
|------------------|---------------------|----------------------|-------------|
| CIRCULATION | OTHER FACILITIES | VOID ON LOWER FLOORS | EGRESS PATH |
| FOOD PREPARATION | STRUCTURAL ELEMENTS | SAFE PLACE | DOOR NUMBER |

Figure 49 – Case study – Floor plans and cross section of the food court

5.2.2 Objectives and performance criteria

The analysis addresses life safety of people potentially exposed to a fire in the facility. It is conducted with quantitative risk analysis methods. First, an event tree is constructed to obtain a complete set of risk scenarios for the facility. Then, likelihoods are calculated for each scenario. Next, unwanted consequences are calculated with an ASET/RSET analysis using the zero-exposure method. Finally, a FN curve is produced to present the risk resulting from a fire in the food court. If the calculated risk is greater than a value of 10^{-5} , the design of fire safety measures is considered unacceptable; between 10^{-5} and 10^{-3} the risk is considered tolerable only if further risk reduction is impracticable (ALARP region); below 10^{-3} the risk level is broadly acceptable (Vrijling, van Hengel & Houben, 1995).

5.2.3 Event tree

The following basic sequence of events is considered based on the characteristics of the facility:

- An accidental fire ignites with flaming combustion with an expected frequency $1 \cdot 10^{-4} \text{ year}^{-1}$.
- Trained staff is unable to suppress the fire, which progressively spreads to adjacent fuels.
- Smoke builds-up and activates the automatic detection system; this in turn activates the notification system and the smoke and heat control system.
- Temperature builds-up and activates the suppression system.

However, the risk assessment is performed also considering the potential failure of one or more of the fire protection measures. In particular, it is assumed that:

- The detection and notification system may fail with a probability of 0.1.
- The mechanical smoke and heat control system may fail with a probability of 0.15.
- The automatic suppression system may fail with a probability of 0.05.

The probabilities of failure are derived from (ISO/TS 16733 : 2006) and adjusted to the specific case using expert judgment.

Moreover, due to the type and location of the facility, it is expected that the fire-related risk for the occupants is greatly affected by the time of the day when the incident occurs, hence the initial occupant load. Therefore, five levels of density are considered as assumed in appendix D:

- Very low, with a probability of 0.11.
- Low, with a probability of 0.18.
- Medium, with a probability of 0.35.
- High, with a probability of 0.18.
- Very high, with a probability of 0.18.

The resulting event tree consists of 30 risk scenarios as shown in Figure 50. The detailed description of every fire and evacuation scenario associated to each risk scenario can be found in appendix D.

Initiating event	Detection + notification	Smoke control	Fire control	Initial density	Risk scenario	Fire scenario	Evacuation scenario	
Fire 1.0E-04	Success 0.90	Success 0.85	Success 0.95	Very low	0.11	S01	F01	E01
				Low	0.18	S02	F01	E02
				Medium	0.35	S03	F01	E03
				High	0.18	S04	F01	E04
				Very high	0.18	S05	F01	E05
		Failure 0.05	Very low	0.11	S06	F02	E01	
			Low	0.18	S07	F02	E02	
			Medium	0.35	S08	F02	E03	
			High	0.18	S09	F02	E04	
			Very high	0.18	S10	F02	E05	
	Failure 0.10	Failure 0.15	Success 0.95	Very low	0.11	S11	F03	E01
				Low	0.18	S12	F03	E02
				Medium	0.35	S13	F03	E03
				High	0.18	S14	F03	E04
				Very high	0.18	S15	F03	E05
		Failure 0.05	Very low	0.11	S16	F04	E01	
			Low	0.18	S17	F04	E02	
			Medium	0.35	S18	F04	E03	
			High	0.18	S19	F04	E04	
			Very high	0.18	S20	F04	E05	
	Failure 0.10	Failure 1.00	Success 0.95	Very low	0.11	S21	F03	E06
				Low	0.18	S22	F03	E07
				Medium	0.35	S23	F03	E08
				High	0.18	S24	F03	E09
				Very high	0.18	S25	F03	E10
		Failure 0.05	Very low	0.11	S26	F04	E06	
			Low	0.18	S27	F04	E07	
			Medium	0.35	S28	F04	E08	
			High	0.18	S29	F04	E09	
			Very high	0.18	S30	F04	E10	

Figure 50 – Case study – Event tree

5.2.4 Evacuation modelling of a single scenario

In this section, evacuation scenario E05 is analysed with both the proposed model and Pathfinder used in SFPE mode to compare the two approaches when applied to a realistic design situation.

The geometry generated with Pathfinder consists of three rooms, each corresponding to one floor of the facility, connected by the open stair. When the proposed mesoscopic model is used, the building is schematised through 6 networks leading to the available final doors. A detailed description of the setup of two evacuation models can be found in appendix E.

One hundred runs of both models are performed, and the outputs are compared using the mean evacuation curves, similarly to what has been done for test cases. The outputs obtained for the six final doors are presented in Figure 51 to Figure 56, which show a very good agreement between the two models. This means that, in similar design situation, the network representation and the mesoscopic simplification do not have a significant impact on the results.

Figure 57 and Figure 58 present two additional evacuation curves derived for intermediate nodes of network 1. The curve represented in Figure 57 provides, for every time step, the number of occupants that still need to evacuate the second floor; this should be compared with the egress time available at the second floor before the smoke layer reaches an elevation $z = 9.2 + 2.0 = 11.2$ m. Similarly, the curve presented in Figure 58 provides the number of occupants remaining at the first floor, and should be compared with the time when smoke descends below $z = 4.8 + 2.0 = 6.8$ m. In these cases, the curves obtained with two models do not show a good agreement, with the proposed model underestimating the number of occupants when compared with Pathfinder. The discrepancies can be explained by the density-speed interactions that emerge when agents are represented microscopically as highlighted in sections 5.1.4. In this case, these are also enhanced by the presence of multiple streams of occupants merging along the stair.

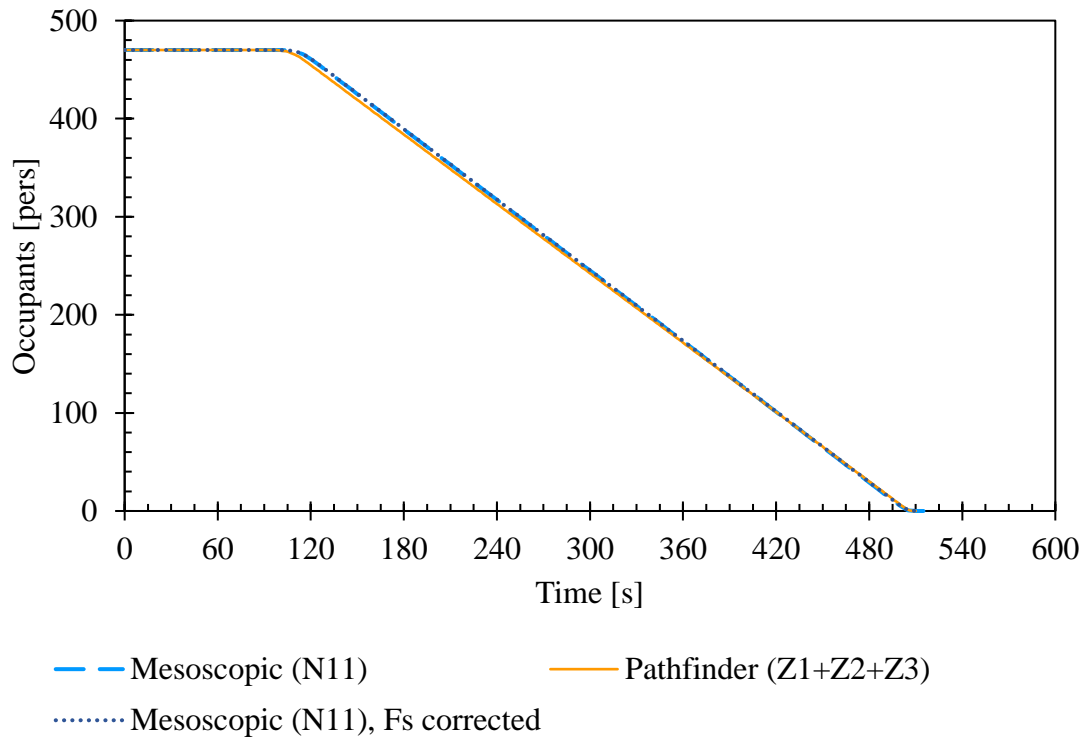


Figure 51 – Case study, Network 1 – Evacuation curve obtained with the proposed mesoscopic model and Pathfinder. The curve represents the sum of the occupants of zones 1, 2 and 3

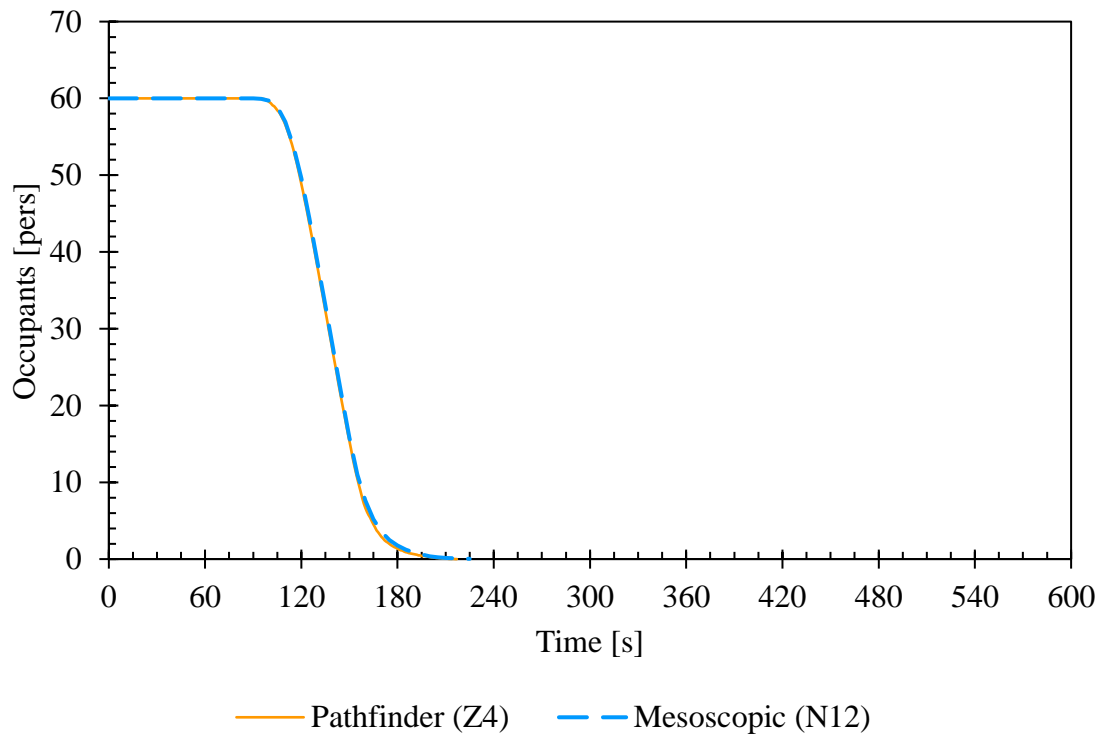


Figure 52 – Case study, Network 2 – Evacuation curve obtained with the proposed mesoscopic model and Pathfinder

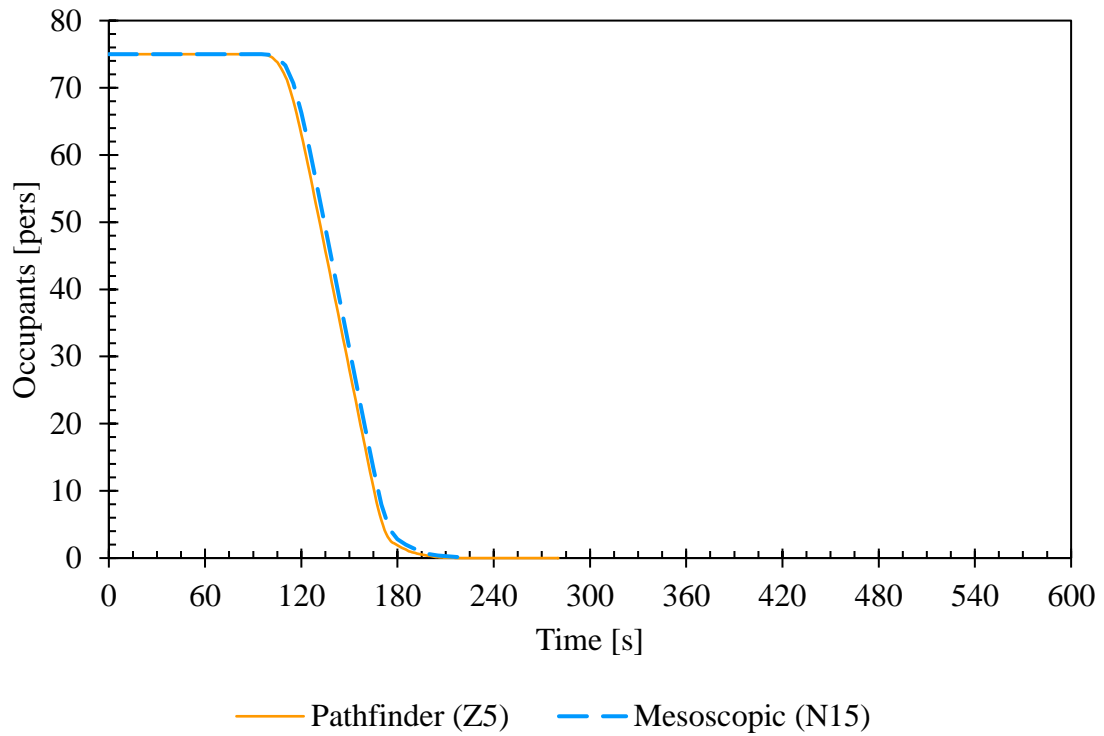


Figure 53 – Case study, Network 3 – Evacuation curve obtained with the proposed mesoscopic model and Pathfinder

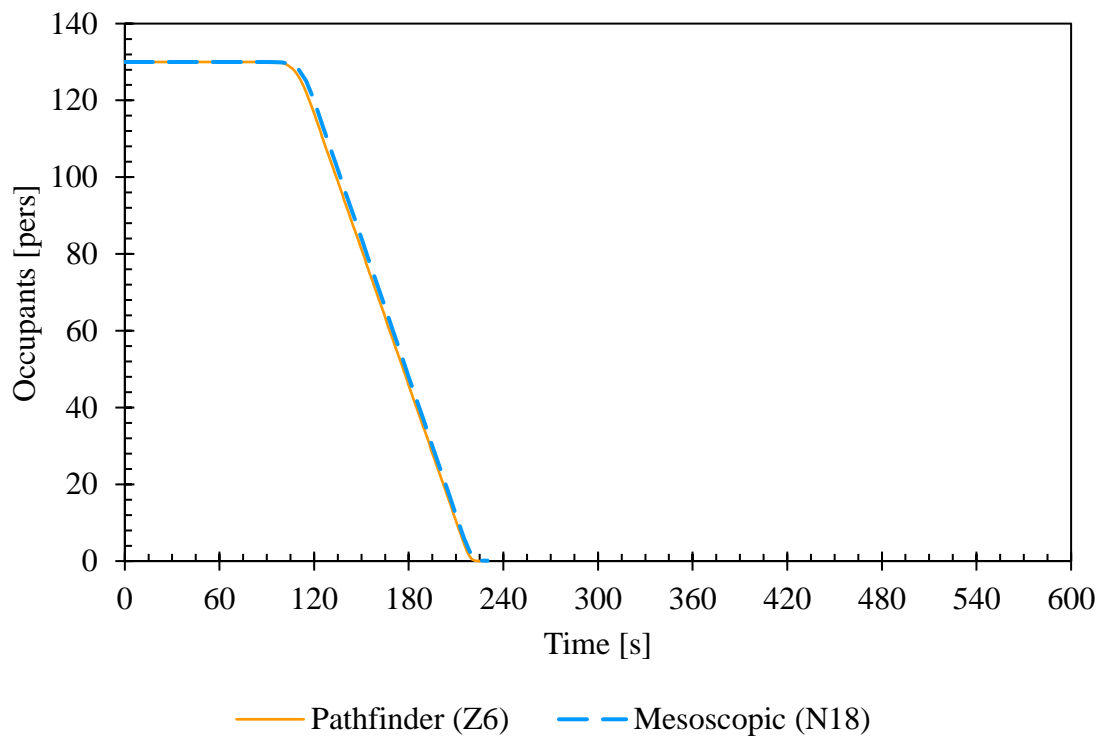


Figure 54 – Case study, Network 4 – Evacuation curve obtained with the proposed mesoscopic model and Pathfinder

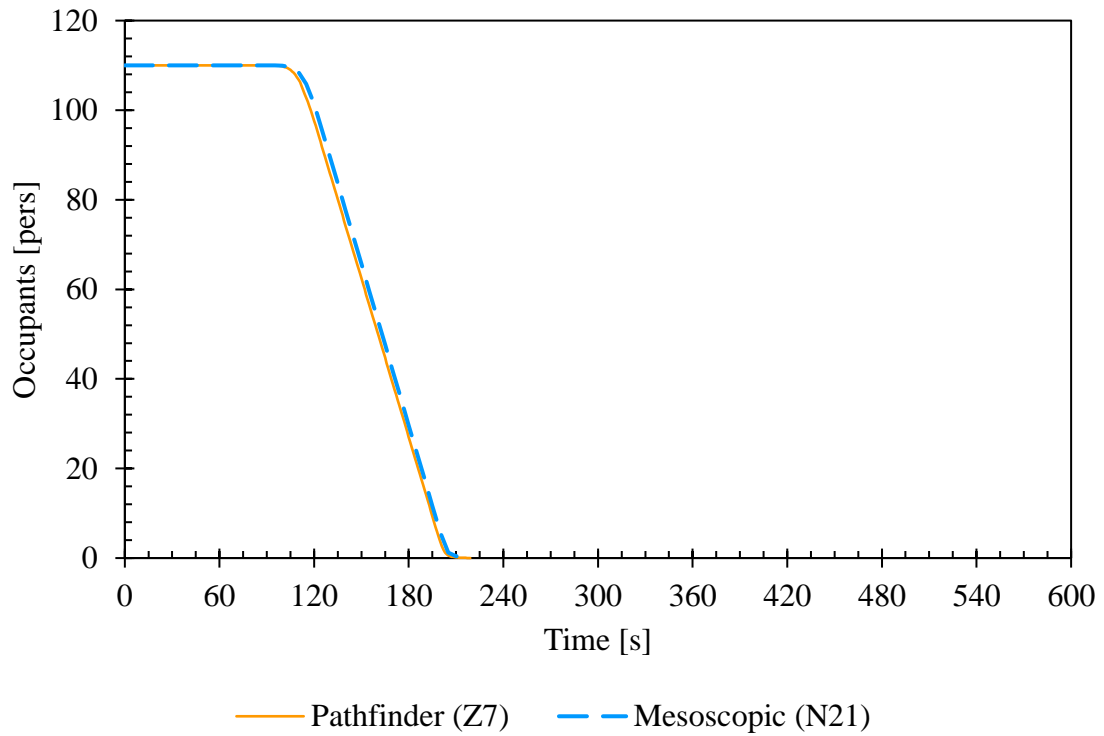


Figure 55 – Case study, Network 5 – Evacuation curve obtained with the proposed mesoscopic model and Pathfinder

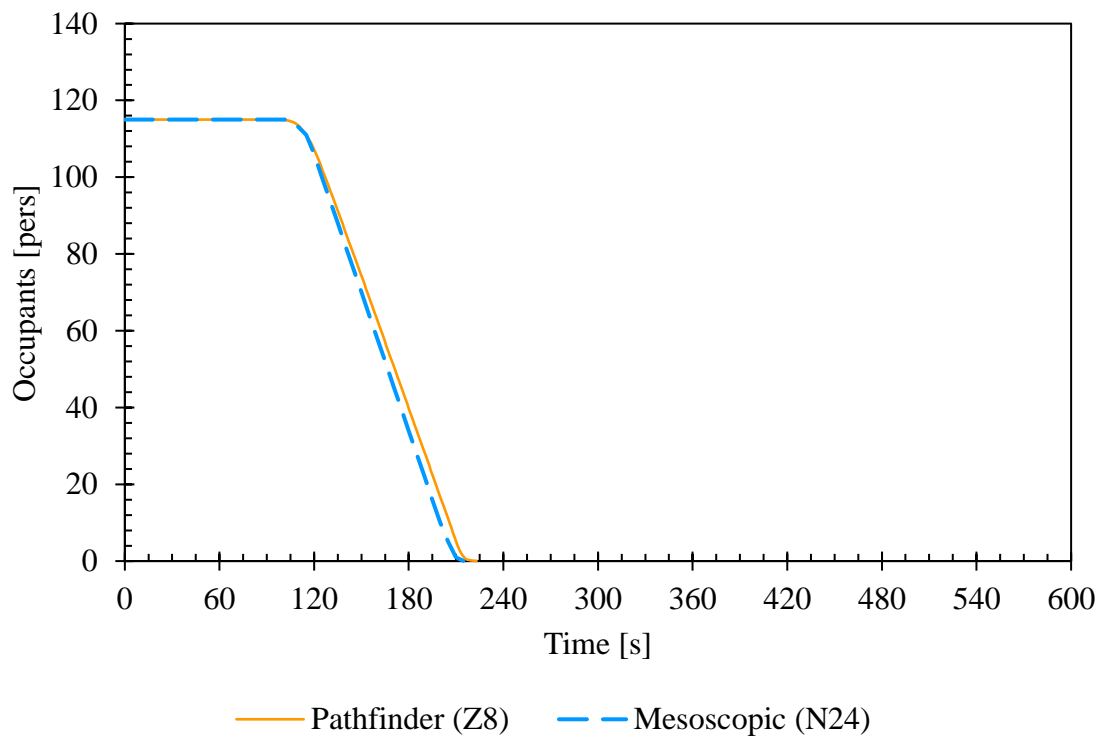


Figure 56 – Case study, Network 6 – Evacuation curve obtained with the proposed mesoscopic model and Pathfinder

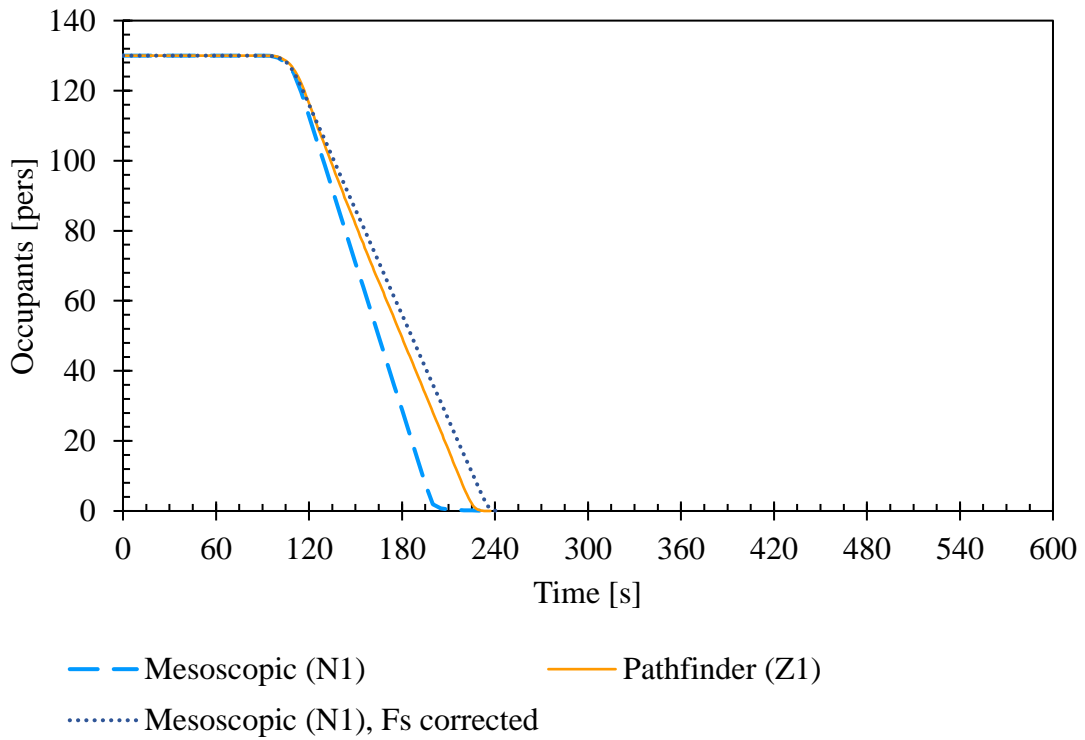


Figure 57 – Case study, Network 1 – Evacuation curve obtained with the proposed mesoscopic model and Pathfinder. The curve represents the occupants of zone 1

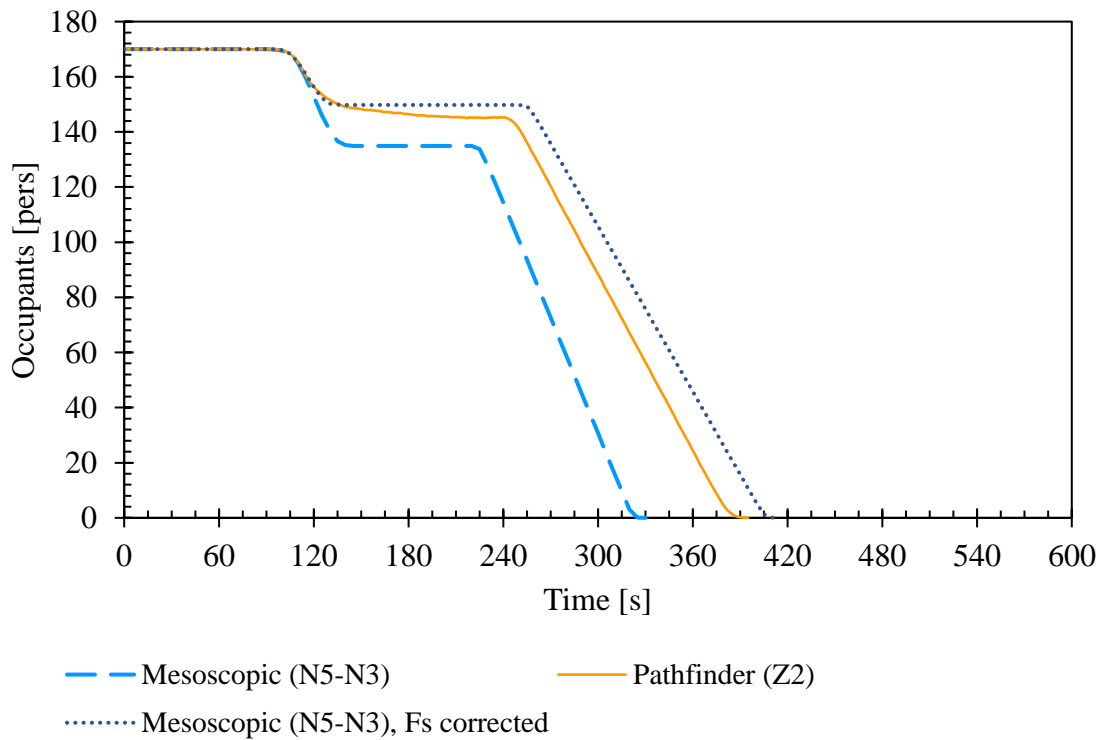


Figure 58 – Case study, Network 1 – Evacuation curve obtained with the proposed mesoscopic model and Pathfinder. The curve represents the occupants of zone 2

5.2.5 Evacuation modelling of the event tree and consequence analysis

For the purpose of demonstrating the use of the tool in a probabilistic framework, this section presents a QRA performed for one of the networks of the analysed food court. Network 1 is chosen for this purpose, in the part that represents the second floor, as this is to location where the occupants are most likely to be exposed to combustion products.

First, the mesoscopic network is setup as shown in the previous section.

Then, one evacuation curve corresponding to each of the ten evacuation scenarios (section D.3) is obtained according to the process described in section 4.3. In particular, Table 9 is used as the scenario generator matrix. The resulting design evacuation curves are presented in Figure 59. As expected, when the initial occupant density is increased progressively, the shape of the evacuation curve changes from free-flow to capacity-controlled.

Next, for every design fire scenario (section D.2), the calculation of ASET is performed with a two-zone fire model as described in appendix E. The available safe egress time obtained for the second floor of the facility ($ASET_2$) in each of the four scenarios can be found in Table 10.

Afterwards, the consequences analysis is performed by comparing the results of the evacuation and fire scenarios associated to every branch of the event tree. For example, risk scenario S20 is associated with fire scenario F04 and evacuation scenario E05; therefore, $ASET_2 = 175$ s is compared with the evacuation curve E05, and a number of $N = 72$ occupants exposed to combustion products is obtained. The consequences calculated for every risk scenario are presented in Table 11 of appendix G.

Ultimately, the frequency of every risk scenario is calculated based on the conditional probabilities along the branches of the event, as shown in Table 12. These are then combined with scenario consequences in Table 13, from which it is possible to obtain the FN curve presented in Figure 60. Since this falls in the ALARP region, risk is tolerable but efforts should be made to reduce it further if practicable.

Note that the calculated curve represents the risk for the occupants of the second floor of the facility of being exposed to combustion products if a kitchen fire occurs at the ground floor. Nevertheless, the analysis of the overall fire-related risk for the facility should also include the calculation of the consequences at first and ground floors. This is a straightforward task with the proposed mesoscopic model, as it is sufficient to repeat the process for every network and sum the number of occupants exposed to smoke in each part of the building. Moreover, the event tree could be extended in order to include more scenarios (e.g., furniture fire, ignition at other floors, etc.). This can be done easily by expanding the scenario matrix.

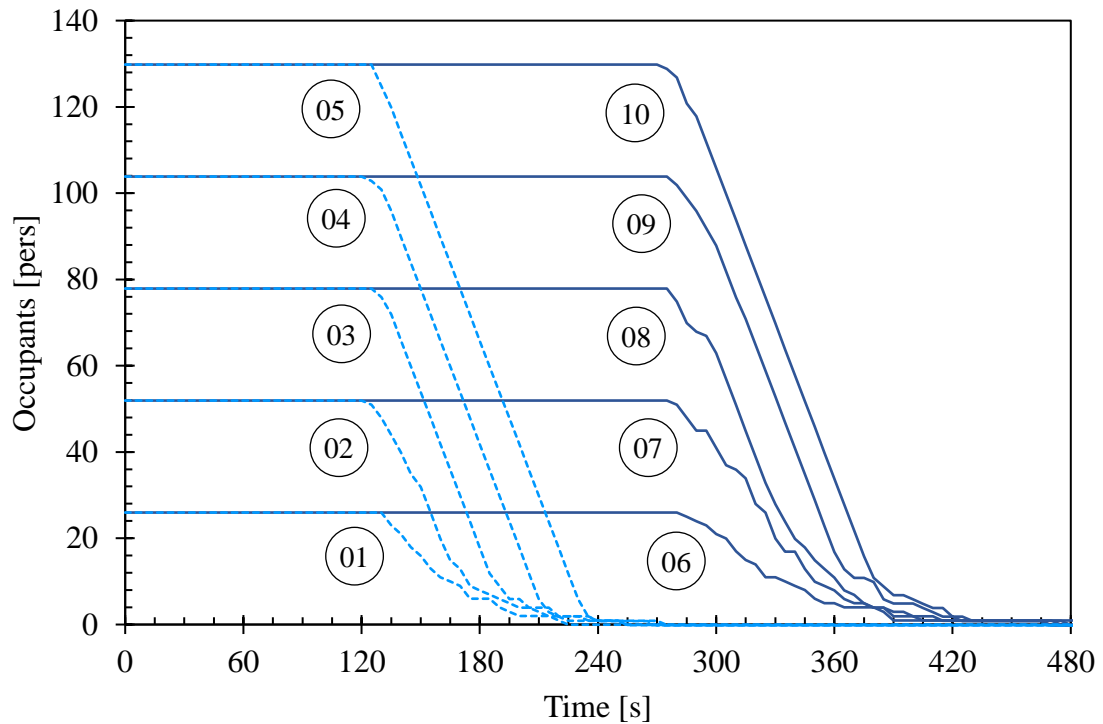


Figure 59 – Case study, Network 1 – Evacuation curves obtained with the proposed mesoscopic model for 10 evacuation scenarios presented in Table 9. Each one represents the number of occupants remaining at the 2nd floor when different initial density, detection and notification time, and pre-evacuation time are considered

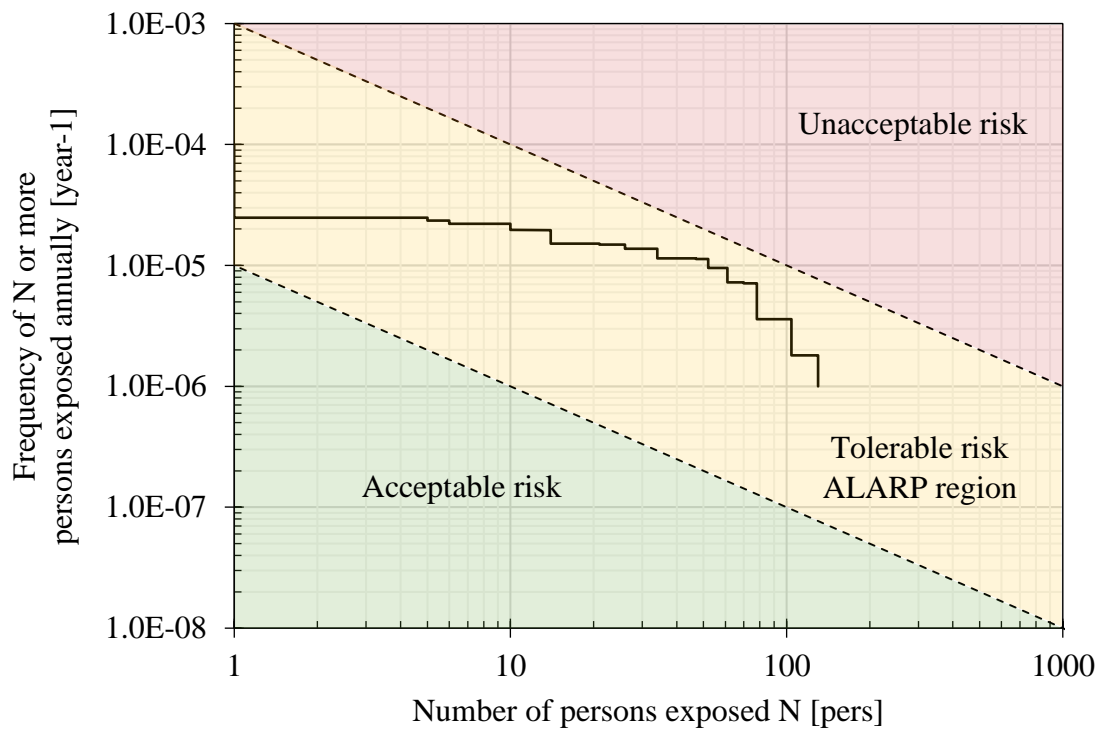


Figure 60 – Case study, Network 1 – FN curve for the occupants of the 2nd floor

5.3 Performance of the proposed model

The application of the proposed model to test scenarios and the case study highlights that the outputs of the mesoscopic tool are satisfactory for the design of evacuation of large gatherings. In fact, when the proposed model is used to analyse the evacuation from an enclosure leading directly to a safe place (i.e., network composed of one zone and one node), which is a typical architectural feature of many assembly buildings such as trade fairs, supermarkets, train stations, etc., the results of the mesoscopic tool fit almost perfectly with the ones produced by a microscopic model. Negligible discrepancies may be attributed to different sampling methods used by the probabilistic models to assign individual characteristics to occupants based on input distributions or to a different discretization of space and time.

The outcomes of the proposed model agree well with microscopic results also when horizontal evacuation through multiple egress components is simulated. The mesoscopic approach leads to a slight overprediction of the evacuation curve compared with microscopic calculations, which is conservative for design purposes. Therefore, the two alternative approaches can be used interchangeably for the design of horizontal egress routes.

If the proposed model is chosen, users can benefit from the following features:

- Short modelling time: the mesoscopic model requires users to specify a small set of input parameters (the characteristics of the occupants, zones, and nodes) as described in annex B. There is no need to model in detail the building geometry as in evacuation tools that are based on a 2D/3D representation of space.
- Short calculation time: the deterministic calculation of a network is almost instantaneous. The iterative calculation process required to reach convergence and perform the evacuation modelling of an event tree with a conventional laptop¹ is in the order of few minutes. For instance, the calculation time required to simulate test scenario 2 (4 components, 225 agents, 100 runs) is 50 seconds versus 4 minutes required by Pathfinder. The simulation time required to calculate network 1 of the case study (14 components, 470 agents, 100 runs) is 90 seconds with the proposed mesoscopic model and 100 minutes with Pathfinder. The iterative calculation process required to perform the evacuation calculation for a whole event tree presented in the case study (about 500 runs) is 5 minutes, while it is expected to be at least in the order of 40 minutes if Pathfinder is used (4 minutes/scenario x 10 scenarios).
- Zero post-processing time: the proposed model automatically provides the plots of the evacuation curves for every node of the network.
- Dynamic convergence assessment: the proposed model automatically performs iterative simulations of an evacuation scenario, stops as soon as the outputs converge, and automatically produces a design evacuation curve. This allows to account for behavioural uncertainty while reducing the computational cost to the minimum. Such an automatic feature is generally not available in microscopic evacuation models.

¹ The machine used to run the simulations presented in this thesis has the following characteristics. Model: Asus ZenBook UX443F. Processor: Intel Core i7-8565U Processor @ 1.8 GHz (8M Cache, up to 4.6 GHz, 4 cores). Graphics: Intel UHD 620, NVIDIA GeForce MX150, 2GB GDDR5. Memory: 16GB LPDDR3 on board, total system memory:16GB. Storage: 512GB M.2 NVMe PCIe 3.0 SSD.

- Probabilistic framework: the proposed model includes features that allow to automatically simulate a set of design evacuation scenarios so that it can be used for quantitative risk assessments or uncertainty analysis. This is generally not implemented in many commercial microscopic evacuation models.

The scenarios concerning vertical egress routes show discrepancies when the mesoscopic approach is used instead of the microscopic one. In the analysed cases, the proposed model underpredicts the time required for evacuation, hence the results are less conservative than the outputs of Pathfinder. When a stair is incorporated in a network, the use of a coefficient that modifies its theoretical maximum capacity may represent a strategy to mitigate the discrepancies between model outcomes. For example, Figure 57 and Figure 58 show that if the stair capacity $F_{s,max}$ is reduced by a factor of 0.9, the outputs of the two models get closer. Nevertheless, the agreement between the evacuation curves is not perfect, and it is important to bear in mind that the magnitude of the correction is case-specific (e.g., the coefficient may vary based on the staircase configuration, on the number of served floors, etc.). Hence, this has not been embedded in the proposed model and further research is recommended to refine the algorithms that predict movement on stairs.

Although this limitation, the proposed tool can still be used to get a qualitative representation and a rough estimate of the evacuation process in the context of vertical egress. This information may still be satisfactory to consultants that need to implement fire safety at preliminary stages of a building design, when the layout is likely to be modified multiple times and it is important to quickly assess the impact of alterations. Moreover, it can inform fire safety engineers about the most critical locations of a facility and highlight the need of further analysis with more refined microscopic tools.

Overall, it is worth to emphasise that the benchmarking with a microscopic model is performed here with the objective of testing the performance of the proposed tool and to underline the differences between mesoscopic and microscopic approaches. When discrepancies are found, the comparison should not be intended as a statement about the reliability of the results of one approach over the other. In fact, both of the models analysed in this study include simplifications and assumptions that may affect the results in different ways. In the corridor case, for example, Pathfinder (used in SFPE mode) reduces the speed of the occupants at the beginning the corridor due to the presence of a queue at the opposite end (30 m far away). Is this reasonable or is it a better to modify the speed based on hydraulic calculations as done with the proposed mesoscopic model? Or again, is it realistic to allow agents to move at individual speeds, or is it more accurate to assume that in a narrow corridor people will adjust their movement according to the surrounding flow? A formal verification and validation process that includes comparison with real world data is necessary to draw conclusions about the representativeness of model results.

A further acknowledged limitation of the proposed mesoscopic tool is that the setup of the network, although very quick, may be less intuitive than modelling a 2D/3D continuous geometry that provides a realistic representation of the building. The same may be true concerning the interpretation/communication of the model outcomes, since the proposed model only provides plots of the relevant quantities rather than a visualization of the agents moving across the computational mesh.

Moreover, many of the limitations of the SFPE hydraulic model also apply with the proposed mesoscopic model. In fact, in contrast with microscopic tools based on social force models, the hydraulic analogy does not consider the following aspects of crowd movement:

- Variable body dimensions (hence fundamental diagrams).
- Navigation around obstacles.
- Movement through non-standard egress components (e.g., staircases with irregular steps, landings with unusual geometry, etc.).
- Local variations of occupant density.
- Local acceleration, deceleration, and collision of occupants due to congestion.
- Counterflows (e.g., two streams of occupants moving in opposite directions).
- Backtrack (e.g., a queue that fills a corridor and spills back into the previous room).
- Group behaviours (e.g., uniform walking speed of smaller groups within the crowd).
- Dynamic exit choice and rerouting.
- Speed reduction due to visibility.

On the other hand, some other limitations of SFPE hand calculations are resolved with the proposed mesoscopic model, such as:

- Occupants possess individual movement characteristic in initial zones.
- This can be used to generate a realistic presentation flow of occupants moving in open plan enclosures.
- Results are probabilistic and allow users to account for behavioural uncertainty.

Lastly, in the prototypical version of the mesoscopic model, the statistic monitored for convergence assessment ZET is comparable to the Total Evacuation Time TET often used in the literature on this topic, however the method is easily applicable to any other output of the proposed model. Since the convergence of the average value of ZET does not necessarily imply the convergence of its standard deviation nor of other relevant outputs (e.g., evacuation curve, flow rates, queuing times, etc.) future developments should aim to include multiple convergence criteria as proposed in (Ronchi, Reneke & Peacock, 2013), (Grandison, 2020), or (Smedberg, Kinsey & Ronchi, 2021).

Moreover, the calculation of σ_{\max} has been performed using normal-based confidence intervals after a qualitative check of the distribution of $P(t)$. Since departure from normality can cause inaccuracies in the estimation of the confidence intervals for the variance, a quantitative test for normality or lognormality could be implemented in the iterative process as proposed in (Tinaburri, 2022). In case a skewed distribution was found, the method proposed by Bonett could be used with a larger number of model runs (Bonett, 2006).

Another possible improvement of the model concerns the technique used for sampling the realizations of the stochastic variables from input distribution. In fact, a simple random sampling method is implemented in the current version of the proposed model. Nevertheless, more complex methods such as Latin hypercube, stratified or inversed stratified may lead to convergence at a lower computational cost (Lovreglio, Spearpoint & Girault, 2019).

On a final note, it is worth to highlight that the use of a design evacuation curve is a simplistic conservative approach for the treatment of behavioural uncertainty. In fact, this leads to a loss of information due to the averaging of the evacuation curves obtained until convergence. A more refined approach could be achieved using probabilistic distributions also in the consequence analysis e.g., using the distribution of evacuation curves to calculate the probability of different numbers N of incapacitated persons at ASET. This would ultimately lead to a more refined (smooth) FN curve, especially towards high consequences.

6 Conclusion and outlook

When predicting the evacuation process from building fires, modellers have to deal with several input parameters and assumptions that are stochastic variables in the real world. Probabilistic methods such as quantitative risk assessment represent an optimal way to address life safety in performance-based designs while accounting for variability and uncertainty. This is of particular importance when a large number of occupants is involved i.e., large gatherings.

Working in a probabilistic framework requires the use of modelling tools that are sufficiently fast and accurate in the prediction of the evacuation process. Microscopic models may be computationally inefficient for this purpose, while macroscopic models may represent evacuation in a too simplistic way. Thus, a mesoscopic model is developed in VBA for Microsoft Excel, which combines both the microscopic and macroscopic techniques.

The model relies on a coarse network representation of the building, where egress routes are schematised through sequences of zones and nodes. A zone represents a part of an enclosure where the crowd is represented microscopically. Here individual characteristics are attributed to each occupant through random sampling from user-defined probability distributions, then individual timelines are used to determine the initial occupant flow. Nodes represent sections of egress routes where occupants are treated macroscopically. Here the SFPE hydraulic model is applied to predict how the evacuation process evolves according to the characteristics of egress components (doors, corridors, stairs, etc.). As a result, the model provides plots of essential parameters such as the evacuation curve, occupants flowrate, queue size, etc. This approach allows to account for variability of occupants' characteristics while demanding a negligible time to run. Therefore, it allows to perform iterations efficiently and obtain accurate representations of the crucial phenomena that occur during the evacuation of large crowds.

Due to the probabilistic approach used in the zones, the model needs to be run multiple times to analyse a single evacuation scenario and account for behavioural uncertainty. Therefore, an automatic routine is implemented for this purpose, and a dynamic convergence assessment based on inferential statistics is designed to halt the iterative process as soon as a user-defined accuracy level is reached. Given the multitude of output data obtained with the repeated simulations, an additional algorithm calculates a design evacuation curve for each node of the network.

Furthermore, another automatic feature allows to repeat the aforementioned cycle for a multitude of evacuation scenarios (e.g., determined with an event tree) and quickly obtain the evacuation curves to be used in a quantitative risk assessment.

The performance of the proposed model has been tested with a series of test scenarios and a case study involving a food court. Benchmarking against the outputs of a microscopic simulator (Pathfinder used in SFPE mode) highlights that the proposed tool produces reliable results at a

fraction of the computational cost. In particular, for horizontal egress routes, the evacuation curves generated by the two models nearly coincide despite the mesoscopic simplification. For vertical egress routes, the mesoscopic predictions capture reasonably well the qualitative evolution of the egress process, but numerical results are underestimated. These discrepancies may be corrected with a safety factor, but further research is desirable to improve the accuracy of the proposed mesoscopic when a stair is included in the network. A full quantitative risk analysis is also performed for a floor of the food court, which shows the efficiency of the proposed model then it is employed in a probabilistic framework.

Therefore, it can be concluded that the prototypical version of the probabilistic mesoscopic model satisfies the initial objectives of this study, and the model can potentially be used for:

- Quick preliminary design of egress systems (e.g., capacity of egress components).
- Quick comparison of design alternatives (e.g., exit width, occupant load, crowd management strategy).
- Identify critical locations of the building where congestion may occur.
- Evacuation modelling for quantitative risk assessment.
- Uncertainty/sensitivity analysis.
- Assess the need for more detailed analysis (e.g., with microscopic models).
- Investigate many scenarios to determine the credible worst case to be used as an input for microscopic models.
- Sanity check of the outputs of microscopic models.
- Faster than real time calculations.

Albeit the satisfactory results, the proposed model comes with some simplifications and acknowledged limitations that have been highlighted in sections 1.4, 3.4 and 5.3. Thus, future research and model development may address the following topics in order to improve its performance with regards to:

- Implementation of a more elaborate algorithm to predict movement on stairs.
- Improvement of the pseudo-random sampling technique.
- Implementation of multiple convergence criteria.
- Integration with a fire model so that consequences analysis can be performed automatically.
- Implementation of correlations to account for speed reduction due to smoke.
- Implementation of correlations or different fundamental diagrams to account for other body sizes than average adult.
- Implementation of correlations to account for backtrack.

Acknowledgements

This work is the final thesis of the International Master of Science in Fire Safety Engineering (IMFSE). It has been completed in collaboration with the division of Division of Fire Safety Engineering at Lund University (Sweden) and the R&D department of GAe Engineering (Italy). A number of people brought significant contributions to the accomplishment of this work.

First, I would like to thank Prof. Enrico Ronchi for being a great mentor who always took the time for discussion and constructive feedback. I appreciate the valuable inputs and excellent guidance I received along this journey.

Further, I wish to express my gratitude to Dr. Giuseppe Amaro and Dr. Ada Malagnino for co-supervising this work. Thank you for your availability and support that made possible the testing of the tool and the finalization of the project.

My sincere thanks also go to Dr. Gianluca De Sanctis and Dr. Juan Blond, who sparked my interest for this research topic. I have learned so much from the great collaboration and discussions about risk and uncertainty, which contributed to shape the current form of this work.

Last but not least, thanks to my family, always supportive of my choices, academic or other. Thanks to my friends, old and new, close or far away, for contributing to my happiness and resilience. And thanks to Luca, the oxygen that keeps my fire burning.

Lund, May 2020

Lorenzo Contini

References

- Alpert, R. L. (2016). Ceiling Jet Flows, in *SFPE Handbook of Fire Protection Engineering, Fifth Edition*, Springer.
- Averill, J. D. (2011). Five Grand Challenges in Pedestrian and Evacuation Dynamics, *Pedestrian and Evacuation Dynamics*.
- Baker, G., Wade, C., Nilsson, D. & Olsson, P. (2022). Results Are In: International Fire Engineering Tools Survey, *Fire Protection Engineering Magazine*.
- Bonett, D. G. (2006). Approximate Confidence Interval for Standard Deviation of Nonnormal Distributions, *Computational Statistics and Data Analysis*.
- Borrmann, A., Kneidl, A., Köster, G., Ruzika, S. & Thiemann, M. (2012). Bidirectional Coupling of Macroscopic and Microscopic Pedestrian Evacuation Models, *Safety Science*.
- British Standards Institution. (2003). PD 7974-4:2003 Application of Fire Safety Engineering Principles to the Design of Buildings - Part 4: Detection of Fire and Activation of Fire Protection Systems (Sub-System 4).
- British Standards Institution. (2004). PD 7974-6:2004 The Application of Fire Safety Engineering Principles to Fire Safety Design of Buildings - Part 6: Human Factors: Life Safety Strategies - Occupant Evacuation, Behaviour and Condition (Sub-System 6).
- British Standards Institution. (2019a). PD 7974-1:2019 - Application of Fire Safety Engineering Principles to the Design of Buildings - Part 1: Initiation and Development of Fire within the Enclosure of Origin (Sub-System 1).
- British Standards Institution. (2019b). BS 9999:2019 - Fire Safety in the Design, Management and Use of Buildings - Code of Practice.
- Burghardt, S., Seyfried, A. & Klingsch, W. (2013). Performance of Stairs - Fundamental Diagram and Topographical Measurements, *Transportation Research Part C*, [e-journal], Available Online: <http://dx.doi.org/10.1016/j.trc.2013.05.002>.
- Canter, D., Breaux, J. & Sime, J. (1980). Domestic, Multiple Occupancy and Hospital Fires, *Fires and Human Behaviour*.
- Chen, H. N. & Mao, Z. L. (2018). Study on the Failure Probability of Occupant Evacuation with the Method of Monte Carlo Sampling, *Procedia Engineering*, [e-journal], Available Online: <https://doi.org/10.1016/j.proeng.2017.12.137>.
- De Sanctis, G. (2015). Generic Risk Assessment for Fire Safety: Performance Evaluation and Optimisation of Design Provisions, *ETH Zurich Research Collection*.
- De Sanctis, G., Moos, M. & Aumayer, C. (2019). Survey of Occupant Load Densities in Retail Buildings, *SFPE Foundation*.
- Devore, J. L. (2012). Probability & Statistics for Engineering and the Sciences, edited by Brooks/Cole Cengage Learning, Eighth edi.
- Dressler, D., Groß, M., Kappmeier, J. P., Kelter, T., Kulbatzki, J., Plümpe, D., Schlechter, G., Schmidt, M., Skutella, M. & Temme, S. (2010). On the Use of Network Flow Techniques for Assigning Evacuees to Exits, *Procedia Engineering*.
- Frantzych, H. (1998). Uncertainty and Risk Analysis in Fire Safety Engineering, *Lund University*.

- Grandison, A. (2020). Determining Confidence Intervals, and Convergence, for Parameters in Stochastic Evacuation Models, *Fire Technology*, [e-journal], Available Online: <https://link.springer.com/article/10.1007/s10694-020-00968-0>.
- Gustafsson, P. (2016). A Study on Movement Down Spiral Staircases, *Lund University*, [e-journal], Available Online: www.brand.lth.se.
- Gwynne, S. M. V. & Boyce, K. E. (2016). Engineering Data, in *SFPE Handbook of Fire Protection Engineering, Fifth Edition*, [e-book] Springer, Available Online: https://link.springer.com/chapter/10.1007/978-1-4939-2565-0_64.
- Gwynne, S. M. V., Hulse, L. M. & Kinsey, M. J. (2016). Guidance for the Model Developer on Representing Human Behavior in Egress Models, *Fire Technology*.
- Gwynne, S. M. V. & Rosenbaum, E. R. (2016). Employing the Hydraulic Model in Assessing Emergency Movement, in *SFPE Handbook of Fire Protection Engineering, Fifth Edition*, [e-book] Springer, Available Online: https://link.springer.com/chapter/10.1007/978-1-4939-2565-0_59.
- Hadjisophocleous, G. V. & Benichou, N. (2000). Development of Performance-Based Codes, Performance Criteria and Fire Safety Engineering Methods, *International Journal on Engineering Performance-Based Fire Codes*.
- Hanisch, A., Tolujew, J., Richter, K. & Schulze, T. (2003). Online Simulation of Pedestrian Flow in Public Buildings, *Winter Simulation Conference Proceedings*.
- Hartson, H. R. (2003). Cognitive, Physical, Sensory, and Functional Affordances in Interaction Design, *Behaviour and Information Technology*.
- Hopkin, D., Van Coile, R. & Lange, D. (2017). Certain Uncertainty - Demonstrating Safety in Fire Engineering Design and the Need for Safety Targets, *SFPE Europe*.
- Hurley, M. J., Gottuk, D., Hall, J. R., Harada, K., Kuligowski, E., Puchovsky, M., Torero, J., Watts, J. M. & Wieczorek, C. (2016). *SFPE Handbook of Fire Protection Engineering, Fifth Edition*, Springer.
- Hurley, M. J. & Rosenbaum, E. R. (2015). *Performance-Based Fire Safety Design*, CRC Press.
- International Organisation for Standardization. (2009). ISO/TR 16738 - Fire-Safety Engineering - Technical Information on Methods for Evaluating Behaviour and Movement of People, *Technical report 16738*.
- International Organisation for Standardization. (2020). ISO 20414:2020 - Fire Safety Engineering — Verification and Validation Protocol for Building Fire Evacuation Models, Available Online: <https://www.iso.org/standard/78348.html>.
- International Organization for Standardization. (2006). ISO/TS 16733 - Fire Safety Engineering - Selection of Design Scenarios and Design Fires, *Technical specification 16733*.
- Italy - Ministry of Interiors. (2019). D.M. 18.10.2019 - Codice Di Prevenzione Incendi (Fire Safety Code).
- Kaplan, S. & Garrick, B. J. (1981). On The Quantitative Definition of Risk, *Risk Analysis*.
- Kong, D., Lu, S. xiang, Kang, Q. sheng, Lo, S. ming & Xie, Q. (2014). Fuzzy Risk Assessment for Life Safety Under Building Fires, *Fire Technology*.
- Kuligowski, E. D. (2016). Computer Evacuation Models for Buildings, in *SFPE Handbook of*

- Fire Protection Engineering, Fifth Edition*, [e-book] Springer, Available Online: https://link.springer.com/chapter/10.1007/978-1-4939-2565-0_60.
- Kuligowski, E. D., Gwynne, S. M. V., Kinsey, M. J. & Hulse, L. (2017). Guidance for the Model User on Representing Human Behavior in Egress Models, *Fire Technology*.
- Latané, B. & Darley, J. (1970). Where There's Smoke..., in Appleton-Century Crofts (ed.), *The Unresponsive Bystander*.
- Lord, J., Meacham, B., Moore, A., Fahy, R. & Proulx, G. (2005). Guide for Evaluating the Predictive Capabilities of Computer Egress Models, *NIST GCR 06-886*.
- Lovreglio, R., Kuligowski, E., Gwynne, S. M. V. & Boyce, K. (2019). A Pre-Evacuation Database for Use in Egress Simulations, *Fire Safety Journal*.
- Lovreglio, R., Ronchi, E. & Kinsey, M. J. (2020). An Online Survey of Pedestrian Evacuation Model Usage and Users, *Fire Technology*, [e-journal], Available Online: <https://link.springer.com/article/10.1007/s10694-019-00923-8>.
- Lovreglio, R., Ronchi, E. & Nilsson, D. (2015). A Model of the Decision-Making Process during Pre-Evacuation, *Fire Safety Journal*, [e-journal], Available Online: <http://dx.doi.org/10.1016/j.firesaf.2015.07.001>.
- Lovreglio, R., Spearpoint, M. & Girault, M. (2019). The Impact of Sampling Methods on Evacuation Model Convergence and Egress Time, *Reliability Engineering and System Safety*.
- Magnusson, S. E., Frantzich, H. & Harada, K. (1995). Fire Safety Design Based on Calculations. Uncertainty Analysis and Safety Verification, *Lund University, Report 307*.
- McGrattan, K., Hostikka, S., McDermott, R., Floyd, J., Weinschenk, C. & Overholt, K. (2020). Fire Dynamics Simulator Technical Reference Guide Volume 1: Mathematical Model, *NIST Special Publication 1018-1*.
- New Zealand - Ministry of Business Innovation & Employment and Department of Building and Housing. (2017). C/VM2 - Verification Method: Framework for Fire Safety Design.
- Nilsson, D. & Johansson, A. (2009). Social Influence during the Initial Phase of a Fire Evacuation-Analysis of Evacuation Experiments in a Cinema Theatre, *Fire Safety Journal*.
- Notarianni, K. A. & Parry, G. W. (2016). Uncertainty, in *SFPE Handbook of Fire Protection Engineering, Fifth Edition*, [e-book] Springer, Available Online: [https://link.springer-com.ludwig.lub.lu.se/chapter/10.1007/978-1-4939-2565-0_76](https://link.springer.com.ludwig.lub.lu.se/chapter/10.1007/978-1-4939-2565-0_76).
- O'Connor, D. J., Biller, J., Dryden, S., Fahy, R., Gann, R. G., Goodhead, S., Groner, N., Gwynne, S. M. V., Hoskins, B., Kinsey, M. J., Kuligowski, E. D., McAllister, J., Omori, H., Purser, D. A. & Strege, S. (2019). *SFPE Guide to Human Behavior in Fire*, Springer.
- Peacock, R. D., McGrattan, K. B., Forney, G. P. & Reneke, P. A. (2015). CFAST - Consolidated Model of Fire Growth and Smoke Transport (Version 7) Volume 1: Technical Reference Guide, *NIST Technical Note 1889v1*.
- Poh, W. (2010). Tenability in Building Fires: Limits and Design Criteria, *Fire Australia*,.
- Predtechenskii, V. M. & Milinskii, A. I. (1978). Planning for Foot Traffic Flow in Buildings, Amerind Publishing.
- Purser, D. A. (2010). Hazards from Smoke and Irritants, in *Fire Toxicity*, Elsevier.

- Purser, D. A. & Gwynne, S. M. V. (2007). Identifying Critical Evacuation Factors and the Application of Egress Models, *Interflam conference*.
- Rein, G., Torero, J. L., Jahn, W., Stern-Gottfried, J., Ryder, N. L., Desanghere, S., Lázaro, M., Mowrer, F., Coles, A., Joyeux, D., Alvear, D., Capote, J. A., Jowsey, A., Abecassis-Empis, C. & Reszka, P. (2009). Round-Robin Study of a Priori Modelling Predictions of the Dalmarnock Fire Test One, *Fire Safety Journal*.
- Ronchi, E., Corbetta, A., Galea, E., Kinateder, M., Kuligowski, E. D., McGrath, D., Pel, A., Shiban, Y., Thompson, P. & Toschi, F. (2017). New Approaches to Evacuation Modelling, *Summary of the workshop part of the 12th Symposium of the International Association for Fire Safety Science*.
- Ronchi, E., Reneke, P. A. & Peacock, R. D. (2013). A Method for the Analysis of Behavioural Uncertainty in Evacuation Modelling, *Fire Technology*.
- Ronchi, E., Reneke, P. A. & Peacock, R. D. (2014). A Method for the Analysis of Behavioural Uncertainty in Evacuation Modelling, *Fire Technology*.
- Shi, M., Lee, E. W. M. & Ma, Y. (2018). A Novel Grid-Based Mesoscopic Model for Evacuation Dynamics, *Physica A: Statistical Mechanics and its Applications*.
- Sime, J. (1985). Movement toward the Familiar - Person and Place Affiliation in a Fire Entrapment Setting, *Environment and Behavior*.
- Smedberg, E., Kinsey, M. J. & Ronchi, E. (2021). Multifactor Variance Assessment for Determining the Number of Repeat Simulation Runs in Evacuation Modelling, *Fire Technology*, [e-journal], Available Online: <https://doi.org/10.1007/s10694-021-01134-w>.
- Spinardi, G., Bisby, L. & Torero, J. (2016). A Review of Sociological Issues in Fire Safety Regulation, *Fire Technology*.
- Tavares, M. & Ronchi, E. (2015). Uncertainties in Evacuation Modelling: Current Flaws and Future Improvements, *6th Human Behaviour in Fire Symposium 2015*.
- Tehler, H. (2015). A General Framework for Risk Assessment, *Lund University*.
- Teknomo, K. & Gerilla, G. P. (2008). Mesoscopic Multi-Agent Pedestrian Simulation, in *Transportation Research Trends*, Nova Science Publisher.
- Thunderhead Engineering. (2021). Pathfinder Technical Reference Manual.
- Tinaburri, A. (2022). Principles for Monte Carlo Agent-Based Evacuation Simulations Including Occupants Who Need Assistance. From RSET to RiSET, *Fire Safety Journal*, [e-journal], Available Online: <https://doi.org/10.1016/j.firesaf.2021.103510>.
- Tolujew, J. & Alcalá, F. (2004). A Mesoscopic Approach to Modeling and Simulation of Pedestrian Traffic Flow, *Proceedings 18th European Simulation Multiconference*.
- Tong, D. & Canter, D. (1985). The Decision to Evacuate: A Study of the Motivations Which Contribute to Evacuation in the Event of Fire, *Fire Safety Journal*.
- Van Weyenberge, B., Deckers, X., Caspeele, R. & Merci, B. (2016). Development of a Risk Assessment Method for Life Safety in Case of Fire in Rail Tunnels, *Fire Technology*.
- Vanumu, L. D., Ramachandra Rao, K. & Tiwari, G. (2017). Fundamental Diagrams of Pedestrian Flow Characteristics: A Review, *European Transport Research Review*, [e-journal], Available Online: <https://etrr.springeropen.com/articles/10.1007/s12544-017-0264-6>.

- Vrijling, J. K., van Hengel, W. & Houben, R. J. (1995). A Framework for Risk Evaluation, *Journal of Hazardous Materials*.
- Xiong, M., Tang, S. & Zhao, D. (2013). A Hybrid Model for Simulating Crowd Evacuation, *New Generation Computing*.
- Zambrano, J. A., Huertas, J. A., Segura-Duran, E. & Medaglia, A. L. (2020). Time Estimation and Hotspot Detection in the Evacuation of a Complex of Buildings: A Mesoscopic Approach and Case Study, *IEEE Transactions on Engineering Management*.

Appendices

Appendix A: Inferential statistics

Let X denote the ‘population’ of all possible model outcomes having a mean μ , and a standard deviation σ . For instance, this is represented by the population of *all* possible ZETs generated with the mesoscopic model (or at least with a very large number of runs in the order of 10^4 or 10^5). μ , and σ are the population *parameters*, hence fixed unknown numerical values that designers want to estimate.

Since engineers wish to minimise the number of model realizations to reduce the computational cost of egress analyses, a limited number of simulations is typically run, which can be seen as a subset or a ‘sample’ of observations drawn randomly from the population. In this case, inferential statistics are needed to draw conclusions about the population from the sample characteristics. Let $X_1, X_2, \dots, X_i, \dots, X_n$ denote a random sample having a mean \bar{X} , and a standard deviation S . These are the sample *statistics*, and the use of uppercase letters highlights that, before sampling, the observations are random variables. After sampling, each observation is a number, denoted by a lowercase letter $x_1, x_2, \dots, x_i, \dots, x_n$. The statistics \bar{x} and s are also numerical values known to designers, as they can be computed from the sampled observations. However, their value may vary from sample to sample. For instance, a sample can be composed of 50 values of ZET determined through 50 model runs, for which it is possible to calculate the mean and the standard deviation. If another sample of 50 ZETs is generated, new values of \bar{x} and s may be found.

As \bar{X} and S are random variables whose values \bar{x} and s depend on the sample, they only represent the best guess of the population parameters μ and σ , but they are never exact. In fact, it can be expected that for some samples the estimate is larger than the true value, and in other cases the contrary occurs. This approximation inevitably generates an error of estimation Δ . Due to the law of large numbers, as the simple size increases, the error of estimation decreases, and the sample statistics tend to the population parameters. Ideally engineers aspire to know the population parameters by running large numbers of simulations, but practically the available resources only allow them to perform a limited number of runs to obtain the sample statistics. Therefore, the sample mean \bar{X} is the *estimator* of the population mean μ , and \bar{x} is the *point estimate* of μ i.e., a single number computed from the sampled data that can be regarded as the most plausible value of μ . Similarly, s is the point estimate that is used to make inferences about σ . Due to this approximation, it is important to quantify the error of estimation.

If the sample size n is sufficiently large, Δ can be estimated with z statistics. In fact, if $n > 40$ (Devore, 2012), the Central Limit Theorem can be applied and it is possible to state that the sample mean \bar{X} has approximately a normal distribution regardless of the population distribution X , with an expected value μ and a standard deviation σ/\sqrt{n} . When \bar{X} is standardized, the random variable $Z = \frac{\bar{X}-\mu}{\sigma/\sqrt{n}}$ is obtained, which has approximately a standard normal distribution.

Based on z statistics, it is now possible to state that:

$$P(-z_{\alpha/2} < Z < z_{\alpha/2}) \approx 1 - \alpha \quad \text{Equation 15 (Devore, 2012)}$$

$$P\left(-z_{\alpha/2} < \frac{\bar{X} - \mu}{\sigma/\sqrt{n}} < z_{\alpha/2}\right) \approx 1 - \alpha \quad \text{Equation 16 (Devore, 2012)}$$

$$P\left(\bar{X} - z_{\alpha/2} \frac{\sigma}{\sqrt{n}} < \mu < \bar{X} + z_{\alpha/2} \frac{\sigma}{\sqrt{n}}\right) \approx 1 - \alpha \quad \text{Equation 17 (Devore, 2012)}$$

As the value of the population standard deviation σ is unknown a priori, Z is typically standardized using the sample standard deviation S instead. Now both \bar{X} and S vary from sample to sample. However, if n is large, S adds negligible variability to Z because s will be close to σ (Devore, 2012). Therefore, it is possible to write:

$$P\left(\bar{X} - z_{\alpha/2} \frac{S}{\sqrt{n}} < \mu < \bar{X} + z_{\alpha/2} \frac{S}{\sqrt{n}}\right) \approx 1 - \alpha \quad \text{Equation 18 (Devore, 2012)}$$

After observing $X_1 = x_1, X_2 = x_2, \dots, X_n = x_n$ and computing the observed sample mean \bar{x} and standard deviation s , it is possible to rewrite Equation 18 as:

$$P\left(\bar{x} - z_{\alpha/2} \frac{s}{\sqrt{n}} < \mu < \bar{x} + z_{\alpha/2} \frac{s}{\sqrt{n}}\right) \approx 1 - \alpha \quad \text{Equation 19 (Devore, 2012)}$$

This represents the large-sample confidence interval for μ $\left(\bar{x} - z_{\alpha/2} \frac{s}{\sqrt{n}}; \bar{x} + z_{\alpha/2} \frac{s}{\sqrt{n}}\right)$ with a confidence level of approximately $100(1 - \alpha) \%$. Typical values of α and $z_{\alpha/2}$ are reported in Table 6 for commonly used confidence levels.

Table 6 – Values of α and $z_{\alpha/2}$ for commonly used confidence levels

Confidence level CL	α	$z_{\alpha/2}$
0.80	0.20	1.28
0.85	0.25	1.44
0.90	0.10	1.65
0.95	0.05	1.96
0.98	0.02	2.33
0.99	0.01	2.58

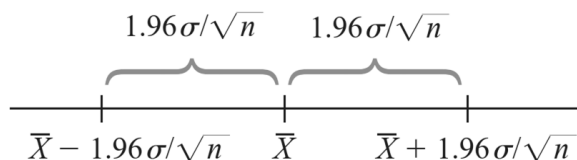


Figure 61 – Representation of a confidence interval centered at \bar{X} with a confidence level of approximately 95%. Figure from (Devore, 2012)

Conceptually, a confidence interval represents a range of plausible values for the parameter being estimated through the sample statistics. The centre of the interval is the sample mean \bar{x} and it extends by the quantity $z_{\alpha/2} \frac{s}{\sqrt{n}}$ on each side. This is often referred as ‘standard error’ and denoted by Δ . Therefore, it is possible to express the confidence interval alternatively as:

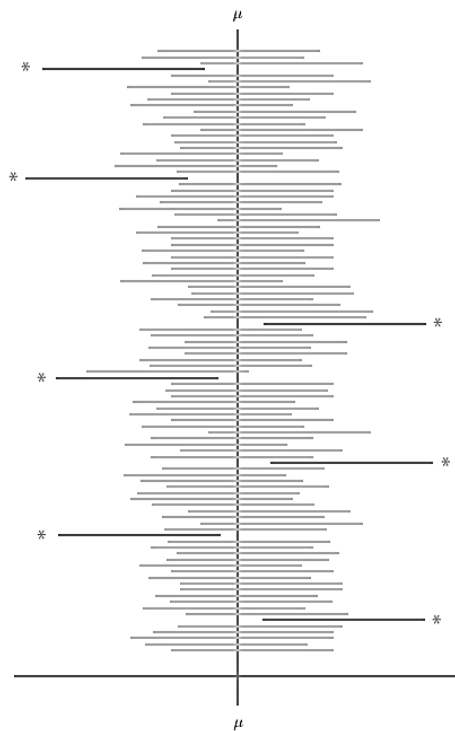
$$\bar{x} - \Delta < \mu < \bar{x} + \Delta \quad \text{Equation 20 (Devore, 2012)}$$

$$\mu = \bar{x} \pm \Delta \quad \text{Equation 21 (Devore, 2012)}$$

Both the interval center and the error are random variables for each sample. However, when n increases the error reduces. Therefore, it is possible to think at the width of the interval as its accuracy or precision.

The confidence level expresses the probability for the random interval to include the true value of μ . For instance, a 95% confidence level means that if a random sample of size n is generated 100 times, and the confidence interval is computed for each sample, approximately 95 of the intervals will include the true value of the population mean μ (Figure 62). If the confidence level is increased, the value of $z_{\alpha/2}$ also increases and interval becomes wider. Therefore, we can see the confidence level as the reliability of the confidence interval: the higher the confidence level, the more likely it is for the interval to include the population parameter, because it is wider.

As a result, estimating a confidence interval is a compromise between accuracy and reliability: a reliable interval (high confidence level) tends to be imprecise (wide), while a precise (narrow) interval is less reliable (low confidence level). For design purposes, a confidence level of 95% is often chosen. Values of 90% or 99% are also used frequently (Devore, 2012).



*Figure 62 – Representation of one hundred confidence intervals with confidence level of approximately 95%. Asterisks identify intervals that do not include the population mean μ .
Figure from (Devore, 2012)*

In a similar manner, the sample variance s^2 can be used to draw inferences about the population variance σ^2 . When the population has a normal distribution, the chi-squared probability distribution χ^2 having $v = n - 1$ degrees of freedom replaces the Z distribution used previously, and it is possible to state that:

$$P\left(\chi^2_{1-\alpha/2,v} < \frac{(n-1)S^2}{\sigma^2} < \chi^2_{\alpha/2,v}\right) = 1 - \alpha \quad \text{Equation 22 (Devore, 2012)}$$

$$\frac{(n-1)s^2}{\chi^2_{\alpha/2,v}} < \sigma^2 < \frac{(n-1)s^2}{\chi^2_{1-\alpha/2,v}} \quad \text{Equation 23 (Devore, 2012)}$$

Equation 23 represents the confidence interval for the variance σ^2 of a normal population with a confidence level $100(1 - \alpha) \%$. The interval for the standard deviation σ can be calculated as:

$$\sqrt{\frac{(n-1)s^2}{\chi^2_{\alpha/2,v}}} < \sigma < \sqrt{\frac{(n-1)s^2}{\chi^2_{1-\alpha/2,v}}} \quad \text{Equation 24 (Devore, 2012)}$$

Appendix B: User manual

This section represents a user manual of the probabilistic mesoscopic model for fire evacuation in large gatherings developed by Lorenzo Contini.

Users are informed that the tool is a prototype that may lack of accuracy in the prediction of real-world phenomena. Expert judgement is necessary to evaluate the appropriateness of its use and its predictive capabilities.

Feedback to the author is encouraged to guide future developments of the tool.

Model setup and deterministic run

The modelling process starts from the sheet named 'Input'. First, compile the sheet with the parameters concerning the characteristics of occupants, zones and nodes.

Inputs for occupants:

- Unimpeded walking speed S_{\max} : choose a distribution shape $\text{Distr}[S_{\max}]$ (Normal by default), and input values for its mean $E[S_{\max}]$ and standard deviation $\text{Var}[S_{\max}]^{1/2}$ in [m/s].

Inputs for zones:

- Component ID: input the letter 'Z' followed by a zone number (e.g., Z1, Z2, Z3, etc.)
- Component type T: input a text description.
- Floor length X and width Y: input values for the dimensions of the zones in [m].
- Path shape PS: choose between 'Diagonal' (shortest distance that represents the absence of obstacles) or 'X+Y' (longer distance that represents the path around obstacles).
- Occupant density D: input a value in [pers/m²].
- Detection + notification time t_{d+n} : choose a distribution shape $\text{Distr}[t_{d+n}]$ (Normal by default), and input values for its mean $E[t_{d+n}]$ and standard deviation $\text{Var}[t_{d+n}]^{1/2}$ in [s].
- Pre-evacuation time t_{pre} : choose a distribution shape $\text{Distr}[t_{\text{pre}}]$ (Log-normal by default), and input values for its location $E[t_{\text{pre}}]$ and scale $\text{Var}[t_{\text{pre}}]^{1/2}$ in [s]. A calculator is available in the same sheet to derive $E[t_{\text{pre}}]$ and $\text{Var}[t_{\text{pre}}]^{1/2}$ from the pre-evacuation times of the 1st and 99th percentiles ($t_{\text{pre},1\text{st}}$ and $t_{\text{pre},99\text{th}}$).

Inputs for nodes:

- Component ID: input the letter 'N' followed by a node number (e.g., N1, N2, N3, etc.)
- Previous components: input the names of the previous components in the network.
- Component type T: input a text description.
- Measured width W: input a value in [m].
- Boundary layer BL: input a value in [m]. See Table 59.1 in (Gwynne & Rosenbaum, 2016).
- Max specific flow $F_{s,\max}$: input a value in [pers/(ms)]. See Table 59.5 in (Gwynne & Rosenbaum, 2016).

- Unimpeded walking speed S_{\max} : input a value in [m/s]. See Table 59.4 in (Gwynne & Rosenbaum, 2016).
- Component constant k : input a value. See Table 59.2 in (Gwynne & Rosenbaum, 2016).
- Component length L : enter a value in [m].

Once the inputs have been compiled, update the sheet by pressing F9, and click the button ‘Create Network’. A new sheet for every zone/node will be generated. Update again the sheet to perform the calculation of the network using a random sample from input distributions. Every the sheet is updated, a new random sample is generated and a deterministic calculation of the network is performed. The outputs for every zone/node can be found in the respective sheet. The outputs for the whole network can be found in the sheet ‘Output’.

If a new network needs to be generated, click the button ‘Restore’, then repeat the process.

Iterative runs for convergence

After the model has been setup and a deterministic run has been calculated, it is possible to perform and record a number of iterative runs until convergence is reached. To do so, in the sheet named ‘Iterations’, specify a maximum number of iterations N_{\max} (the minimum value is 50). Then choose if the model should stop when convergence is reached.

- If ‘NO’ is selected, the model performs a number of simulations $n = N_{\max}$.
- If ‘YES’ is selected and convergence is achieved for $n < N_{\max}$, the model stops the iterative process; if convergence is not achieved before N_{\max} , the model stops anyways when $n = N_{\max}$.

In this second case, after selecting ‘YES’, go to the sheet named ‘Convergence’, in the field ‘Component ID’ choose the first zone of the network, then specify a design confidence level CL and a desired percentile for the calculation of the design evacuation curve. Update ‘Convergence’ sheet and return to ‘Iterations’ sheet.

Click the button ‘Reiterate’. A new group of lines (outputs for every node/zone) will be recorded in the ‘Iterations’ sheet for every new model run. To visualise the mean, min, max and design curves go to the sheet ‘Convergence’, choose the desired component ID and update the sheet.

If new iterations need to be generated, click the button ‘Clear’, then repeat the process.

Iterative runs for convergence

After convergence runs have been calculated, it is possible to perform and record a number of iterative runs to analyse multiple evacuation scenarios. To do so, in the sheet named ‘Bins’, specify the scenario matrix.

- Scenario ID: input numbers from 1 to the max number of scenarios (e.g., 1, 2, 3, etc.)
- Description: input a text description.
- Par 1 to 12: specify the parameters that vary in different evacuation scenarios and their values. Update the sheet. Then link the cells in the ‘Input’ sheet to the corresponding cells in the ‘Bins’ sheet (range R6:R17). Update the sheet.

In the sheet 'Scenarios' click the button 'Calculate scenarios'. A new group of lines (design curves for every zone/node) will be recorded in the 'Scenarios' sheet for every new scenario. To visualise the groups of curves generated for every zone/node of the network go to the sheet 'Consequences', choose the desired component ID and update the sheet.

If new scenarios need to be generated, click the button 'Clear', then repeat the process.

Appendix C: Test scenarios – Setup of the evacuation models

All scenarios

UNIMPEDED WALKING SPEED			
Distribution	Distr[S _{max}]	-	Normal
Mean	E[S _{max}]	m/s	1.19
Standard deviation	Var[S _{max}] ^{1/2}	m/s	0.30

Scenario T1_A

ZONES										N of zones	1	
Component ID	Component type	Floor length (side with door)	Floor width	Path shape	Occupant density	Detection + notification time	t _{d+n} = t _d + t _n			Pre- evacuation time	t _{pre}	
-	T	X	Y	PS	D	Distr[t _{d+n}]	E[t _{d+n}]	Var[t _{d+n}] ^{1/2}	Distr[t _{pre}]	E[t _{pre}]	Var[t _{pre}] ^{1/2}	
Z1	Room	30.0	15.0	Diagonal	0.5	Normal	0	0	Log-normal	4.21	0.27	

NODES										N of nodes	1
Component ID	Previous components		Component type	Measured width	Boundary layer	Max specific flow	Unimpeded walking speed	Component constant	Component length		
-	A	B	T	W	BL	F _{s,max}	S _{max}	k	L		
N1	Z1	0	Door	4.00	0.30	1.316	1.19	1.40	0.0		

Scenario T1_B

ZONES										N of zones	1	
Component ID	Component type	Floor length (side with door)	Floor width	Path shape	Occupant density	Detection + notification time	t _{d+n} = t _d + t _n			Pre- evacuation time	t _{pre}	
-	T	X	Y	PS	D	Distr[t _{d+n}]	E[t _{d+n}]	Var[t _{d+n}] ^{1/2}	Distr[t _{pre}]	E[t _{pre}]	Var[t _{pre}] ^{1/2}	
Z1	Room	30.0	15.0	Diagonal	0.5	Normal	0	0	Log-normal	4.21	0.27	

NODES										N of nodes	1
Component ID	Previous components		Component type	Measured width	Boundary layer	Max specific flow	Unimpeded walking speed	Component constant	Component length		
-	A	B	T	W	BL	F _{s,max}	S _{max}	k	L		
N1	Z1	0	Door	2.00	0.30	1.316	1.19	1.40	0.0		

Scenario T1_C

ZONES										N of zones	1	
Component ID	Component type	Floor length (side with door)	Floor width	Path shape	Occupant density	Detection + notification time	t _{d+n} = t _d + t _n			Pre- evacuation time	t _{pre}	
-	T	X	Y	PS	D	Distr[t _{d+n}]	E[t _{d+n}]	Var[t _{d+n}] ^{1/2}	Distr[t _{pre}]	E[t _{pre}]	Var[t _{pre}] ^{1/2}	
Z1	Room	30.0	15.0	Diagonal	1.0	Normal	0	0	Log-normal	4.21	0.27	

NODES										N of nodes	1
Component ID	Previous components		Component type	Measured width	Boundary layer	Max specific flow	Unimpeded walking speed	Component constant	Component length		
-	A	B	T	W	BL	F _{s,max}	S _{max}	k	L		
N1	Z1	0	Door	4.00	0.30	1.316	1.19	1.40	0.0		

Scenario T1_D

ZONES										N of zones	1	
Component ID	Component type	Floor length (side with door)	Floor width	Path shape	Occupant density	Detection + notification time	$t_{d+n} = t_d + t_n$			Pre- evacuation time	t_{pre}	
-	T	X m	Y m	PS	D pers/m ²	Distr[t _{d+n}]	E[t _{d+n}] s	Var[t _{d+n}] ^{1/2} s	Distr[t _{pre}]	E[t _{pre}] s	Var[t _{pre}] ^{1/2} s	
Z1	Room	30.0	15.0	Diagonal	1.0	Normal	0	0	Log-normal	4.21	0.27	

NODES										N of nodes	1
Component ID	Previous components		Component type	Measured width	Boundary layer	Max specific flow	Unimpeded walking speed	Component constant	Component length		
-	A	B	T	W m	BL m	F _{s,max} pers/(m·s)	S _{max} m/s	k	L m		
N1	Z1	0	Door	2.00	0.30	1.316	1.19	1.40	0.0		

Scenario T1_E

ZONES										N of zones	1	
Component ID	Component type	Floor length (side with door)	Floor width	Path shape	Occupant density	Detection + notification time	$t_{d+n} = t_d + t_n$			Pre- evacuation time	t_{pre}	
-	T	X m	Y m	PS	D pers/m ²	Distr[t _{d+n}]	E[t _{d+n}] s	Var[t _{d+n}] ^{1/2} s	Distr[t _{pre}]	E[t _{pre}] s	Var[t _{pre}] ^{1/2} s	
Z1	Room	30.0	15.0	Diagonal	2.0	Normal	0	0	Log-normal	4.21	0.27	

NODES										N of nodes	1
Component ID	Previous components		Component type	Measured width	Boundary layer	Max specific flow	Unimpeded walking speed	Component constant	Component length		
-	A	B	T	W m	BL m	F _{s,max} pers/(m·s)	S _{max} m/s	k	L m		
N1	Z1	0	Door	4.00	0.30	1.316	1.19	1.40	0.0		

Scenario T1_F

ZONES										N of zones	1	
Component ID	Component type	Floor length (side with door)	Floor width	Path shape	Occupant density	Detection + notification time	$t_{d+n} = t_d + t_n$			Pre- evacuation time	t_{pre}	
-	T	X m	Y m	PS	D pers/m ²	Distr[t _{d+n}]	E[t _{d+n}] s	Var[t _{d+n}] ^{1/2} s	Distr[t _{pre}]	E[t _{pre}] s	Var[t _{pre}] ^{1/2} s	
Z1	Room	30.0	15.0	Diagonal	2.0	Normal	0	0	Log-normal	4.21	0.27	

NODES										N of nodes	1
Component ID	Previous components		Component type	Measured width	Boundary layer	Max specific flow	Unimpeded walking speed	Component constant	Component length		
-	A	B	T	W m	BL m	F _{s,max} pers/(m·s)	S _{max} m/s	k	L m		
N1	Z1	0	Door	2.00	0.30	1.316	1.19	1.40	0.0		

Scenario T2_A

ZONES										N of zones	1	
Component ID	Component type	Floor length (side with door)	Floor width	Path shape	Occupant density	Detection + notification time	$t_{d+n} = t_d + t_n$			Pre- evacuation time	t_{pre}	
-	T	X m	Y m	PS	D pers/m ²	Distr[t _{d+n}]	E[t _{d+n}] s	Var[t _{d+n}] ^{1/2} s	Distr[t _{pre}]	E[t _{pre}] s	Var[t _{pre}] ^{1/2} s	
Z1	Room	30.0	15.0	Diagonal	0.5	Normal	0	0	Log-normal	4.21	0.27	

NODES										N of nodes	1
Component ID	Previous components		Component type	Measured width	Boundary layer	Max specific flow	Unimpeded walking speed	Component constant	Component length		
-	A	B	T	W	BL	$F_{s,max}$	S_{max}	k	L		
-	-	-	-	m	m	pers/(m·s)	m/s	-	m		
N1	Z1	0	Door	4.00	0.30	1.316	1.19	1.40	0.0		
N2	N1	0	Corridor	4.00	0.40	1.316	1.19	1.40	30.0		
N3	N2	0	Door	4.00	0.30	1.316	1.19	1.40	0.0		

Scenario T2_B

ZONES										N of zones	1
Component ID	Component type	Floor length (side with door)	Floor width	Path shape	Occupant density	Detection + notification time	$t_{d+n} = t_d + t_n$	Pre- evacuation time	t_{pre}		
-	T	X	Y	PS	D	Dist(t_{d+n})	$E[t_{d+n}]$	Var(t_{d+n}) ^{1/2}	Dist(t_{pre})	$E[t_{pre}]$	Var(t_{pre}) ^{1/2}
-	-	m	m	-	pers/m ²	-	s	s	-	s	s
Z1	Room	30.0	15.0	Diagonal	0.5	Normal	0	0	Log-normal	4.21	0.27

NODES										N of nodes	1
Component ID	Previous components		Component type	Measured width	Boundary layer	Max specific flow	Unimpeded walking speed	Component constant	Component length		
-	A	B	T	W	BL	$F_{s,max}$	S_{max}	k	L		
-	-	-	-	m	m	pers/(m·s)	m/s	-	m		
N1	Z1	0	Door	2.00	0.30	1.316	1.19	1.40	0.0		
N2	N1	0	Corridor	4.00	0.40	1.316	1.19	1.40	30.0		
N3	N2	0	Door	2.00	0.30	1.316	1.19	1.40	0.0		

Scenario T2_C

ZONES										N of zones	1
Component ID	Component type	Floor length (side with door)	Floor width	Path shape	Occupant density	Detection + notification time	$t_{d+n} = t_d + t_n$	Pre- evacuation time	t_{pre}		
-	T	X	Y	PS	D	Dist(t_{d+n})	$E[t_{d+n}]$	Var(t_{d+n}) ^{1/2}	Dist(t_{pre})	$E[t_{pre}]$	Var(t_{pre}) ^{1/2}
-	-	m	m	-	pers/m ²	-	s	s	-	s	s
Z1	Room	30.0	15.0	Diagonal	0.5	Normal	0	0	Log-normal	4.21	0.27

NODES										N of nodes	1
Component ID	Previous components		Component type	Measured width	Boundary layer	Max specific flow	Unimpeded walking speed	Component constant	Component length		
-	A	B	T	W	BL	$F_{s,max}$	S_{max}	k	L		
-	-	-	-	m	m	pers/(m·s)	m/s	-	m		
N1	Z1	0	Door	2.00	0.30	1.316	1.19	1.40	0.0		
N2	N1	0	Corridor	2.00	0.40	1.316	1.19	1.40	30.0		
N3	N2	0	Door	2.00	0.30	1.316	1.19	1.40	0.0		

Scenario T2_D

ZONES										N of zones	1
Component ID	Component type	Floor length (side with door)	Floor width	Path shape	Occupant density	Detection + notification time	$t_{d+n} = t_d + t_n$	Pre- evacuation time	t_{pre}		
-	T	X	Y	PS	D	Dist(t_{d+n})	$E[t_{d+n}]$	Var(t_{d+n}) ^{1/2}	Dist(t_{pre})	$E[t_{pre}]$	Var(t_{pre}) ^{1/2}
-	-	m	m	-	pers/m ²	-	s	s	-	s	s
Z1	Room	30.0	15.0	Diagonal	0.5	Normal	0	0	Log-normal	4.21	0.27

NODES										N of nodes	1
Component ID	Previous components		Component type	Measured width	Boundary layer	Max specific flow	Unimpeded walking speed	Component constant	Component length		
-	A	B	T	W	BL	$F_{s,max}$	S_{max}	k	L		
-	-	-	-	m	m	pers/(m·s)	m/s	-	m		
N1	Z1	0	Door	2.00	0.30	1.316	1.19	1.40	0.0		
N2	N1	0	Corridor	2.00	0.40	1.316	1.19	1.40	30.0		
N3	N2	0	Door	1.00	0.30	1.316	1.19	1.40	0.0		

Scenario T3

ZONE S											N of zones	1
Component ID	Component type	Floor length (side with door)	Floor width	Path shape	Occupant density	Detection + notification time $t_{d+n} = t_d + t_n$			Pre- evacuation time t_{pre}			
-	T	X	Y	PS	D	Dist(t_{d+n})	E(t_{d+n})	Var(t_{d+n}) ^{1/2}	Dist(t_{pre})	E(t_{pre})	Var(t_{pre}) ^{1/2}	
-	-	m	m	-	pers/m ²	-	s	s	-	s	s	
Z1	Room	30.0	15.0	Diagonal	0.5	Normal	0	0	Log-normal	4.21	0.27	

NODES										N of nodes	1
Component ID	Previous components		Component type	Measured width	Boundary layer	Max specific flow	Unimpeded walking speed	Component constant	Component length		
-	A	B	T	W	BL	$F_{s,max}$	S_{max}	k	L		
-	-	-	-	m	m	pers/(m·s)	m/s	-	m		
N1	Z1	0	Door	4.00	0.30	1.316	1.19	1.40	0.0		
N2	N1	0	Transit	30.00	0.40	1.316	1.19	1.40	15.0		
N3	N2	0	Door	4.00	0.30	1.316	1.19	1.40	0.0		

Scenario T4_A

ZONE S											N of zones	1
Component ID	Component type	Floor length (side with door)	Floor width	Path shape	Occupant density	Detection + notification time $t_{d+n} = t_d + t_n$			Pre- evacuation time t_{pre}			
-	T	X	Y	PS	D	Dist(t_{d+n})	E(t_{d+n})	Var(t_{d+n}) ^{1/2}	Dist(t_{pre})	E(t_{pre})	Var(t_{pre}) ^{1/2}	
-	-	m	m	-	pers/m ²	-	s	s	-	s	s	
Z1	Room	30.0	15.0	Diagonal	0.5	Normal	0	0	Log-normal	4.21	0.27	

NODES										N of nodes	1
Component ID	Previous components		Component type	Measured width	Boundary layer	Max specific flow	Unimpeded walking speed	Component constant	Component length		
-	A	B	T	W	BL	$F_{s,max}$	S_{max}	k	L		
-	-	-	-	m	m	pers/(m·s)	m/s	-	m		
N1	Z1	0	Door	4.00	0.30	1.316	1.19	1.40	0.0		
N2	N1	0	Landing	4.00	0.40	1.316	1.19	1.40	2.0		
N3	N2	0	Stair	4.00	0.30	0.940	0.85	1.00	7.0		
N4	N3	0	Landing	4.00	0.40	1.316	1.19	1.40	2.0		
N5	N4	0	Door	4.00	0.30	1.316	1.19	1.40	0.0		

Scenario T4_B

ZONE S											N of zones	1
Component ID	Component type	Floor length (side with door)	Floor width	Path shape	Occupant density	Detection + notification time $t_{d+n} = t_d + t_n$			Pre- evacuation time t_{pre}			
-	T	X	Y	PS	D	Dist(t_{d+n})	E(t_{d+n})	Var(t_{d+n}) ^{1/2}	Dist(t_{pre})	E(t_{pre})	Var(t_{pre}) ^{1/2}	
-	-	m	m	-	pers/m ²	-	s	s	-	s	s	
Z1	Room	30.0	15.0	Diagonal	0.5	Normal	0	0	Log-normal	4.21	0.27	

NODES										N of nodes	1
Component ID	Previous components		Component type	Measured width	Boundary layer	Max specific flow	Unimpeded walking speed	Component constant	Component length		
-	A	B	T	W	BL	$F_{s,max}$	S_{max}	k	L		
-	-	-	-	m	m	pers/(m·s)	m/s	-	m		
N1	Z1	0	Door	2.00	0.30	1.316	1.19	1.40	0.0		
N2	N1	0	Landing	2.00	0.40	1.316	1.19	1.40	2.0		
N3	N2	0	Stair	2.00	0.30	0.940	0.85	1.00	7.0		
N4	N3	0	Landing	2.00	0.40	1.316	1.19	1.40	2.0		
N5	N4	0	Door	2.00	0.30	1.316	1.19	1.40	0.0		

Scenario T4_C

ZONES										N of zones	1	
Component ID	Component type	Floor length (side with door)	Floor width	Path shape	Occupant density	Detection + notification time	$t_{d+n} = t_d + t_n$			Pre-evacuation time	t_{pre}	
-	T	X	Y	PS	D	Distr[t_{d+n}]	E[t_{d+n}]	Var[t_{d+n}] ^{1/2}	Distr[t_{pre}]	E[t_{pre}]	Var[t_{pre}] ^{1/2}	
-	-	m	m	-	pers/m ²	-	s	s	-	s	s	
Z1	Room	30.0	15.0	Diagonal	0.5	Normal	0	0	Log-normal	4.21	0.27	

NODES										N of nodes	1
Component ID	Previous components		Component type	Measured width	Boundary layer	Max specific flow	Unimpeded walking speed	Component constant	Component length		
-	A	B	T	W	BL	$F_{s,max}$	S_{max}	k	L		
-	-	-	-	m	m	pers/(m·s)	m/s	-	m		
N1	Z1	0	Door	4.00	0.30	1.316	1.19	1.40	0.0		
N2	N1	0	Landing	4.00	0.40	1.316	1.19	1.40	2.0		
N3	N2	0	Stair	4.00	0.30	1.160	1.05	1.23	7.0		
N4	N3	0	Landing	4.00	0.40	1.316	1.19	1.40	2.0		
N5	N4	0	Door	4.00	0.30	1.316	1.19	1.40	0.0		

Scenario T4_D

ZONES										N of zones	1	
Component ID	Component type	Floor length (side with door)	Floor width	Path shape	Occupant density	Detection + notification time	$t_{d+n} = t_d + t_n$			Pre-evacuation time	t_{pre}	
-	T	X	Y	PS	D	Distr[t_{d+n}]	E[t_{d+n}]	Var[t_{d+n}] ^{1/2}	Distr[t_{pre}]	E[t_{pre}]	Var[t_{pre}] ^{1/2}	
-	-	m	m	-	pers/m ²	-	s	s	-	s	s	
Z1	Room	30.0	15.0	Diagonal	0.5	Normal	0	0	Log-normal	4.21	0.27	

NODES										N of nodes	1
Component ID	Previous components		Component type	Measured width	Boundary layer	Max specific flow	Unimpeded walking speed	Component constant	Component length		
-	A	B	T	W	BL	$F_{s,max}$	S_{max}	k	L		
-	-	-	-	m	m	pers/(m·s)	m/s	-	m		
N1	Z1	0	Door	2.00	0.30	1.316	1.19	1.40	0.0		
N2	N1	0	Landing	2.00	0.40	1.316	1.19	1.40	2.0		
N3	N2	0	Stair	2.00	0.30	1.160	1.05	1.23	7.0		
N4	N3	0	Landing	2.00	0.40	1.316	1.19	1.40	2.0		
N5	N4	0	Door	2.00	0.30	1.316	1.19	1.40	0.0		

Scenario T5_A

ZONES										N of zones	1	
Component ID	Component type	Floor length (side with door)	Floor width	Path shape	Occupant density	Detection + notification time	$t_{d+n} = t_d + t_n$			Pre-evacuation time	t_{pre}	
-	T	X	Y	PS	D	Distr[t_{d+n}]	E[t_{d+n}]	Var[t_{d+n}] ^{1/2}	Distr[t_{pre}]	E[t_{pre}]	Var[t_{pre}] ^{1/2}	
-	-	m	m	-	pers/m ²	-	s	s	-	s	s	
Z1	Room 1	15.0	15.0	Diagonal	0.5	Normal	0	0	Log-normal	4.21	0.27	
Z2	Room 2	15.0	15.0	Diagonal	0.5	Normal	0	0	Log-normal	4.21	0.27	

NODES										N of nodes	1
Component ID	Previous components		Component type	Measured width	Boundary layer	Max specific flow	Unimpeded walking speed	Component constant	Component length		
-	A	B	T	W	BL	$F_{s,max}$	S_{max}	k	L		
-	-	-	-	m	m	pers/(m·s)	m/s	-	m		
N1	Z1	0	Door	2.00	0.30	1.316	1.19	1.40	0.0		
N2	N1	0	Transit	15.00	0.40	1.316	1.19	1.40	17.0		
N3	Z2	0	Door	2.00	0.30	1.316	1.19	1.40	0.0		
N4	N3	0	Transit	15.00	0.40	1.316	1.19	1.40	17.0		
N5	N2	N4	Merging point	15.00	0.40	1.316	1.19	1.40	0.0		
N6	N5	0	Door	2.00	0.30	1.316	1.19	1.40	0.0		

Scenario T5_B

ZONES									N of zones	1	
Component ID	Component type	Floor length (side with door)	Floor width	Path shape	Occupant density	Detection + notification time	$t_{d+n} = t_d + t_n$		Pre-evacuation time	t_{pre}	
-	T	X	Y	PS	D	Distr[t_{d+n}]	$E[t_{d+n}]$	$Var[t_{d+n}]^{1/2}$	Distr[t_{pre}]	$E[t_{pre}]$	$Var[t_{pre}]^{1/2}$
-	-	m	m	-	pers/m ²	-	s	s	-	s	s
Z1	Room 1	15.0	15.0	Diagonal	0.5	Normal	0	0	Log-normal	4.21	0.27
Z2	Room 2	15.0	15.0	Diagonal	0.5	Normal	90	0	Log-normal	4.21	0.27

NODES									N of nodes	1
Component ID	Previous components		Component type	Measured width	Boundary layer	Max specific flow	Unimpeded walking speed	Component constant	Component length	
-	A	B	T	W	BL	$F_{s,max}$	S_{max}	k	L	
-	-	-	-	m	m	pers/(m·s)	m/s	-	m	
N1	Z1	0	Door	2.00	0.30	1.316	1.19	1.40	0.0	
N2	N1	0	Transit	15.00	0.40	1.316	1.19	1.40	17.0	
N3	Z2	0	Door	2.00	0.30	1.316	1.19	1.40	0.0	
N4	N3	0	Transit	15.00	0.40	1.316	1.19	1.40	17.0	
N5	N2	N4	Merging point	15.00	0.40	1.316	1.19	1.40	0.0	
N6	N5	0	Door	2.00	0.30	1.316	1.19	1.40	0.0	

Appendix D: Case study – Modelling assumptions and inputs

D.1 Design scenarios

D.1.1 Fire characteristics

Since the objective of the analysis is life safety of occupants, design fires are assumed to be in the pre-flashover stage. This is assumed to grow at a quadratic rate ($HRR = \alpha_g t^2$).

The walls, the floors and the ceilings of the facility are made of incombustible materials. Thus, the majority of the fuel load is represented by the furniture in the dining areas (e.g., tables and chairs) and the combustible materials in the kitchens (e.g., food, oils and fats, packaging, etc.). Therefore, two types of fires are identified as representative for the food court: kitchen fires, which can originate in the food preparation areas located along the perimeter of the facility, and furniture fires that can originate in the dining areas.

In both cases a medium fire growth rate is considered ($\alpha_g = 0.011 \text{ kW/s}^2$) until a peak heat release of 5000 kW is reached. The combustion reaction of a generic fuel $\text{CH}_2\text{O}_{0.5}$ is assumed to occur with a heat of combustion $\Delta H_c = 20 \text{ MJ/kg}$, a radiative fraction $\chi_r = 0.35$ and a soot yield $y_s = 0.07 \text{ kg/kg}$ (Italian Fire Safety Code, 2019).

Since food preparation areas are protected by an automatic suppression system, it is assumed that the growth of kitchen fires is controlled when a temperature sensing element activates the discharge of the extinguishing agent (despite it is likely that the system will suppress the fire).

D.1.2 Building characteristics

The detection time t_d of the automatic smoke detection system is estimated with the two-zone model CFAST 7.6.0 developed by NIST (Peacock et al., 2015). A point smoke detector is located below the ceiling at an elevation of 4 m and radial distance of 7 m the fire. It is assumed that the smoke detector activates when the obscuration per unit length rises above a value of 20 %/m. The initial ambient temperature is set at 20 °C. The detection time obtained with the fire simulation is $t_d = 60 \text{ s}$. The notification time is set as $t_n = 0 \text{ s}$ since it is assumed that the fire alarm is activated automatically throughout the enclosure as soon as smoke is detected. Therefore $t_{d+n} = 60 \text{ s}$.

If the automatic detection and alarm system fails, it is assumed that some occupants become aware of the emergency when the smoke produced by a fire at one end of the enclosure has traversed the entire length of the space. It is assumed that 60 s are necessary for a stable ceiling jet to form. Considering a ceiling jet velocity $u = 1 \text{ m/s}$ and a maximum ceiling length of about 50 m, the smoke traverse time can be assumed to be 50 s. Therefore, $t_d = 60 + 50 = 110 \text{ s}$. Next, it is estimated that a notification time $t_n = 60 \text{ s}$ is required for the first occupants who perceive the smoke to reach a manual push button or inform directly other occupants. Hence, in case of failure of the automatic detection and notification system, it is assumed $t_{d+n} = 110 + 60 = 170 \text{ s}$.

The activation time of the suppression system t_a is also calculated with CFAST, introducing a temperature sensing element above the burner. It is assumed that fast response heat sensing elements are installed, characterised by a RTI of 50 $(\text{ms})^{0.5}$ and an activation temperature of 74 °C. The activation time obtained with the zone model is $t_a = 160 \text{ s}$. Conservatively, it is

assumed that the automatic system controls the fire without suppressing it. Therefore, after t_a , it is assumed that the fire burns with a steady heat release rate $HRR(t_a) \approx 285 \text{ kW}$.

D.1.3 Occupants' characteristics

The unimpeded walking speed and the pre-evacuation time are assumed to have the same distributions presented in section 5.1. In case of failure of the automatic detection and alarm system, the distribution of t_{pre} is assumed to be wider, with the values of the 1st and 99th percentiles corresponding respectively to 60 and 240 s (ISO TR 16738 : 2009). This corresponds to lognormal distribution with a location of 4.79 and a scale of 0.23.

The occupant load is expected to vary accordingly to the time of the day. The distribution is estimated using aggregated and anonymized data collected by Google, publicly available on www.google.com. The usage of similar facilities located into the analysed train station on an average day of the week is shown in Figure 63. The same shape is used in this study, assuming that the peak corresponds to a conservative occupant density of 1.0 pers/m^2 (the design value suggested in (Italian Fire Safety Code, 2019) for restaurants is 0.7 pers/m^2). The occupant load in other hours of the day is scaled accordingly. Based on this distribution, five levels of occupant load are selected for egress analyses, and the associated probability is calculated as shown in Table 7. Before ignition, occupants are assumed to be distributed uniformly within the facility.

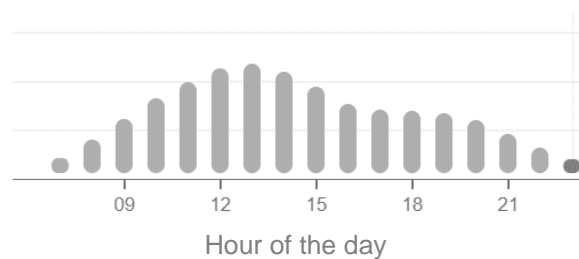


Figure 63 – Case study – Customer visits to similar facilities located in the analysed train station. Figure from www.google.com

Table 7 – Case study – Design occupant loads and associated probability

Density level	Occupant density [pers/m ²]	Probability
Very low	0.2	0.11
Low	0.4	0.18
Medium	0.6	0.35
High	0.8	0.18
Very high	1.0	0.18

D.2 Fire scenarios

The two types of fires (kitchen and furniture) may originate at any of the three floors of the facility. For model testing, only a kitchen fire located at the ground floor is considered further.

Based the activation/failure of the smoke and heat control system and automatic suppression system, four design fire scenarios are considered as presented in Table 8.

Occupants are deemed incapacitated when the smoke layer reaches an elevation of 2 m above the floor level or a temperature of 200 °C. Therefore, three values of ASET are calculated, corresponding to the time required for smoke to generate untenable conditions at the second floor, the first floor, and the ground floor (called respectively ASET₂, ASET₁ and ASET₀).

Table 8 – Case study – Design fire scenarios

Fire scenario	Type of fire	Location	α_g [kW/s ²]	SHC activates	FS activates	HRR _{max} [kW]
F01	Kitchen	GF	0.0111	Yes	Yes	285
F02	Kitchen	GF	0.0111	Yes	No	5000
F03	Kitchen	GF	0.0111	No	Yes	285
F04	Kitchen	GF	0.0111	No	No	5000

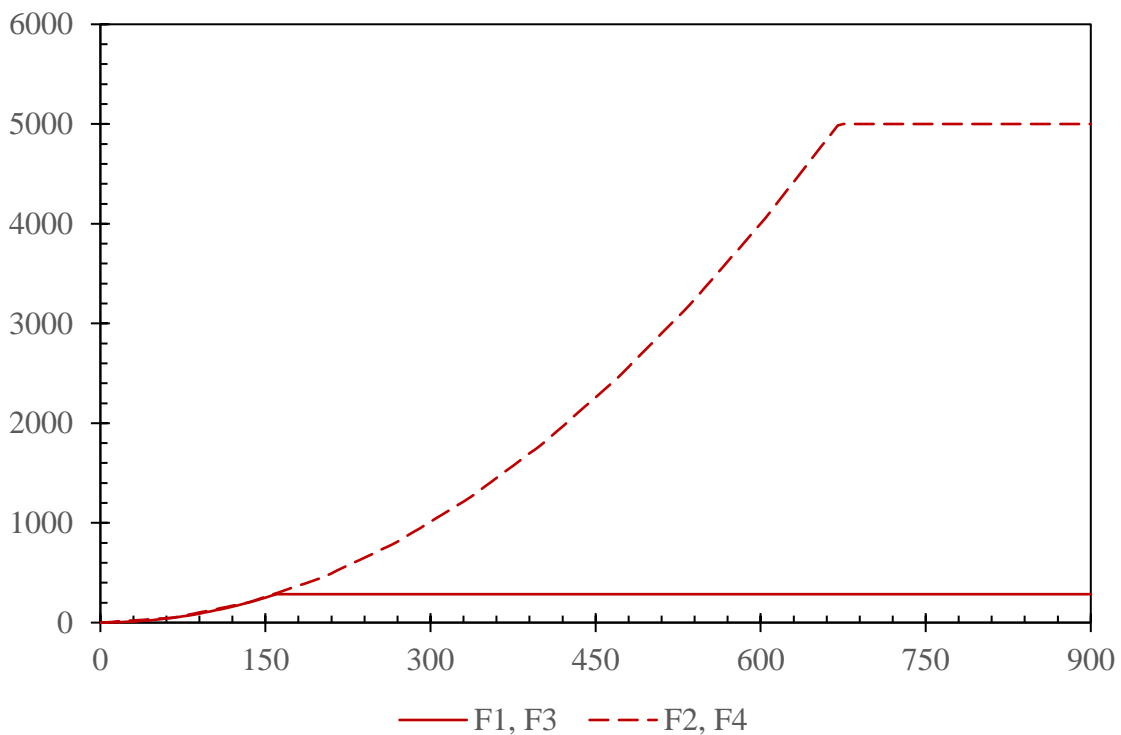


Figure 64 – Case study – Heat release rate curves

D.3 Evacuation scenarios

Based the activation/failure of the automatic smoke detection and notification system, the initial occupant load, and the reactivity of occupants, ten evacuation scenarios are considered as presented in Table 9. The timelines of the initial phases of the evacuation process in case of activation/failure of the SDN system are presented in Figure 65 and Figure 66.

In every case, it is assumed that when a fire is notified (automatically or manually) evacuation proceeds simultaneously at all floors. Conservatively, the main entrance (door n. 1) is discarded (e.g., blocked by the fire) and the occupants at the ground floor are assumed to distribute evenly across the remaining exits. It is assumed that occupants of the first floor split between the stair leading to the ground floor and exit n. 8. Since this door is not used by visitors in ordinary conditions, a proportion of 75% (stair) and 25% (exit) is considered to account for affiliation to familiar areas of the facility. All the occupants of the second floor use the stair as it is the only available egress path. It is assumed that all the occupants arriving at the ground floor from the stair will complete evacuation using exit n. 3, as it is the closest and most visually accessible.

Occupants are deemed safe when they have traversed a door leading to the exterior or to adjacent areas of the train station. Moreover, the occupants initially located at the first and second floor are deemed temporarily safe when they have moved to the lower floor. Therefore, three values of RSET need to be calculated, corresponding to the time required to evacuate the second floor, the first floor, and the ground floor (called respectively RSET₂, RSET₁ and RSET₀).

Table 9 – Case study – Design evacuation scenarios

Evacuation scenario	Detection + notification time [s]	Location of pre-evac time [s]	Scale of pre-evac time [s]	Occupant density [pers/m²]
E01	60	4.21	0.27	0.2
E02	60	4.21	0.27	0.4
E03	60	4.21	0.27	0.6
E04	60	4.21	0.27	0.8
E05	60	4.21	0.27	1.0
E06	170	4.79	0.23	0.2
E07	170	4.79	0.23	0.4
E08	170	4.79	0.23	0.6
E09	170	4.79	0.23	0.8
E10	170	4.79	0.23	1.0

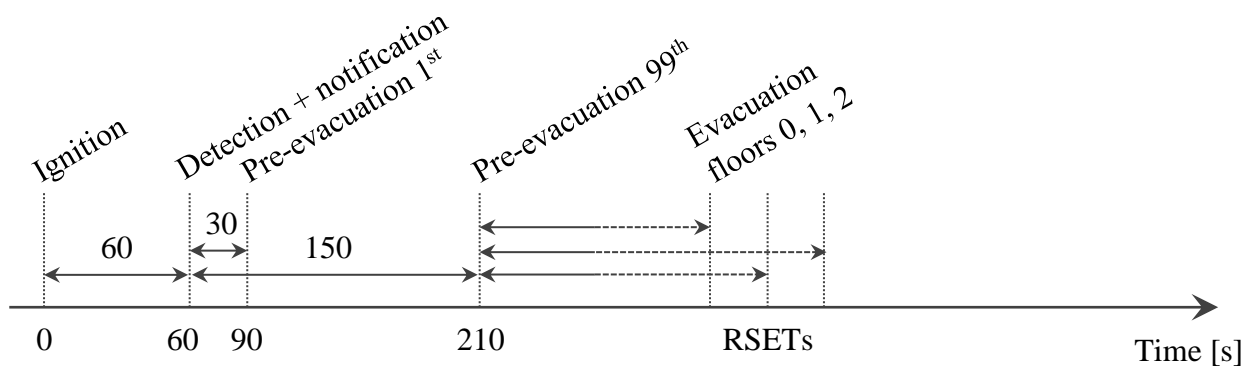


Figure 65 – Case study – Timeline of the evacuation process in case of success of the automatic detection and notification system

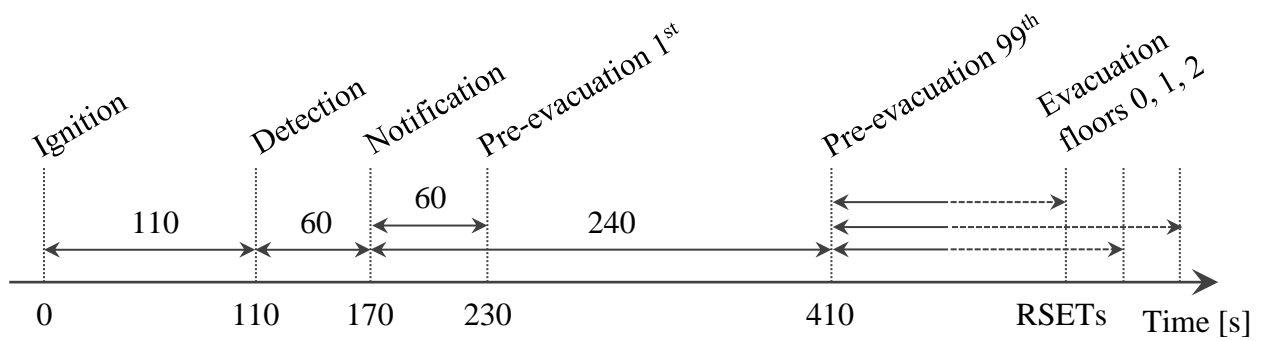


Figure 66 – Case study – Timeline of the evacuation process in case of failure of the automatic detection and notification system

Appendix E: Case study – Fire modelling

The evolution of the smoke layer properties is predicted with the two-zone model CFAST 7.6.0 developed by NIST (Peacock et al., 2015).

The modelled domain coincides with the internal gross volume of the enclosure. This is schematised as two interconnected rooms, without modelling explicitly the first and second floor (Figure 67). In fact, as these areas are completely open towards ground floor, hence it is expected that smoke dynamics are not affected greatly by the presence of the two floor slabs. As a result, when smoke progressively fills the enclosure, it initially engulfs the second floor, then the first floor, and ultimately the ground floor.

The thermal properties of lightweight concrete are applied to the walls: thickness $t = 15$ cm, thermal conductivity $k = 1.75$ W/(m K), density $\rho = 2200$ kg/m³, specific heat $c = 1$ kJ/(kg K), emissivity $\varepsilon = 0.94$. Ambient temperature is set at 20 °C.

The burner is placed at the centre of the ground floor, in the area with the greatest internal height. The four scenarios summarised in Table 8 are modelled. In scenarios F01 and F02 the smoke and heat control system activates after 60 s (detection time) and reaches the maximum extraction capacity of 16 m³/s after additional 30 s. In the same timeframe doors n. 2, 3, 4 and 5 open automatically to allow the inflow of fresh air.

The results show that the smoke layer temperature remains well below 200 °C for the duration of the whole simulations (Figure 68). Therefore, the smoke layer height is the controlling criterion for ASET. Its values obtained for every floor of the facility in each fire scenario are derived from Figure 69 as summarised in Table 10.

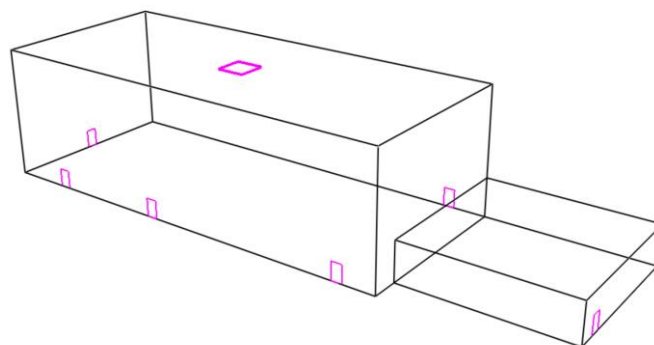


Figure 67 – Case study – 3D view of CFAST model

Table 10 – Case study – ASETs obtained with CFAST

	F01	F02	F03	F04
ASET₂ (+ 11.2 m) [s]	350	265	185	175
ASET₁ (+ 6.8 m) [s]	> 900	530	475	370
ASET₀ (+ 2.0 m) [s]	> 900	> 900	> 900	750

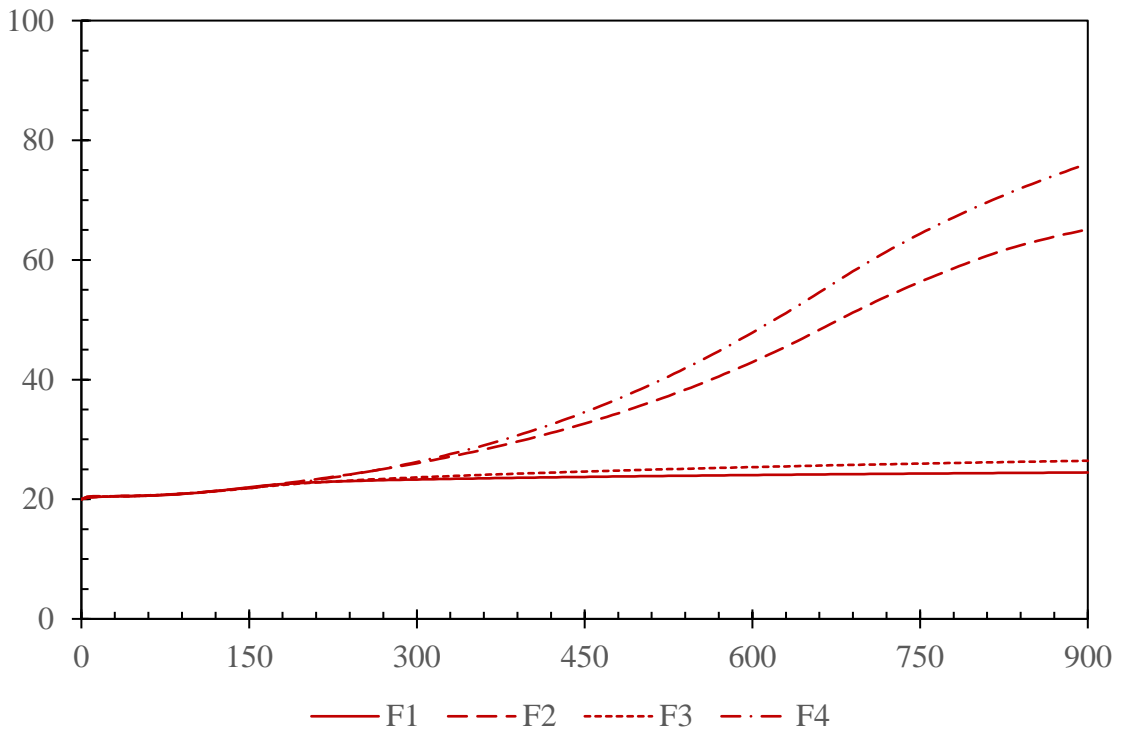


Figure 68 – Case study – Smoke layer temperature obtained with CFAST

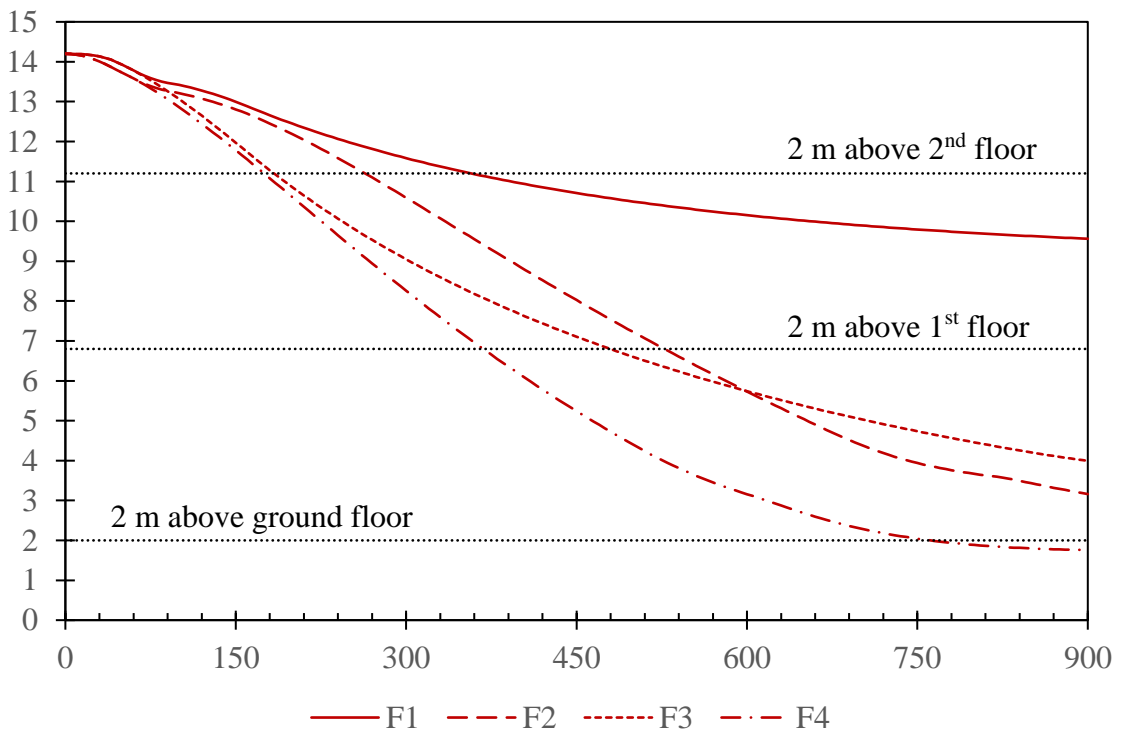


Figure 69 – Case study – Smoke layer height obtained with CFAST

Appendix F: Case study – Setup of the evacuation models

This appendix describes how the case study is modelled in Pathfinder and in the proposed mesoscopic model.

The geometry generated with Pathfinder consists of three rooms, each corresponding to one floor of the facility, located at an elevation of ± 0.0 m, + 4.8 m and + 9.2 m. Only the circulation and food consumption areas accessible to the public are modelled. The kitchens are not included in the model as they have independent exits towards a safe place; therefore, the evacuation of the vendors does not affect the evacuation of the customers. The footprint of obstructions such as counters and furniture is subtracted from the room surface. The three rooms are connected by a stair composed of multiple flights. The width is 150 cm, with risers of 16.5 cm and treads of 30.5 cm. All the doors are modelled ‘always open’ except for the main entrance which is discarded. Every door width is 120 cm. Figure 70 and Figure 71 provide a 3D and 2D visualization of the described geometry.

When the proposed mesoscopic model is used, the building is represented by 8 zones: 1 at the second floor, 2 at the first floor, and 5 at the ground floor. Only the dimensions of the circulation and food consumption areas are considered. However, since zones are defined as rectangles, an approximation is sometimes necessary to represent the parts of the building that are not perfectly rectangular (Figure 72). The presence of obstructions is considered by setting a ‘x+y’ type of path shape (section 4.1.2). A total of 24 nodes is generated to represent doors, passageways, corridors, transits, and merging points. They are characterised by the geometrical dimensions described previously, and the component properties summarised in Table 1 and Table 5. Zones and nodes are then combined into 6 networks, each leading to one of the six available final doors, as presented in the following images.

In pathfinder, occupants are randomly scattered over the room surfaces with a density of 1.0 pers/m². Thus, the resulting number of occupants generated at the ground, first and second floor is respectively of 600, 230, and 130 pers. In the proposed model, the same density is considered, but a reduction coefficient is introduced to account for the footprint of obstructions and obtain the same initial number of occupants. Their behaviour is set according to the evacuation scenarios presented in Annex D.

F.1 Pathfinder model

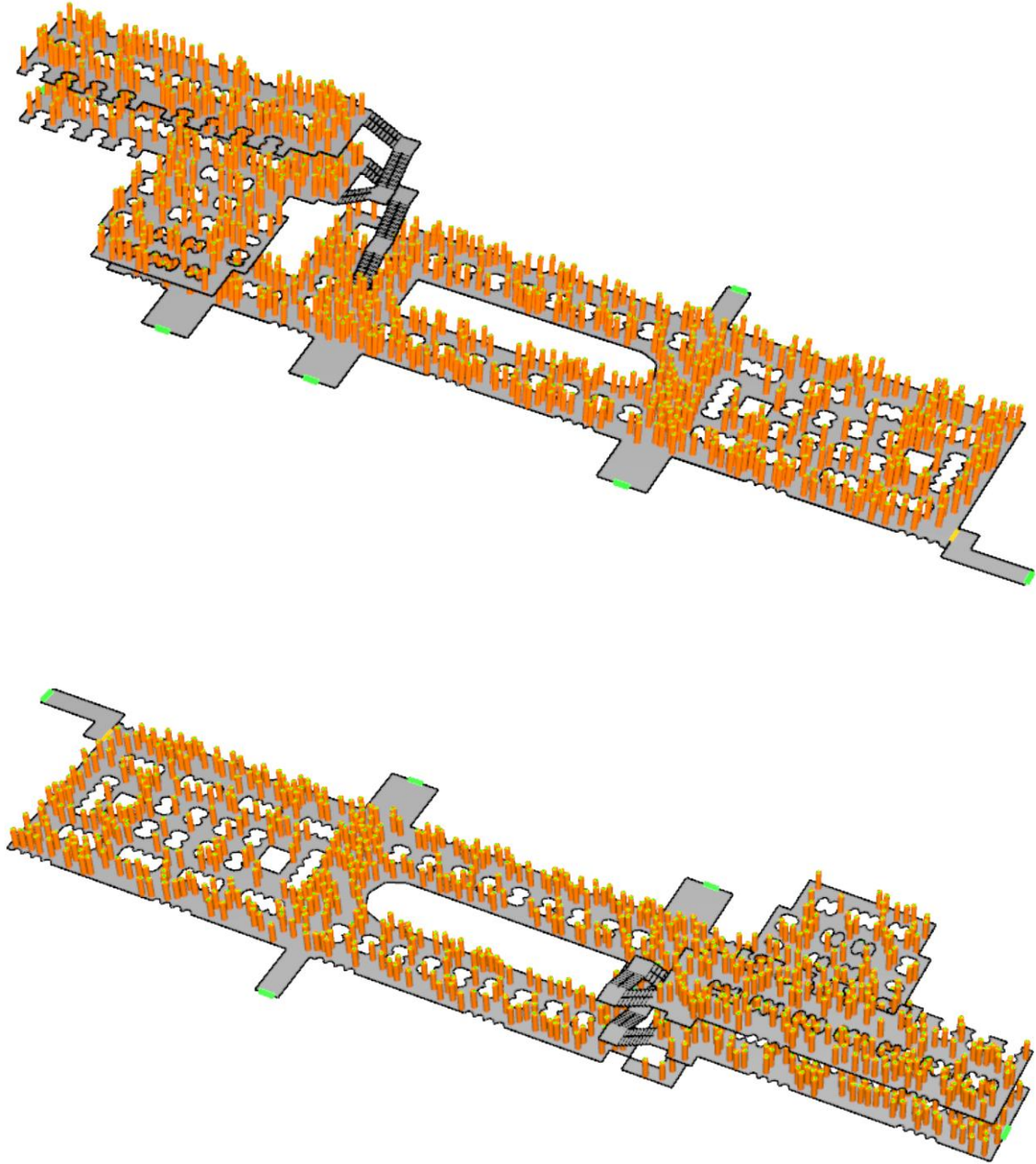
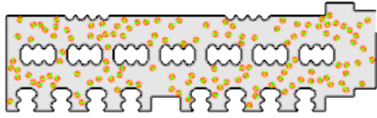
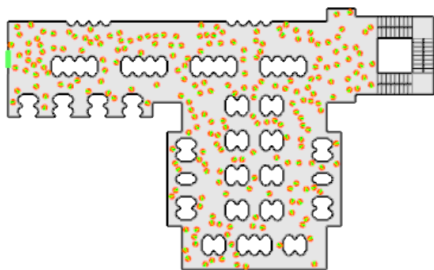


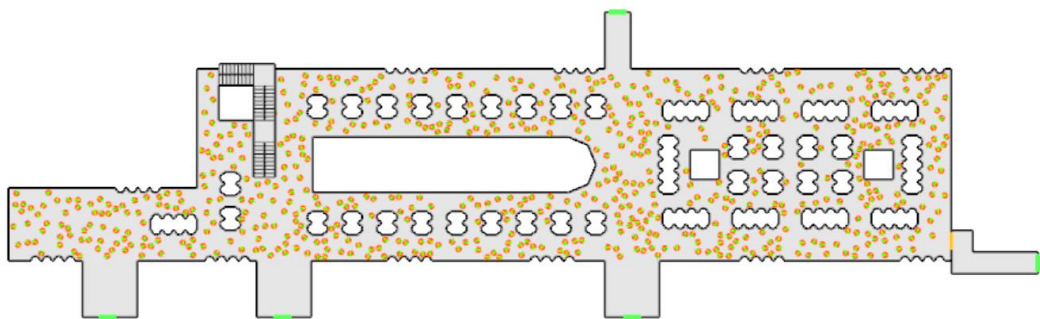
Figure 70 – Case study – 3D views of Pathfinder model



SECOND FLOOR (+ 9.2 m)



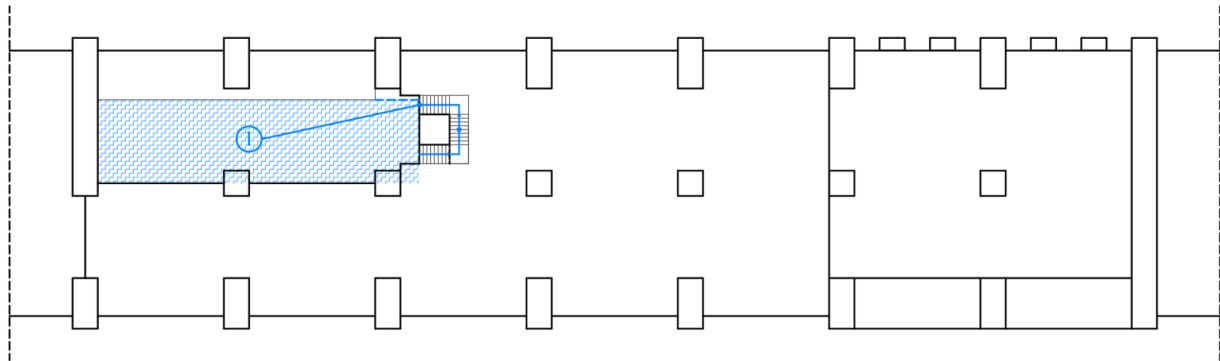
FIRST FLOOR (+ 4.8 m)



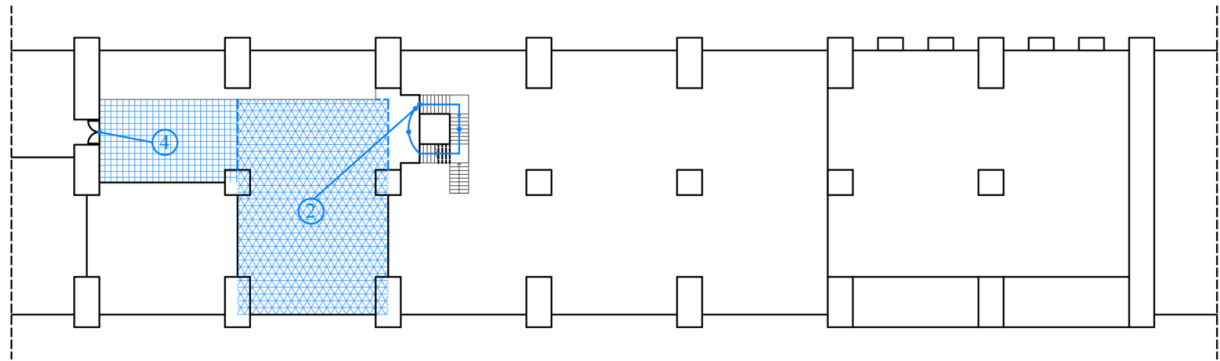
GROUND FLOOR (± 0.0 m)

Figure 71 – Case study – 2D views of Pathfinder model

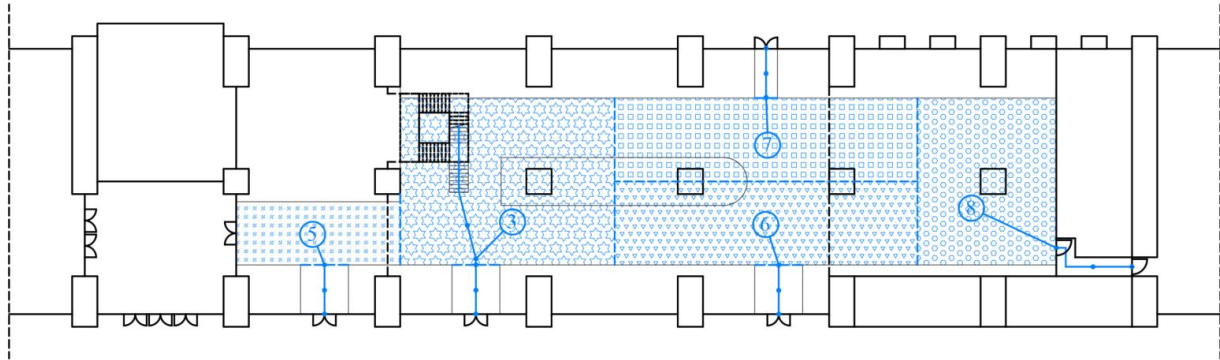
F.2 Mesoscopic model



SECOND FLOOR (+ 9.2 m)



FIRST FLOOR (+ 4.8 m)



GROUND FLOOR (± 0 m)






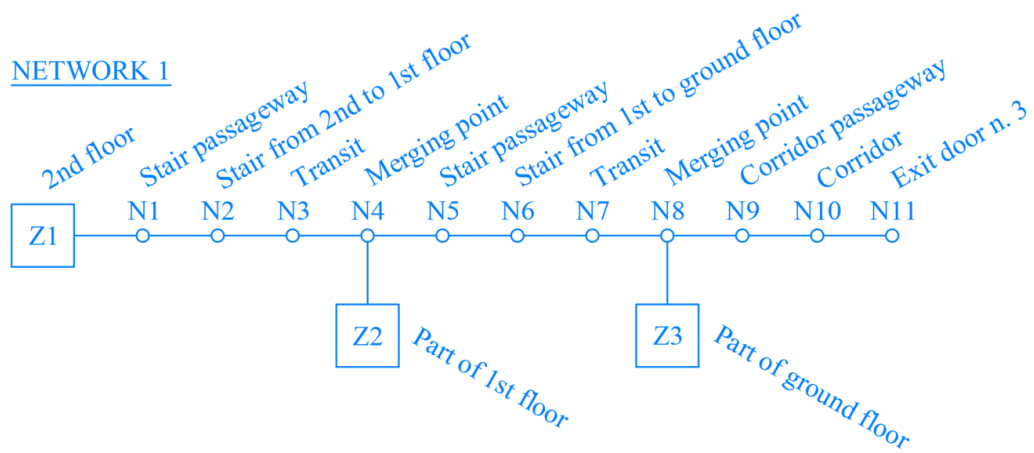
- | | | | |
|--|--|--|--|
|  ZONE 1 |  ZONE 3 |  ZONE 5 |  ZONE 7 |
|  ZONE 2 |  ZONE 4 |  ZONE 6 |  ZONE 8 |

Figure 72 – Case study – Simplification of the building geometry into zones and nodes

Network 1

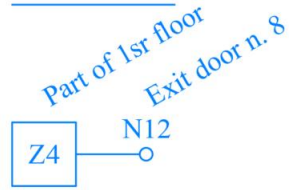


ZONES										N of zones	3
Component ID	Component type	Floor length (side with door)	Floor width	Path shape	Occupant density	Detection + notification time	$t_{d+n} = t_d + t_n$	15	Pre-evacuation time	t_{pre}	
-	T	X	Y	PS	D	Distr[t_{d+n}]	E[t_{d+n}]	Var[t_{d+n}] ^{1/2}	Distr[t_{pre}]	E[t_{pre}]	Var[t_{pre}] ^{1/2}
Z1	Zone 1	25.5	6.5	X+Y	1.0	Normal	60	0	Log-normal	4.21	0.27
Z2	Zone 2	12.0	17.0	X+Y	1.0	Normal	60	0	Log-normal	4.21	0.27
Z3	Zone 3	17.0	17.0	X+Y	1.0	Normal	60	0	Log-normal	4.21	0.27

NODES										N of nodes	11
Component ID	Previous components		Component type	Measured width	Boundary layer	Max specific flow	Unimpeded walking speed	Component constant	Component length		
-	A	B	T	W	BL	$F_{s,max}$	S_{max}	k	L		
N1	Z1	0	Passageway	1.50	0.30	1.090	1.00	1.16	0.0		
N2	N1	0	Stair	1.50	0.30	1.090	1.00	1.16	11.5		
N3	N2	0	Transit	1.50	0.30	1.316	1.19	1.40	6.0		
N4	N3	Z2	Merging	1.50	0.30	1.316	1.19	1.40	0.0		
N5	N4	0	Passageway	1.50	0.30	1.090	1.00	1.16	0.0		
N6	N5	0	Stair	1.50	0.30	1.090	1.00	1.16	11.5		
N7	N6	0	Transit	10.00	0.30	1.316	1.19	1.40	5.0		
N8	N7	Z3	Merging	10.00	0.30	1.316	1.19	1.40	0.0		
N9	N8	0	Passageway	5.00	0.30	1.316	1.19	1.40	0.0		
N10	N9	0	Corridor	5.00	0.30	1.316	1.19	1.40	4.0		
N11	N10	0	Exit n. 3	1.20	0.30	1.316	1.19	1.40	0.0		

Network 2

NETWORK 2

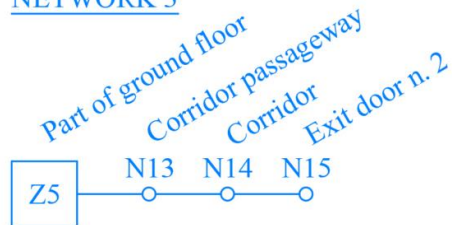


ZONES										N of zones	1
Component ID	Component type	Floor length (side with door)	Floor width	Path shape	Occupant density	Detection + notification time	$t_{d+n} = t_d + t_n$	15	Pre-evacuation time	t_{pre}	
-	T	X	Y	PS	D	Distr[t_{d+n}]	E[t_{d+n}]	Var[t_{d+n}] ^{1/2}	Distr[t_{pre}]	E[t_{pre}]	
-	-	m	m	-	pers/m ²	-	s	s	-	s	
Z4	Zone 4	6.5	11.0	X+Y	1.0	Normal	60	0	Log-normal	4.21	0.27

NODES										N of nodes	1
Component ID	Previous components		Component type	Measured width	Boundary layer	Max specific flow	Unimpeded walking speed	Component constant	Component length		
-	A	B	T	W	BL	$F_{s,max}$	S_{max}	k	L		
-	-	-	-	m	m	pers/(m·s)	m/s	-	m		
N12	Z4	0	Exit n. 8	1.20	0.30	1.316	1.19	1.40	0.0		

Network 3

NETWORK 3

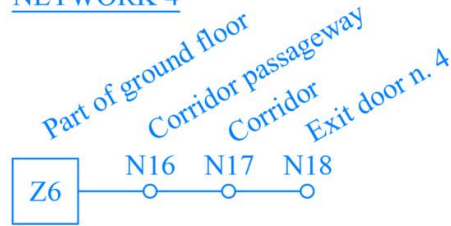


ZONES										N of zones	1
Component ID	Component type	Floor length (side with door)	Floor width	Path shape	Occupant density	Detection + notification time	$t_{d+n} = t_d + t_n$	15	Pre-evacuation time	t_{pre}	
-	T	X	Y	PS	D	Distr[t_{d+n}]	E[t_{d+n}]	Var[t_{d+n}] ^{1/2}	Distr[t_{pre}]	E[t_{pre}]	
-	-	m	m	-	pers/m ²	-	s	s	-	s	
Z5	Zone 5	13.0	5.0	X+Y	1.0	Normal	60	0	Log-normal	4.21	0.27

NODES										N of nodes	3
Component ID	Previous components		Component type	Measured width	Boundary layer	Max specific flow	Unimpeded walking speed	Component constant	Component length		
-	A	B	T	W	BL	$F_{s,max}$	S_{max}	k	L		
-	-	-	-	m	m	pers/(m·s)	m/s	-	m		
N13	Z5	0	Passageway	3.80	0.30	1.316	1.19	1.40	0.0		
N14	N13	0	Corridor	3.80	0.40	1.316	1.19	1.40	4.0		
N15	N14	0	Exit n. 2	1.20	0.30	1.316	1.19	1.40	0.0		

Network 4

NETWORK 4

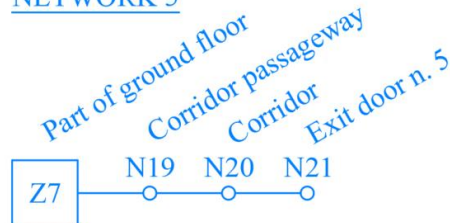


ZONES										N of zones	1
Component ID	Component type	Floor length (side with door)	Floor width	Path shape	Occupant density	Detection + notification time	$t_{d+n} = t_d + t_n$	15	Pre- evacuation time	t_{pre}	
-	T	X m	Y m	PS	D pers/m ²	Distr[t _{d+n}]	E[t _{d+n}] s	Var[t _{d+n}] ^{1/2} s	Distr[t _{pre}]	E[t _{pre}] s	Var[t _{pre}] ^{1/2} s
Z6	Zone 6	24.0	5.5	X+Y	1.0	Normal	60	0	Log-normal	4.21	0.27

NODES										N of nodes	3
Component ID	Previous components		Component type	Measured width	Boundary layer	Max specific flow	Unimpeded walking speed	Component constant	Component length		
-	A	B	T	W m	BL m	F _{s,max} pers/(m·s)	S _{max} m/s	k	L m		
N16	Z6	0	Passageway	3.80	0.30	1.316	1.19	1.40	0.0		
N17	N16	0	Corridor	3.80	0.40	1.316	1.19	1.40	4.0		
N18	N17	0	Exit n. 4	1.20	0.30	1.316	1.19	1.40	0.0		

Network 5

NETWORK 5

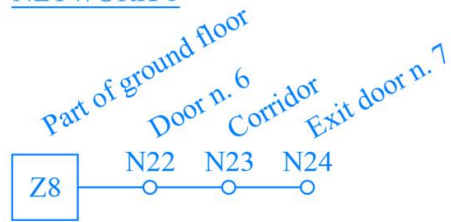


ZONES										N of zones	1
Component ID	Component type	Floor length (side with door)	Floor width	Path shape	Occupant density	Detection + notification time	$t_{d+n} = t_d + t_n$	15	Pre- evacuation time	t_{pre}	
-	T	X m	Y m	PS	D pers/m ²	Distr[t _{d+n}]	E[t _{d+n}] s	Var[t _{d+n}] ^{1/2} s	Distr[t _{pre}]	E[t _{pre}] s	Var[t _{pre}] ^{1/2} s
Z7	Zone 7	24.0	5.5	X+Y	1.0	Normal	60	0	Log-normal	4.21	0.27

NODES										N of nodes	3
Component ID	Previous components		Component type	Measured width	Boundary layer	Max specific flow	Unimpeded walking speed	Component constant	Component length		
-	A	B	T	W m	BL m	F _{s,max} pers/(m·s)	S _{max} m/s	k	L m		
N19	Z7	0	Passageway	1.80	0.30	1.316	1.19	1.40	0.0		
N20	N19	0	Corridor	1.80	0.40	1.316	1.19	1.40	4.0		
N21	N20	0	Exit n. 5	1.20	0.30	1.316	1.19	1.40	0.0		

Network 6

NETWORK 6



ZONES										N of zones	1
Component ID	Component type	Floor length (side with door)	Floor width	Path shape	Occupant density	Detection + notification time	$t_{d+n} = t_d + t_n$	15	Pre- evacuation time	t_{pre}	
-	T	X m	Y m	PS -	D pers/m ²	Distr[t _{d+n}]	E[t _{d+n}] s	Var[t _{d+n}] ^{1/2} s	Distr[t _{pre}]	E[t _{pre}] s	Var[t _{pre}] ^{1/2} s
Z8	Zone 8	11.0	13.0	X+Y	1.0	Normal	60	0	Log-normal	4.21	0.27

NODES										N of nodes	3
Component ID	Previous components		Component type	Measured width	Boundary layer	Max specific flow	Unimpeded walking speed	Component constant	Component length		
-	A	B	T	W m	BL m	F _{s,max} pers/(m·s)	S _{max} m/s	k	L m		
N22	Z8	0	Door	1.20	0.30	1.316	1.19	1.40	0.0		
N23	N22	0	Corridor	1.50	0.40	1.316	1.19	1.40	7.5		
N24	N23	0	Exit n. 7	1.20	0.30	1.316	1.19	1.40	0.0		

Appendix G: Case study – Quantitative risk assessment

Table 11 – Case study, Network 1 – Consequences of risk scenarios

Risk scenario	Fire scenario	Available Safe Egress Time	Evacuation scenario	Number of occupants exposed
S_i [-]	F_i [-]	ASET_i [s]	E_i [-]	N_i [pers]
S01	F01	350	E01	0
S02	F01	350	E02	0
S03	F01	350	E03	0
S04	F01	350	E04	0
S05	F01	350	E05	0
S06	F02	265	E01	0
S07	F02	265	E02	1
S08	F02	265	E03	0
S09	F02	265	E04	1
S10	F02	265	E05	1
S11	F03	185	E01	4
S12	F03	185	E02	6
S13	F03	185	E03	12
S14	F03	185	E04	36
S15	F03	185	E05	61
S16	F04	175	E01	6
S17	F04	175	E02	9
S18	F04	175	E03	24
S19	F04	175	E04	48
S20	F04	175	E05	72
S21	F03	185	E06	26
S22	F03	185	E07	52
S23	F03	185	E08	78
S24	F03	185	E09	104
S25	F03	185	E10	130
S26	F04	175	E06	26
S27	F04	175	E07	52
S28	F04	175	E08	78
S29	F04	175	E09	104
S30	F04	175	E10	130

Table 12 – Case study, Network 1 – Likelihood of risk scenarios

Risk scenario	Probability	Frequency
S_i [-]	P_i [-]	F_i [year ⁻¹]
S01	7.99E-02	7.99E-06
S02	1.31E-01	1.31E-05
S03	2.54E-01	2.54E-05
S04	1.31E-01	1.31E-05
S05	1.31E-01	1.31E-05
S06	4.21E-03	4.21E-07
S07	6.89E-03	6.89E-07
S08	1.34E-02	1.34E-06
S09	6.89E-03	6.89E-07
S10	6.89E-03	6.89E-07
S11	1.41E-02	1.41E-06
S12	2.31E-02	2.31E-06
S13	4.49E-02	4.49E-06
S14	2.31E-02	2.31E-06
S15	2.31E-02	2.31E-06
S16	7.43E-04	7.43E-08
S17	1.22E-03	1.22E-07
S18	2.36E-03	2.36E-07
S19	1.22E-03	1.22E-07
S20	1.22E-03	1.22E-07
S21	1.05E-02	1.05E-06
S22	1.71E-02	1.71E-06
S23	3.33E-02	3.33E-06
S24	1.71E-02	1.71E-06
S25	1.71E-02	1.71E-06
S26	5.50E-04	5.50E-08
S27	9.00E-04	9.00E-08
S28	1.75E-03	1.75E-07
S29	9.00E-04	9.00E-08
S30	9.00E-04	9.00E-08
Total	1.00	1.00E-04

Table 13 – Case study, Network 1 – Consequences and frequency of risk scenarios

Consequences	Frequency	Cumulative frequency	Risk scenario
N_i [pers]	F_i [year⁻¹]	ΣF_i [year⁻¹]	S_i [-]
N > 130	0.00E+00	0.00E+00	-
104 < N ≤ 130	1.80E-06	1.80E-06	S25, S30
78 < N ≤ 104	1.80E-06	3.60E-06	S24, S29
70 < N ≤ 78	3.50E-06	7.10E-06	S23, S28
61 < N ≤ 70	1.22E-07	7.22E-06	S20
52 < N ≤ 61	2.31E-06	9.53E-06	S15
47 < N ≤ 52	1.80E-06	1.13E-05	S22, S27
34 < N ≤ 47	1.22E-07	1.15E-05	S19
26 < N ≤ 34	2.31E-06	1.38E-05	S14
21 < N ≤ 26	1.10E-06	1.49E-05	S21, S26
14 < N ≤ 21	2.36E-07	1.51E-05	S18
10 < N ≤ 14	4.49E-06	1.96E-05	S13
6 < N ≤ 10	1.22E-07	1.97E-05	S17
5 < N ≤ 6	2.38E-06	2.21E-05	S12, S16
1 < N ≤ 5	1.41E-06	2.35E-05	S11
0 < N ≤ 1	1.34E-06	2.48E-05	S08
N = 0	7.52E-05	1.00E-04	S01-07, S09, S10